DOI:10.14753/SE.2023.2882

SEMMELWEIS EGYETEM

DOKTORI ISKOLA

Ph.D. értekezések

2882.

PAULA MUT ARBONA

Funkcionális idegtudományok
című program

Programvezető: Dr. Sperlágh Beáta, egyetemi tanár

Témavezető: Dr. Sperlágh Beáta, egyetemi tanár

DOI:10.14753/SE.2023.2882

The role of the P2X7 receptor as a key player in neuronal development and implications for schizophrenia animal models

PhD thesis

Paula Mut Arbona

János Szentágothai Doctoral School of Neuroscience

Semmelweis University

Supervisor: Beata Sperlágh, MD, D.Sc

Official reviewers: Judit Lazáry, MD, D.Sc

Éva Mikics, MD, Ph.D

Head of the Complex Examination Committee: György Lévay, C.Sc

Members of the Examination Committee: László Köles, PharmD

Zelena Dóra, D.Sc

Budapest

2023

DOI:10.14753/SE.2023.2882

Table of Contents

DOI:10.14753/SE.2023.2882

DOI:10.14753/SE.2023.2882

DOI:10.14753/SE.2023.2882

1. Abbreviations

5HT2A: serotonin (5-HT) 5-HT2A receptor

ACC: Anterior cingulate cortex

ANOVA: analysis of variance

ASD: Autism spectrum disorder

ATP: Adenosine 5'-triphosphate

BSA: bovine serum albumin

BzATP: 2′ (3′)-O-(4-benzoyl benzoyl) adenosine 5′-triphosphate triethylammonium salt

cDNA: complementary deoxyribonucleic acid

DAMP: damage-associated molecular pattern

DLPFC: Dorsolateral prefrontal cortex

E-NPPs: ectonucleotidase pyrophosphatase/phosphodiesterase family

E-NTPDase: ectonucleoside triphosphate diphosphohydrolase

FC: fold change

i.p.: intra-peritoneal

IL-1β: Interleukin-one beta

KO: knock-out, P2rx7-/- C57Bl/6J strain

LPS: Lipopolysaccharide

MIA: Maternal immune activation

NDD: Neurodevelopmental disorder

NF-κB: nuclear factor-κB

NOR: Novel object recognition

OL: Object location

P2X7R: P2X7 receptor

PAR: Parietal cortex

PFC: Prefrontal cortex

PIC: Polyinosinic: polycytidylic acid; Poly (I:C)

RNA: ribonucleic acid

RT: reverse transcription

RT: Room temperature, 18-23 °C

RT-qPCR: quantitative reverse transcription-polymerase chain reaction

SCZ: Schizophrenia

SNc: Substantia nigra pars compacta

TLR: Toll-like receptors

TNF-α: tumour necrosis factor-alpha

TOR: Temporal object recognition

VTA: Ventral tegmental área

WT: wild-type, P2rx7+/+ C57Bl/6J strain

CNS: central nervous system

DOI:10.14753/SE.2023.2882

2. Introduction

Extracellular ATP is an important signalling molecule that regulates several cellular functions and activates purinergic P2 receptors, which are expressed in the early embryonic stage during brain development, thus influencing cellular differentiation, proliferation, and apoptosis. At high levels, extracellular ATP operates as a “danger” molecule under pathologic conditions through purinergic receptors, including the ionotropic P2X7 receptor (P2X7R). The ionotropic receptors P2X and particularly the P2X7R have received considerable attention in the past decade because of their involvement in diseases of the central nervous system (CNS), including psychiatric disorders. Indeed. P2X7R endogenous activation is associated with neurodevelopmental disorders. However, its function during early embryonic stages remains largely unclear despite the fact that purinergic signalling has been shown to play a role in physiological brain development.

This PhD thesis aims to assess the regulatory effect of P2X7R on neuronal outgrowth and morphology in primary cultures of murine hippocampal neurons and acute hippocampal slices. As well, this thesis will focus on the study of role of the receptor on the pathogenesis of schizophrenia. Schizophrenia is regarded as a neurodevelopmental psychiatric disorder, a dynamic disorder, in which changes in brain development and maturation might be because of the interaction of various genetic, epigenetic, and environmental factors.

2.1. Purinergic signalling system

The purinergic signalling system ("purinome") is a form of extracellular signalling mediated by purine nucleotides and nucleosides, mainly adenosine and Adenosine 5'-triphosphate (ATP) and pyrimidines. Purines and pyrimidine nucleotides are released to the extracellular medium from living cells by several physiological mechanisms, such as exocytosis or diffusion through the transporters and membrane channels (1).

The purinergic pathway mediates both pro-inflammatory and anti-inflammatory responses being the breakdown of ATP to extracellular process critical for this equilibrium. In physiological conditions, extracellular ATP is kept at concentrations in the nanomolar range. Whether released into the medium from lytic (e.g., stressed or apoptotic/necrotic cells) and non-lytic (e.g., pannexin-1 and connexins) routes, following

tissue damage, inflammation, or hypoxia, ATP acts as a clear indicator or "danger signal" for cell damage. Once ATP is released into the extracellular space, it gets enzymatically degraded by a large cascade of ectonucleotidases (e.g. the ectonucleoside triphosphate diphosphohydrolase (E-NTPDase) family (CD39), the ecto-nucleotide pyrophosphatase/phosphodiesterase family (E-NPPs) and the ecto-5′-nucleotidase (CD73)) (2). As ATP is suggested as primitive danger signal, this might indicate a common evolution of purinergic receptors with the damage-associated molecular patterns (DAMPs). Eventually, ATP metabolites, i.e. Adenosine diphosphate (ADP), Adenosine monophosphate (AMP), and ultimately adenosine act as well as purine signalling molecules (schemed in Fig. 1).

This process involves the activation of purinergic receptors in the cell and nearby cells, thereby regulating cellular functions. These purinergic receptors are divided mainly into three subfamilies (3):

- The G protein-coupled metabotropic adenosine receptors (also known as P1) present four subunits (P1A1, 2A, 2B and 3 subunits), activated by adenosine to convey pro-inflammatory and anti-inflammatory responses, depending on the receptor subtype and cell types involved.
- The trimeric ionotropic P2X receptors subfamily presents seven (P2X1, 2, 3, 4, 5, 6, 7) subunits activated by ATP to promote pro-inflammatory responses.
- The G protein-coupled metabotropic P2Y receptors subfamily presents eight subunits (P2Y1, 2, 4, 6, 11, 12, 13, 14) activated by ATP and other nucleotides (ADP, uridine diphosphate (UDP), uridine triphosphate (UTP), or UDP-glucose) to promote pro-inflammatory responses.

DOI:10.14753/SE.2023.2882

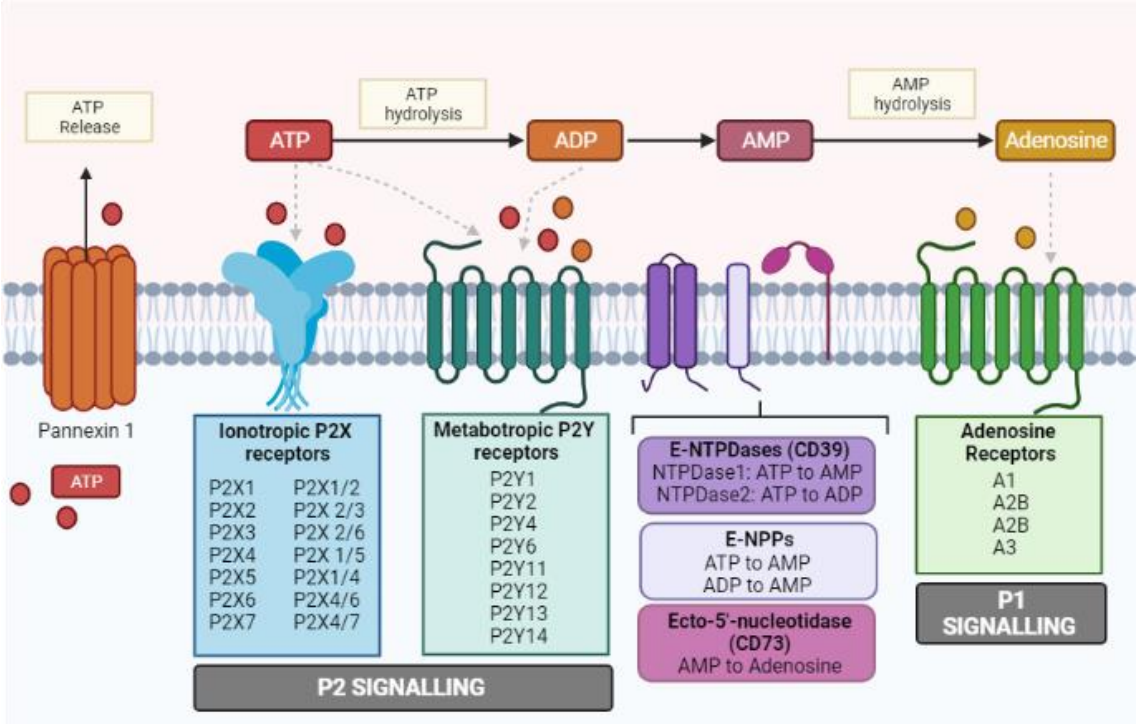

Figure 1. Scheme of the purinergic system complex. Created with Biorender.

2.1.1. Purinergic signalling in the nervous system

Purinergic receptors are abundantly expressed in different cell types and systems, including the central nervous system (CNS), as purinergic signalling appeared early in evolution, being present already in invertebrates (4). ATP acts as a fast excitatory co-transmitter stored in all nerve types in the central and peripheral nerves and released from synaptic terminals, binding to many purinergic receptors.

In the CNS, ATP and adenosine mediate neuromodulatory function (5,6). ATP and adenosine also modulate the communication between neural cells by mediating neuron-glia communication (7). This communication is commonly associated with pathological conditions, but it is gaining attention recently under physiological conditions. For example, adenosine and ATP induce astrocyte cell proliferation (8) and modulate synaptic plasticity (9). Moreover, the immune cells of the CNS, the microglia, recognise purinergic somatic junctions and control the correct neuronal function of the cells. Therefore, it has been hypothesised that microglia might be highly sensitive to subtle changes in the brain's extracellular space, as is the primary immune-competent cell type resident in the CNS. Recently, the expression of several proteins of the purinergic signalling system in microglia *in vivo* and *ex vivo* has been reviewed (10). A1 and A2A adenosine receptors are abundantly expressed in the CNS, principally located at synapses,

to modulate synaptic transmission promptly. Whereas A1 display an inhibitory effect, A2A counteracts by facilitating long-term potentiation in response to high-frequency activity. Likely both A1A and A2A receptors are functionally expressed in microglia to facilitate a phenotypic microglial anti- and pro-inflammatory shift, respectively (11).

In the peripheral nervous system, ATP and adenosine modulate the release of neurotransmitters in response to nerve stimulation (12). Therefore, it is essential for several homeostatic processes of the nervous system, such as controlling blood flow.

2.1.2. Purinergic signalling during nervous system development

The ubiquity of purinergic signalling in the nervous system hypothesizes whether the nucleotides and nucleosides present multiple roles in neurogenesis and plastic remodelling during development. The process of brain development entails a complexity of processes, such as cellular programming or cell-to-cell communication, leading to the early neural induction of the central and peripheral nervous systems. Purinergic receptors present different roles, mediated by purines and other agonists and might act as modulators or enhancers of the signal or direct functional switches of the purinergic pathways (13). Extracellular ATP is an important signalling molecule that regulates several cellular functions while activating purinergic P2 receptors and, expressed in the early embryonic stage during brain development, influences cellular differentiation, proliferation and apoptosis (14,15). The main processes of brain development can be enumerated mainly as the control of proliferation and cell fate of glial cells, neurons and oligodendrocytes, cell migration and maturation, elimination of the excess of cellular contacts and dead cells by synaptic pruning and apoptosis, cell migration and maturation, neurite outgrowth and synapse formation, plasticity and network consolidation (16). Therefore, the transient expression of some purinergic receptor subtypes and ectonucleotidases hints that those nucleotides and nucleosides might affect stage-specific developmental processes.

During the nervous system development, progenitor cells and neural stem cells convert into macroglia cells (astrocytes and oligodendrocytes) and neurons by symmetric and asymmetric divisions. The process of neurogenesis occurs firstly the embryogenesis, while the glial cells develop mainly after birth. Cell survival regulation is a highly

regulated process essential for the correct function in developing and maintaining the nervous system.

At prenatal and early postnatal stages, the neurogenesis is located in two actively proliferating zones: the ventricular zone (VZ) and the subventricular zone (SVZ). The VZ is a transient embryonic thin layer of tissue containing the radial glial cells, progenitor cells responsible for producing all neuronal cell types and specific lineages of glia. In embryonic neural stem cells, ATP increases the intracellular calcium release in radial glial cells, promoting neuronal proliferation in neocortex development (17). In contrast, the SVZ refers to a secondary proliferative zone containing neural progenitor cells, a region situated on the lateral ventricle of the vertebrate brain present in both the embryonic and adult brains. Progressively, these layers will disappear to establish the mature nervous system. Neurogenesis is maintained in selected forebrain regions of the adult brain, such as the adult SVZ on the lateral ventricles or the subgranular layer (SGL) of the dentate gyrus of the hippocampus (18). There is increasing evidence of the purinergic system pathways with both the embryonic and adult progenitor's neural processes. For example, in the embryonic chicken retina, ATP stimulates both neuronal and retinal progenitor cells proliferation (19). P2X receptors are also expressed in rat neurospheres cultured in suspension and are mainly linked to neurogenesis and induction of neuronal differentiation (20).

It has been reported that the downregulation of purinergic signalling during neurogenesis and early development prevents the uncontrolled growth of progenitor cells and establishes a suitable environment for neuronal differentiation mediated by ectonucleotidases (21). Also, purines expand the VZ neural stem and progenitor cells, and purine receptor activation is required for the proper cell density maintenance working as a critical regulatory checkpoint Still, in adult neurogenesis, in the neural progenitors from the adult dentate gyrus of the hippocampus, nucleotides activated the cells in acute slices, and ATP provoked an inward current, implying the expression of P2X Receptors (22). Likewise, P2X receptor-mediated inward currents were observed in *in vitro* undifferentiated adult hippocampal progenitors (23). These data indicate that the regulation of purinergic signalling can modulate the process of neuronal differentiation, and after that, it can be hypothesized that a rapid loss of purinergic signalling might accompany it.

2.2. P2X family with emphasis on the P2X7 receptor

The purinergic P2X receptors are trimeric ligand-operated channels. Each subunit comprises two transmembrane domains presenting an intracellular C and N-termini and a large ectodomain. Three ATP binding sites are formed between the interface of two subunits containing highly conserved residues. The C-terminus is formed by a cysteine-rich region, which serves as an anchor to the cell membrane, and a 200-residue extended region denominated as “cytoplasmic ballast” (24).

At physiological conditions, the extracellular ATP (eATP) is relatively low and elevated after a trauma or cell lysis, and therefore, eATP becomes a key messenger in the fanalogues, being sensitive from nanomolar ranges (P2X1 and P2X3 receptors) to lower micromolar concentrations (P2X2 and P2X4 receptors). Exceptionally, P2X7R is sensitive to much higher concentrations of ATP (EC50 of 100 μM). Whether it binds to the P2X7 receptor (P2X7R), it elicits a structural change to an open conformational state, allowing the flow of positive ions: sodium and calcium influx and potassium efflux (25). Especially the longer intracellular C-terminus domain among the P2X receptors is directly interlinked to the capability of P2X7R to produce large pores in the cell membrane, allowing the trafficking of larger hydrophilic molecules (26). Moreover, P2X7R has the highest sensitivity to the ATP analogue 2’,3’-O-(benzoyl-4-benzoyl)-ATP (BzATP), commonly employed as an agonist of the receptor (27). The activation of the P2X receptors generally opens a nonselective pore permeable cellular influx of Na+, K+ and Ca2+, leading to a rapid cellular depolarization and the activation of intracellular Ca2+-dependent signalling cascades. Each receptor subtype displays different desensitization dynamics, i.e. fast (P2X1R and P2X3R) or slow (P2X2R, P2X4R, and P2X7R) (28). Nevertheless, when P2X7R is persistently activated, it leads to apoptosis and cell death, consequently potentiating the P2X7R response by releasing more ATP into the extracellular space (29). This process entitles P2X7R as the gatekeeper of the immune responses in assembling the inflammasome (NLRP3/ASC/Procaspase-1). The cleavage and activation of Caspase-1 promote the process of pro-IL-1β to IL-1β for further secretion in the extracellular space. Finally, the whole cascade results in the induction of proliferation, recruitment and activation of macrophages, microglia, lymphocytes and the other inflammatory cytokines such as TNF-α or Interleukin 6 (IL-6) (30). For these reasons, P2X7R has been associated with inflammatory pathological

conditions in neuroinflammatory and neurodegenerative diseases contributing to disease progression (31,32). However, P2X7R also has several physiological functions in the CNS in cell proliferation and cell growth, neurotransmitter release or intercellular communication (33,34).

2.2.1. P2X expression and function in development

The expression profile of P2X has been followed during perinatal brain development in the rat. While some P2X receptors may at first not play a role in development (P2X1 and P2X6 receptors), other subtypes might participate in different developmental processes depending on their first appearance in the embryo (35) (Fig. 2). Recently, in a rat neuroblastoma cell line, P2X1 receptor-mediated calcium ion influx potentiated the nerve growth factor (NGF)-induced neurite outgrowth. The results obtained in this study imply a possible relationship between P2X1 and neuro-regeneration (36).

The receptors work tightly with the extracellular ATP concentration during development in a conserved manner among living organisms. Already in *Xenopus laevis*, P2X receptors are present in embryonic life. P2X2 is present from gastrulation contrary to P2X4, which is expressed in the egg in segmentation but decreases during gastrulation. However, it is again present during organogenesis until the adult. P2X5 becomes present from neurulation. In the case of P2X6, from egg segregation and gastrulation drops until the adult. Finally, P2X7 appears as the latest receptor in development, present in late organogenesis (37). In developing rat nervous system, P2X receptors appear in early embryonic days. Generally, P2X3 and P2X4 were expressed during mouse embryo neurulation, revealing a possible role in embryogenesis, while P2X1, P2X7, and P2X6 were found in organogenesis (38). Specifically, P2X3 appears from embryonic day (E) 11 hindbrain neural tube and the sensory ganglia. Both P2X2 and P2X3 coexist in the nucleus tractus solitarius, dorsal root ganglion, nodose ganglion, and the taste bud in the E16.5 embryo (39). Although P2X3 seems to appear early at E11 in rat brain development, its expression declines both in brain development in the following stages and in early postnatal brainstems.

On the other hand, P2X2 and P2X7 receptors were expressed from E14 onwards, while P2X4, P2X5 and P2X6 receptors were expressed only from P1 onwards (35). Contrary, P2X5 receptors appeared in the early development of the mouse nervous system

in the neural tube early in E8 in the cortical plate and ventral horn of the spinal cord, increasing its expression to E13, being the E9 the peak of expression, and then continuously decreasing until E17 when the formation of most organs takes place. The specific expression in new-born neurons associates the receptor with neurogenesis and motor neuron development (40). Functionally, P2X3 has been implicated in neurite outgrowth, while P2X7 receptors may be involved in programmed cell death during embryogenesis. Certainly, apoptosis occurs extensively during normal development as a vital process for developing healthy neural precursor cells, differentiated post-mitotic neurons and glial cell populations. Apart from P2X7, multiple receptors, such as P2X4, have been involved in this process (41,42). Due to their expression in developing rat brain, it can be hypothesized that P2X4, P2X5, and P2X6 receptors might be involved in postnatal neurogenesis (35).

P2X receptors might present different roles in development depending on the brain area or cells involved. For example, P2X2 mRNA and protein levels varied inversely with the change of ATP concentration in E18 mouse prefrontal tissue (43). On the other hand, during neuronal differentiation, the P2X2 receptors have been involved in neurogenesis, while P2X7 was involved in gliogenesis (44). P2X5 receptor expression increased specifically during phenotype transitions in embryonic stem cells (ESC) and neuronal progenitor cells (NPCs) (45). However, it has been pointed out that its expression is limited to specific new-born neurons during early development (40). Time, region, and cell type expression pattern of different P2 receptors show the involvement of ATP and its receptors in neuronal development and growth in organotypic slices co-cultures in the dopaminergic system, comprising the ventral tegmental area/substantia nigra (VTA/SN) complex and the prefrontal cortex (PFC) in 3–5 day-old rats (46). GABAergic neurons derived from mouse embryonic stem cells elevate intracellular calcium predominantly via the activation of P2X2 and P2X4 (47).

Expression of P2X2–7 receptor subunits were detected in differentiated neurospheres (48). Interestingly, a substantial increase in P2X2 and P2X6 receptors occurred upon enrichment of neurons following neurosphere differentiation in vitro (20). P2X2 receptors underwent a significant decrease in expression when NPCs differentiated into neurons. P2X4 receptor expression decreased when embryonic stem cells differentiated into NPCs, but it was recovered when NPCs differentiated into neurons

showing its importance in neuronal fate determination (45). Ongoing neuronal differentiation was accompanied by the down-regulation of P2X4 and P2X7 receptor expression in rat telencephalon neurospheres (49). In human embryonic stem cells, embryoid bodies, and human embryonic stem cell-derived oligodendrocyte progenitor cells, all subtypes of P2X are present except for P2X6 (50).

P2 receptors are frequently downregulated postnatal, suggesting a transient developmental role for the purinergic system. It has been reported that the downregulation of purinergic signalling during neurogenesis and early development prevents the uncontrolled growth of progenitor cells and establishes a suitable environment for neuronal differentiation mediated by ectonucleotidases (21). These data might indicate that the regulation of purinergic signalling can modulate neuronal differentiation. After that, it might be accompanied by a rapid loss of purinergic signalling (15).

DOI:10.14753/SE.2023.2882

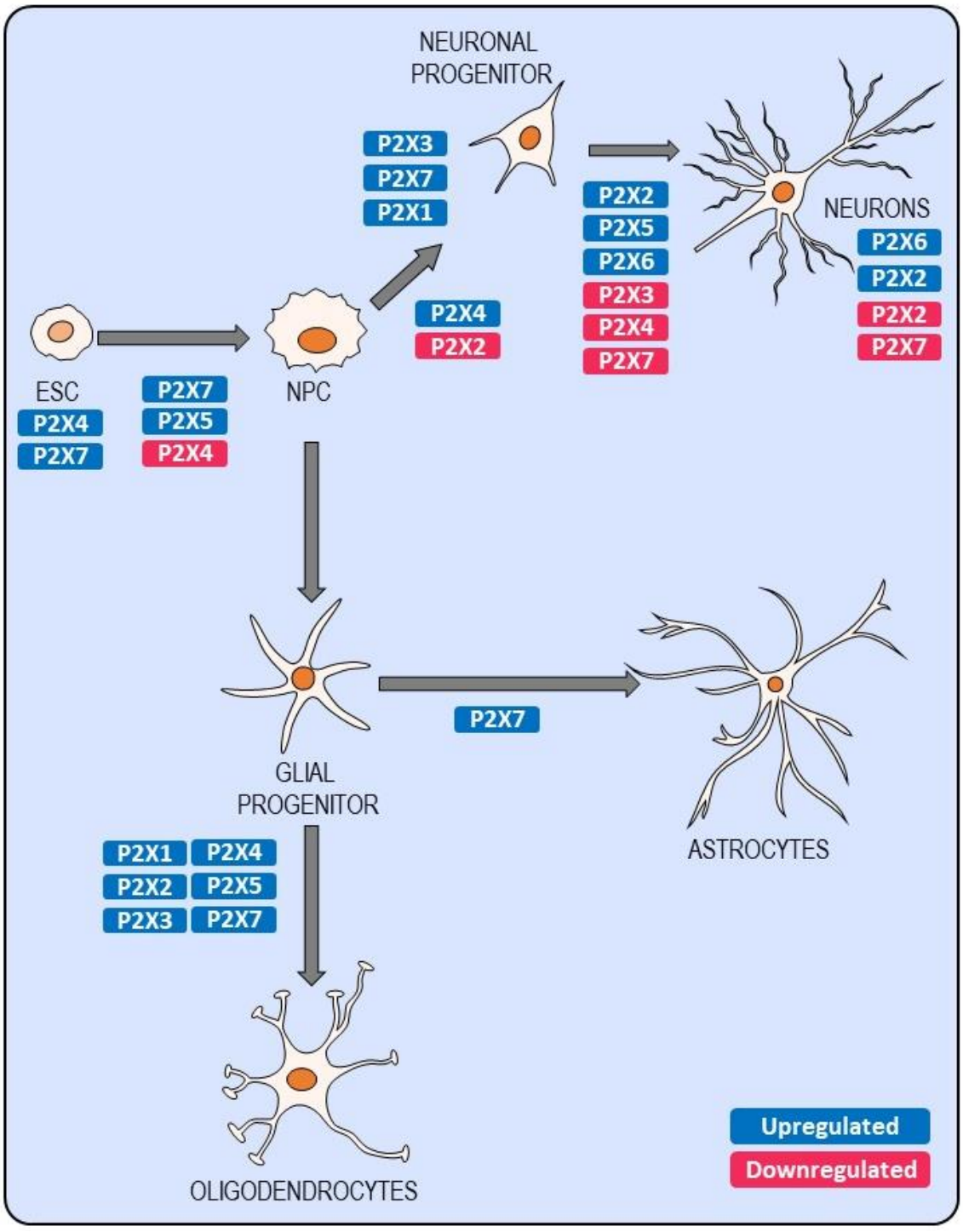

Figure 2. Figure legend in the next page.

Figure 2. Activity of P2 Receptors through neuronal and astroglia differentiation. In embryonic stem cells (ESC), P2X4 and P2X7R expression and activity are upregulated (45,51). Upon differentiation to neural progenitor cell (NPC), the presence of P2X7 (52) was observed while P2X4 needed to be suppressed. As well, P2X5 receptor expression increased specifically during phenotype transitions from ESC to NPC. NPC give rise to both neuronal and glial progenitors. P2X2 receptors underwent a significant decrease in expression when NPCs differentiated into neurons although was recovered when NPCs differentiated into neurons showing its importance in neuronal fate determination (45). P2X3 has been involved in neurite outgrowth (35) while P2X1 and P2X7 are associated with initial axon elongation and neuronal initial proliferation accompanied with a posterior downregulation (49). P2X5 expression is limited to specific new-born neurons during early development (40). In differentiated neuronal cells, a substantial increase in P2X2 and P2X6 receptors occurred upon enrichment of neurons following neurospheres differentiation *in vitro* (20). However, in another study where P2X2 receptors underwent a significant decrease in expression when NPCs differentiated into neurons (45). In P19 murine embryonal carcinoma cells both increase of P2X2 and P2X6 and downregulation of P2X3 were reported during neuronal differentiation (53). In rat-derived embryonic NPCs, decreased expression of P2X7 receptors was reported 14 days after induction of neural differentiation (49). In human embryonic stem cells, oligodendrocyte progenitor cells all subtypes of P2X are present except for P2X6 (50). P2X7 was involved in gliogenesis (44). Image modified from Figure 2 from the review of Mut-Arbona and Sperlágh, 2023 (54) .

2.2.2. P2X7 receptor in physiological conditions: new insights in brain development

P2X7R is sensitive to high concentrations of ATP, suggesting a specific role of the receptor under pathological conditions when cell loss or inflammation provides an ATP-rich extracellular milieu. Nevertheless, a wealth of data indicates now that P2X7R is also involved in the regulation of physiological functions such as neurotransmitter release (55), memory (56) and cognition (57), as well as the development of the nervous system. Moreover, P2X7R is found to be expressed early on rat embryonic days (35) and recently on human induced pluripotent stem cells (hiPSC) derived microglia-like cells and hiPSC-derived neuronal progenitors and hiPSC-derived matured neuronal cells (58). Extracellular levels of ATP are closely associated with the development of neuritic processes in cultured hippocampal neurons mediated by a tissue-nonspecific alkaline phosphatase, which at the same time is functionally interrelated with P2X7R. Both are significant for axonal development showing different regulatory effects *in vitro* (59). However, it is still being determined how their presence and absence impact the development and morphology of the primary pyramidal neurons from the hippocampus *in vitro.*

It has been hypothesised that P2X7R promotes initial proliferation as its expression is higher in rat telencephalon neurospheres in earlier *days in vitro* while getting down-regulated during the 14 days in culture during neuronal differentiation (49). During development, P2X7R seems involved in necrosis and apoptosis (60), whereas other *in vitro* studies demonstrated different regulatory effects in axonal growth and branching (61). Extracellular ATP provokes avian retinal cholinergic neurons mediated via P2X7R during normal development as control of proper density (62).

Therefore, P2X7R might be related to regulating the uncontrolled differentiation and migration of cells during neurogenesis. Finally, it is hypothesized whether the P2X7R role in maintaining both the neural stem and progenitor pools via inducing the proliferation or apoptosis might depend mainly on the microenvironment (63). In mouse embryonic stem cells, expression and activity of P2X7R are upregulated, maintaining proliferation *in vitro*, while P2X7 expression needs to be suppressed upon induction to neural differentiation (51). On the other hand, P2X7R is present in the embryonic rat brain (embryonic day 15.5) in SVZ and VZ neural progenitor cells, and its activation induced neuronal differentiation *in vitro* (64). Therefore, P2X7R might present different expression activity patterns to guide proliferation and differentiation processes into neuronal cells.

In adult neural progenitor cells, which are located in the neurogenic niches of the brain, P2X7R is still present (65). It has been recently reviewed that P2X7R plays at least three different roles in the adult hippocampus, influencing the hippocampal neurogenic niche, depending on the extracellular ATP concentration. At low extracellular ATP, P2X7R is believed to mediate calcium transduction signals regulating biological functions, such as proliferation and differentiation in adult neurogenic niches. Both in the presence of inflammation, then the high concentration of ATP, or, on the opposite physiological conditions, at a total absence of the nucleotide, P2X7R might elicit different responses, such as promoting cell death or phagocytosis, respectively (66).

2.2.3. Purinergic system in development: chapter overview

Overall, the expression and function of P2X receptors vary depending on the brain area and cells involved. Purinergic signalling is hypothesized to have multiple roles in neurogenesis and plastic remodelling during development, and its later downregulation

may prevent the uncontrolled growth of progenitor cells. Consequently, purinergic receptor subtypes transiently expressed during brain development suggest that nucleotides and nucleosides might affect stage-specific developmental processes. This chapter also highlights the importance of ATP in neuronal development and growth.

Extracellular ATP regulates several cellular functions and is expressed in the early embryonic stage during brain development, influencing cellular differentiation, proliferation, and apoptosis. P2X7R has the highest sensitivity to ATP, and upon binding, it elicits a structural change to an open conformational state, allowing the flow of positive ions. The longer intracellular C-terminus domain among the P2X receptors is directly linked to the capability of P2X7R to produce large pores in the cell membrane, allowing the trafficking of larger hydrophilic molecules. Further research is necessary to fully understand the function of purinergic signaling and especially the P2X7 receptor, in neurogenesis and plastic remodelling during development.

2.3. P2X7 in pathological conditions

There is an explosion of data indicating that both pharmacological or genetic blockage of the P2X7R alter animal model responsiveness in several CNS disorders, such as stroke, epilepsy, neuropathic pain, multiple sclerosis, amyotrophic lateral sclerosis, Alzheimer's disease, Parkinson's disease, Huntington's disease and psychiatric disorders (32).

2.3.1. Schizophrenia

2.3.1.1. Etiology, symptomatology and pathogenesis of schizophrenia

According to the 5th edition of the Diagnostic and Statistical Manual of Mental Disorders (DSM) (67), schizophrenia (SCZ) is a chronic mental disorder up to an estimated prevalence of 0.5% to 1%, with a young-adulthood onset characterized by delusions, hallucinations, and disorganized speech, which cause significant distress and functional impairment. These symptoms involve a range of cognitive, behavioural, and emotional dysfunctions although there is great variation across individuals. The array of psychotic symptoms, deprivation of emotional responses, and cognitive impairments associated with substantial comorbidities such as anxiety, substance abuse and depression, leading to a high incidence of suicide attempts, is why is considered one of the leading cause of disability (68), being the suicide deaths the largest contributor to the decreased life

expectancy in individuals with schizophrenia. The multiple symptoms range is grouped into positive, cognitive and negative symptoms.

Generally, the positive symptoms are related to persistent delusions, habitually paranoia, and hallucinations, where the individual might feel things that are not there, being the auditory the most frequent ones (69). Disorganized thoughts and behaviour such as disorientation, irreverent speech and abnormal motor behaviour are also positive symptoms of the disorder. Although the aetiology of schizophrenia is still unclear as it results from a complex combination of genetic and environmental factors, positive symptoms are often related to changes in the mesolimbic pathway, i.e. the neural projection from the ventral tegmental area (VTA) to the nucleus accumbens, the amygdala and hippocampus. The original hypothesis states that the chemical imbalance in dopamine in the brain regions typically leads to a lack of inhibition in the sensory processing areas in the brain and an abnormal cerebral excitation (70). Indeed, auditory hallucinations are related to a failure of excitation in the areas concerned with inner speech (71). Recently, it has been pointed out that the hypersensitivity of specific dopamine receptors (D2 receptors) might provoke an overreaction to the neurotransmitter. In the mesolimbic pathway, there is hyperstimulation in the VTA of the D2 receptor's activity, which increases dopamine, especially in the nucleus accumbens activity, related to motivation, emotions and reward then, across the neurons in the brain (72).

Despite the multiple clinical impairments in perception, cognitive deficits are now considered a core of the disease as they are durable over time and with high incidence among patients and emerge at the first stages of the disease (73). On the broad range of cognitive impairments, mild to moderate deficits are observed in attention and working memory, verbal memory and executive functioning. Although the severity of these cognitive dysfunctions is different among patients, cognitive impairments remain present in schizophrenia. Therefore, therapeutic interventions to improve cognition gained more importance over time. Cognitive symptoms comprehend impairment of working memory, the capability to retain and manipulate information in task execution and goal-directed behaviours. The elements involved are mainly a central executive component responsible for the attentional control system, which controls the manipulation of information of the other subcomponents, the storage buffers. The primary storage buffers for different information areas are, for example, the phonological loop, responsible for the verbal

working memory and the visuospatial sketchpad, for the visual-spatial working memory. Frontoparietal brain regions such as the dorsolateral prefrontal cortex (DLPFC), the anterior cingulate cortex (ACC), and the parietal cortex (PAR) constitute the working memory neuronal network. The DLPFC is implicated in executive control during demanding tasks such as decision-making. At the same time, PAR works as the area for sensory or perceptual processing, and ACC acts as the "attention controller", adjusting the information based on the task (74). In SCZ, the central executive component is the most affected, particularly the manipulation of transiently stored information, usually accompanied by disruptions in DLPFC. Overall, the disruption in this particular area implicates a cause-and-effect cascade that finally affects the neural networks involved in selective attention control. The patients fail to discern between significant and insignificant stimuli, reacting to all of them as if they were unexpected (75).

Finally, the negative symptoms cover the deficits in typical healthy functions, such as the social withdrawal or flattening of emotional responses, anhedonia (inability to experience pleasure), avolition (lack of motivation) and alogia (poor speech). The negative symptoms might be provoked by a hypo-stimulation in the mesocortical pathway (projections from VTA to the prefrontal cortex (PFC)), notably due to the reduction in D1 receptor activity (76,77).

2.3.1.2. Antipsychotics treatments: need for novel therapeutic targets

Dopamine is a primary neurotransmitter involved in the pathogenesis of schizophrenia. However, it is therapeutically complex to target as its activity is increased in the limbic system during positive symptoms, whereas it is decreased in the cortical areas during negative symptoms. Therefore, it might be a rational approach to inhibit the dopaminergic transmission in the mesolimbic pathway while increasing the transmission in the PFC.

Pharmacologically, antipsychotics predominately work as antagonists or partial agonists for the dopamine receptors. Traditionally, the first-generation or classic antipsychotics strongly block D2 receptors, combined with anticholinergic and antihistaminic actions, targeting mainly positive symptoms (delusions and hallucinations) (78). However, the systemic block of D2 receptors indiscriminately in the brain affects other dopaminergic pathways, such as the nigrostriatal pathway, which connects the substantia nigra pars compacta (SNc) with the dorsal striatum, i.e., the caudate nucleus

and putamen; and the tuberoinfundibular pathway where a population of dopamine neurons that project from infundibular nucleus in the region of the hypothalamus to the median eminence. The dopamine released at this site inhibits prolactin secretion from the anterior pituitary gland. Therefore, this leads to both an increased risk of extrapyramidal side-effects symptoms and an increase in prolactin levels by promoting its release in the pituitary gland. Moreover, it often worsens any negative, cognitive or affective symptoms (79).

Second-generation or atypical antipsychotics were developed, targeting the D2 receptors partially in combination with a potent serotonergic blockade (5HT2A) (80). The 5HT2A receptors belong to the serotonin receptor family and are G protein-coupled receptors that control dopamine release as their activation produces neuronal inhibition in the nigrostriatal pathway, reducing the extrapyramidal side effects. It was observed that pharmacological manipulation of 5HT receptor activity counteracted the increased dopamine function in the mesolimbic pathway (81). Special note to cariprazine, a novel, recently synthesised agent that has proved effective in treating positive and negative symptoms, being the only antipsychotic to date that tackles the latest symptoms. Cariprazine is a partial agonist for dopamine D3- and D2-receptor, with a tenfold higher affinity for D3 receptors than D2 receptors while conserving the 5-HT2A receptor antagonist action of second-generation antipsychotics (82,83). Still, regardless of the widespread use of the atypical antipsychotics, several concerns have been raised regarding their safety and tolerability (84). Furthermore, even after remission of the psychosis, negative and cognitive impairments in schizophrenia are often resistant to treatment, with current antipsychotics limiting their therapeutic efficacy. There is a pressing need to evaluate novel drugs that also consider and deal with cognitive deficits.

2.3.2. Modelling schizophrenia: Animal models

Understanding the neurobiological basis of the SCZ is crucial for the development of novel drugs with improved therapeutic efficacy, and therefore it is needed to develop reliable and predictive animal models. Applicable animal models must present a face (mimicking the core symptoms), construct (replicating the theoretical neurobiological pathology) and predictive (revealing novel information such as discovering a new therapeutic target) validity (85).

2.3.2.1. Phencyclidine (PCP) models

Glutamate is the main excitatory neurotransmitter broadly distributed in the CNS, activating both metabotropic and inotropic receptors. The second category includes the N-Methyl-D-aspartate (NMDA) and the non-NMDA receptors (kainate and alpha-amino-3-hydroxy-5-methyl-4-isoxazolepropionic acid (AMPA)). NMDA receptors are distributed in the brain and are critical postsynaptic mediators of synaptic plasticity. It has been established that the blockage of NMDA receptors is necessary and sufficient for mimicking schizophrenia-like symptoms. Shreds of evidence for glutamatergic dysfunction and dysregulation in schizophrenia for the glutamatergic systems were recently reviewed (86). From these discoveries, it is now widely accepted that both glutamate and dopamine systems are involved in the pathophysiology of schizophrenia. Thus, phencyclidine, a non-competitive NMDA receptor antagonist, is a dissociative hallucinogenic drug that triggers acute psychosis, hallucinations, delusions, and disorganized speech in humans. Accordingly, PCP has been used to induce mainly positive symptoms in mice models of schizophrenia (87,88). However, it has also been shown to exacerbate negative symptoms (89,90) and cognitive malfunction (91).

Reduced activity of NMDA receptors on cortical γ-amino- butyric acid (GABA) interneurons, particularly fast-spiking parvalbumin interneurons, might impact the neurocircuitry of the brain by impairing cognitive capabilities. The hypofunction of the NMDA receptors will lead to changes in cortical network oscillations. Certainly, pyramidal neurons are known as “projection neurons” that can integrate and receive synaptic inputs over long distances to connect different brain regions with their long axons. Therefore, dysregulation in their activity can profoundly affect brain-wide neural circuits. Consequently, the hypofunction of interneurons on the cortex might correlate with an increased tone of glutamatergic projection neurons and therefore overstimulates the non-NMDA receptors on pyramidal neurons, which might promote the overstimulation of GABAergic interneurons in the VTA. Again the disinhibition in the cortex affects the firing of cortical glutamatergic projection neurons, which ultimately causes the hyperactivation of the dopamine release in the mesolimbic pathway and hence the positive symptoms and the onset of psychosis (92,93). Supporting this idea, patients with SCZ showed reduced parvalbumin expression in the DLPFC and abnormal gamma-band oscillations (94), which are associated with working memory and attention. It also

has been reported that systemic administration of PCP to rodents induces schizophrenia-related behavioural alternations in association with initial hyperactivity of prefrontal pyramidal neurons, followed by a delayed depression of activity (95).

2.3.2.2. Maternal immune activation models: a neurodevelopmental approach

Schizophrenia is now regarded as a neurodevelopmental disorder (NDD) since an insult at the prenatal or early life stage might become a possible predisposing factor to the disease. Generally, these insults prime the nervous system to develop in malformed ways, resulting in abnormal brain function, including morphological alterations, aberrant neurotransmission, and connectivity (96,97). Therefore, any disruption during the brain developmental stages may result in a susceptibility to develop subsequent pathologies in response to a second insult later on in the individual that has empathized in the "Two-Hit" hypothesis of schizophrenia. Thus, a prenatal infection during the first or second trimester of the pregnancy, as it might be due to a maternal bacterial or viral infection (e.g., maternal influenza infection), has been pointed out as the principal risk factor causing an increased incidence of schizophrenia in the offspring post-puberty (98–100). The second event, for example, during adolescence or young adulthood, would exacerbate the symptoms and disrupt normal neurological function (e.g., an immune insult, affecting microglial activity, or a stressful life episode) (101).

Recently, it has been identified that the maternal immune-inflammatory response is responsible for neurodevelopmental disruptions through the imbalance of the main maternal interleukins, such as IL-6, TNFα, IL-1β, and IL-17A (102). Consequently, several models subjected to maternal immune activation (MIA) have been used to model schizophrenia to cover the understanding of the whole spectrum of the disease. These models commonly consist of injecting the pregnant rodents at different gestational days with an immunogen, such as polyinosinic:polycytidylic acid, usually abbreviated as poly(I:C) (PIC), influenza virus and/or the bacterial endotoxin lipopolysaccharide (LPS) the most frequent ones (reviewed in (99)).

PIC is a synthetic analogue of a viral double-stranded RNA that activates Toll-like receptors (TLR)-3 and triggers an anti-viral immune response in the absence of the pathogen (103). On the other hand, LPS, as a significant part of gram-negative bacteria's outer membrane, causes an anti-bacterial immune response by the ligation to TRL-4

receptors. The mechanism of action is different, and so are its effects on the offspring (Fig.3B).

When PIC binds to TRL-3, it initiates the TRIF-dependent pathway (Fig. 3A). Toll-IL-1 receptor-domain-containing adapter-inducing interferon-β (TRIF) is an adaptor protein that mediates a signal transduction cascade downstream to TRL-3 and TRL-4 with differential outcomes. When TRIF interacts with TRL-3 and TRL-4 directly, it activates TNF receptor-associated factor-3 (TRAF3) and TNF receptor-associated factor-6 (TRAF6). Tumour necrosis factor receptor-associated factor (TRAF) proteins are key signalling molecules that mediate by direct interactions with various receptors via the TRAF domain the function of various cellular signalling events, including immune response. TRAF3 recruits IKK-related kinases TANK-binding kinase 1 (TBK1), IKKi, and IKKγ for Interferon regulatory factor 3 (IRF3) translocation into the nucleus and further phosphorylation and dimer formation (104) (Fig. 3A).

On the other hand, LPS binds with LPS binding protein (LBP) and CD14 to form the LPS-LBP complex, which activates TLR-4. When TRL-4 is activated, it initiates the TRIF pathway and the MyD88-dependent pathway. MyD88 activates TRAF6. Additionally, TLR-4 recruits TRIF-related adaptor molecule (TRAM), leading to TRAF6 activation. TRAF6 transforms growth factor-β-activated kinase 1 (TAK1), activating IκB kinase (IKK) complex and MAPK family members. Subsequently, NF-κB dimerization and the activator protein 1 (AP-1) transcription factor complex formed. Finally, both of them translocate into the nucleus (105).

In any case, IRF3 and NF-κB, AP-1 translocation induce proinflammatory gene expression. While IRF-3 induces the gene expression of type 1 IFN genes, such as *Ifna* and *Ifnb*, NF-κB and AP-1 induce the expression of proinflammatory genes, such as *Il1b*, *Il6*, and *Tnfa*. Therefore, both immunostimulants induce a robust innate response that precedes cytokine production, inflammation, and, ultimately, fever, which causes a cascade reaction that will affect both the mother and the offspring. The main effects observed in the offspring's behaviour can be summarized as spatial and social deficits or anxiety-linked behaviours. Specifically, PIC and LPS induce other alterations, such as an immune-compromised system in the first case or metabolic dysregulations for LPS (106).

DOI:10.14753/SE.2023.2882

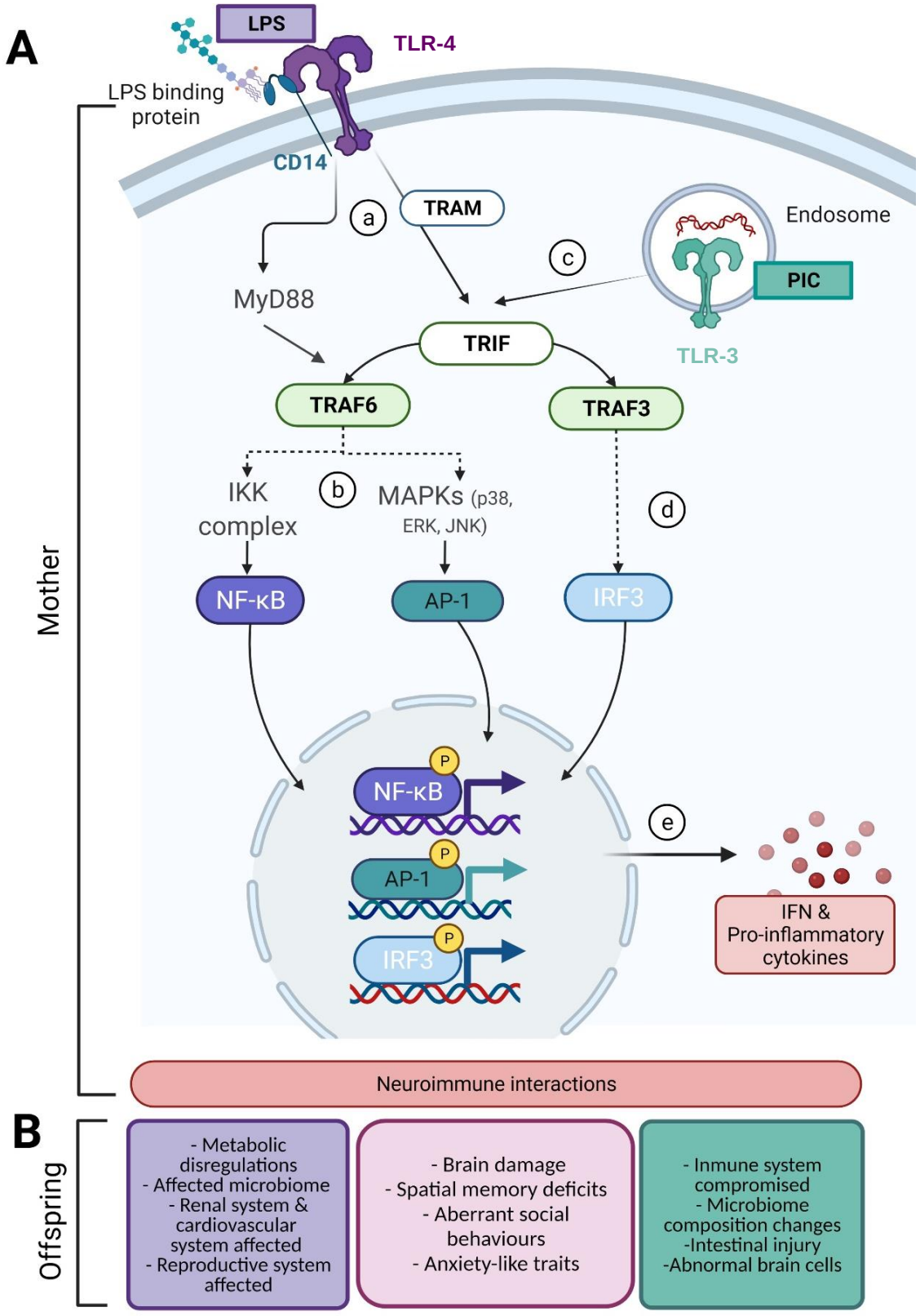

Figure 3. *I*nnate immune activation response by polyinosinic:polycytidylic acid (PIC) and lipopolysaccharide (LPS) through Toll-like receptor (TLR) signalling pathway. Figure modified from (106). Created with Biorender.

Additionally, depending on the time point of the injection, it will also affect several processes in brain development (Fig. 4). For example, critical malformations during cortical development have been observed in the offspring of pregnant dams subjected to MIA, showing repetitive behaviour and social deficits (107). Indeed, cortical patches in the primary somatosensory cortex have been pointed out as a prognostic of MIA-altered behaviours and the severity of the behavioural disruption in offspring from dams injected with PIC at E12.5 but not E15.5 nor E18.5 (108).

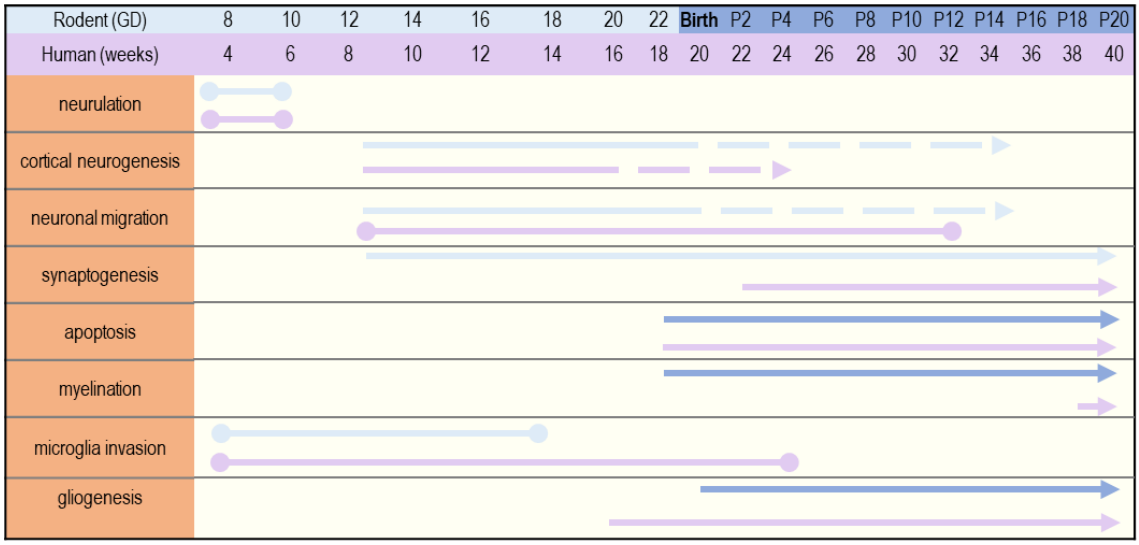

Figure 4. Main brain development processes and timings in rodent and human. A comparison for the key developmental processes for rodents and humans at their respective gestational days (GD), postnatal days (P) and weeks. Data from (109–111).

2.3.3. P2X7R and schizophrenia: a key modulatory element in neuroinflammation

Several epidemiological and genetic studies present the role of inflammation and immunity in schizophrenia associated with numerous infectious agents identified as risk factors and increased serum levels of pro-inflammatory cytokines and markers of endothelial cell activation (reviewed in (112,113)). Indeed, a recent meta-data analysis study showed that patients with schizophrenia present higher levels of pro-inflammatory in the cerebrospinal fluid (114). Overall, neuroinflammation has been acknowledged as one of the putative underlying causes and progression of SCZ. *Neuroinflammation* is defined as an inflammatory response mediated by several key pro-inflammatory cytokines (IL-1β, IL-6, and TNFα), chemokines (CCL2, CCL5, CXCL1), secondary messengers (NO and prostaglandins) and reactive oxygen species (ROS), produced

mainly by activated resident CNS cells including microglia and astrocytes (115). Although there are some examples of beneficial outcomes of neuroinflammation signalling in, for example, modulating learning and memory and brain plasticity (116,117), chronic or exacerbated inflammatory responses has associated with ageing (118) and several neuropsychiatric diseases and such as anxiety (119), depression (120) and mood disorders (121).

P2X7R as a significant driver of inflammation is a key mediator for ATP release in astrocytes and activated microglia. It might drive functional changes due to its role in multiple signal transduction pathways, consequently leading to depressive-like mood disorder reactions(122). Indeed, under psychological stress, glutamate is produced by neuronal cells, which mediates the astrocytes to release ATP into the extracellular space (123), leading to a P2X7R-mediated release of inflammatory cytokines and, ultimately to an immune response. A result of high extracellular ATP and sustained receptor activation will lead to pore formation (29). Consequently, an efflux of intracellular components will, in turn, maintain elevated ATP levels in the extracellular space, which will continuously activate P2X7R and will eventually lead to cell death. Therefore, both the regulatory role of P2X7R in the inflammatory response and as a promoter of an immune response pose the receptor as a potential therapeutical target in psychiatric diseases, including SCZ. Heretofore, P2rx7 genetic deficiency showed decreased in stress-induced behavioural parameters and amphetamine-induced hyperactivity in mice (124), suggesting the receptor's potential role as a modulator in mood disorders. Additionally, it is shown that P2X7R mediates the modulation of 5-HT release from the hippocampal terminals of the median raphe region, underlying a potential role for the receptor in the modulation of cognitive and affective functions and ultimately in psychiatric and mood disorders (125).

The P2RX7 gene is located on chromosome 12 at 12q24.31 and encodes for the P2X7 receptor. Variation in the P2RX7 gene has previously been associated with a higher risk for several psychiatric disorders (126). Linkage studies correlate P2RX7 variants with depressive symptoms in two independent patient samples (127). Recently, a linkage study investigated the effect of P2X7R SNP in interaction with childhood stress on the development and severity of depressive symptoms (128). The 12q24 region has also been implied in schizophrenia as it contains susceptibility genes for SCZ. One of them is DAO (D-amino oxidase), an enzyme that metabolises the NMDAR modulator D-serine, which

hyperactivity leads to impaired NMDAR functioning in the brain (129). Using summary statistics from recent meta-analysis genome-wide association studies (GWAS) in SCZ patients is identified significant enrichment of SCZ risk heritability in excitatory and inhibitory neurons. P2X7R has been indicated as a strong candidate gene, driving a schizophrenia association signal (130). In another genome-wide by environment interaction studies (GWEIS), a single nucleotide polymorphism (SNP) in the P2RX7 gene (rs7958311, Chr12:121167552) was strongly associated with a higher risk of experiencing psychotic symptoms in heavy cannabis users (131).

Regarding the functional studies, in an acute model of PCP, P2X7R genetic deletion or pharmacological blockade alleviates induced hyperlocomotion, stereotype behaviour, ataxia and social withdrawal effects of PCP at lower doses, being the first study linking the receptor with a PCP model of schizophrenia (132). The potential of P2X7R as a therapeutic target for cognitive symptoms in schizophrenia was also investigated in an infant sub-chronic PCP-induced model, where the P2X7R protein expression increased in the hippocampus after the treatment, yet its genetic deficiency pharmacological blockade attenuated schizophrenia-like spatial memory impairments in rodents (133). In a fluorometric Ca2+ assay in a stably hP2X7-expressing cell line (HEKhP2X7), another study showed that some psychoactive drugs such as prochlorperazine and trifluoperazine alter the on- and offset kinetics of the membrane potential of hP2X7, which alleviate schizophrenia-like behavioural alterations in both animals and patients, modulate human P2X7 (134).

Finally, whether inflammation during developmental stages influences the development of SCZ as a neurodevelopmental disease, it was shown how purinergic modulation of subplate neuron activity might lead to disruptions in cortical development (135) and cognitive disturbances in neurodevelopmental disorders such as autism spectrum disorder (ASD) or schizophrenia upon a postnatal challenge. Horváth and colleagues (136) demonstrated the role of P2X7R in neurodevelopmental disease for the first time in an MIA-induced autism-like behavioural model where endogenous receptor activation is needed to develop an autistic phenotype. Recently, it has been proved that ATP-activation of P2X7R results in downstream signalling pathways mediating the development of sociability deficits and repetitive behaviours in an MIA neurodevelopmental model of ASD (137).

Overall, human and rodent studies present shreds of evidence that P2X7R has a potential role as a mediator in early immune responses and the development, severity and, consequently, possible treatment responsiveness of SCZ. Hence, further animal studies are needed to elucidate the pathology and, importantly, the physiological role of P2X7R in brain development.

2.3.4. Schizophrenia and purinergic signalling: chapter overview

This chapter discusses schizophrenia, a chronic mental disorder characterized by psychotic symptoms, deprivation of emotional responses, and cognitive impairments associated with substantial comorbidities such as anxiety, substance abuse and depression. Pharmacologically, antipsychotics predominately work as antagonists or partial agonists for dopamine receptors. However, their systemic block of D2 receptors indiscriminately in the brain affects other dopaminergic pathways, leading to both an increased risk of extrapyramidal side-effects symptoms and an increase in prolactin levels by promoting its release in the pituitary gland. Therefore, there is a need for novel therapeutic targets.

This passage discusses two main topics: maternal immune activation (MIA) models and the role of P2X7R in schizophrenia. MIA models involve injecting pregnant rodents with an immunogen to simulate a maternal immune-inflammatory response, leading to neurodevelopmental disruptions in the offspring, which can manifest as spatial and social deficits or anxiety-linked behaviours. The immunogens commonly used in MIA models include polyinosinic:polycytidylic acid (PIC), influenza virus, and lipopolysaccharide (LPS). PIC activates Toll-like receptor-3 (TLR-3) and triggers an anti-viral immune response, while LPS activates TLR-4 and causes an anti-bacterial immune response. The TRIF-dependent pathway is activated by PIC, which leads to the induction of proinflammatory gene expression. Both PIC and LPS induce a robust innate reaction that precedes cytokine production, inflammation, and fever. The passage also discusses the role of P2X7R in schizophrenia, a critical modulatory element in neuroinflammation. However, further research is necessary to fully understand the mechanism of action of the endogenous activation of the P2X7 receptor in the development of positive, negative and cognitive symptoms in an MIA model of schizophrenia.

DOI:10.14753/SE.2023.2882

3. Objectives

Two main objectives were established to study the role of P2X7R in the development of individual neurons and neurodevelopmental psychiatric disorders. Consequently, it was explored how its pathological activation is associated with schizophrenia-like behaviours in rodent animal models. Therefore, P2X7R was studied in detail in physiological and pathological conditions during development to young adulthood. The specific objectives were:

1. Establish the cell-specific expression and function of P2X7R in physiological conditions during development. Then:
    a. To investigate the role of P2X7R in dendritic outgrowth during neuronal development, proliferation, and maturation in the hippocampus.
    b. To assess the cognitive performance of P2X7R-deficient mice at different stages of development and youth to determine the role of the receptor on cognitive performance.
2. Establish the cell-specific expression and function of P2X7R in pathological conditions in schizophrenia mouse models.
    a. To better understand the over-activation of P2X7R in a mouse PCP model of schizophrenia.
    b. To determine the effects of endogenous activation of P2X7R on dendritic outgrowth *in vitro* and its behavioural outcome in a neurodevelopmental model of schizophrenia.

4. Methods

4.1. Animal studies with mice

The studies were conducted by the procedures and principles outlined in the NIH Guide for the Care and Use of Laboratory Animals, approved by the local Animal Welfare Care Committee of the Institute of Experimental Medicine and by the respective authorities (Budapest, Hungary, ref. No. PEI/001/778–6/2015, PE/EA/297-1/2021) by the European Communities Council Directive of 24 November 1986 (86/609/EEC). All mice were backcrossed onto the C57BL/6N background at least 8 to 10 times, and experiments were performed with littermates as controls. The animals were housed on a 12-hour light-dark cycle under specific pathogen-free conditions and had access to food and water *ad libitum*. Homozygous *P2rx7*+/+ mice were bred on a background of C57Bl/6J. Christopher Gabel from Pfizer, Inc. (Groton, CT, USA) kindly supplied the original breeding pairs of *P2rx7*−/− mice. The *P2rx7*−/− mice contained the DNA construct P2X7-F1 (5′-CGGCGTGCGTTTTGACATCCT-3′) and P2X7-R2 (5′-AGGGCCCTGCGGTTCTC-3′), previously shown to invalidate the P2X7 receptor (132). Embryonic day (E)17.5-E18.5 *P2rx7*+/+ (wild-type; WT) and P2X7 receptor *P2rx7*−/− (knockout; KO) mouse embryos were used for primary cultures. Postnatal (P)60-P90 WT and KO mice were used for behavioural tests. The overexpressing P2X7-EGFP C57Bl/6J mouse (line 17 in C57Bl6N) was obtained from Annette Nicke (138) and bred heterozygously. Mice were raised in grouped cages until P60. Male animals were used for the acute PCP model. In behavioural experiments, all the experiments were run during the light phase (within 10:00–17:00) in dim light. All mice were handled on alternate days during the week preceding the first behavioural testing. To avoid olfactory cues, all the arenas were wiped with 20% ethanol between trials.

4.2. Experimental time-flow for experiments *in vitro*

To investigate the impact of P2X7R deficiency on neuronal growth, we bred P2rx7+/+ (WT) mice and P2rx7-/- mice (knockout; KO), respectively. Mice embryos from embryonic day 17.5 were chosen as cortical neurogenesis is actively occurring (Fig. 4), and neurons in the cerebral cortex are being developed. This will allow the study of the role of the receptor in higher cognitive processes. Control and KO primary hippocampal neurons were maintained until day *in vitro* (DIV) 10 when the dendrites were fully

developed. In order to retrain the study on the role of P2X7R on neuronal growth, the indirect effect of astroglia on neurons was blocked by adding cytosine-arabinofuranoside (CAR, 10µM), an anti-mitogen agent at DIV 3. To study P2X7R expression in our model, RNA was collected each day *in vitro* for these ten days and the transcript level of the *P2rx7* gene was measured by RT-qPCR and validated with Western Blot. Consequently, to study neuronal activity, calcium imaging was performed in KO and WT primary hippocampal neurons to validate the maximum expression level in both RT-qPCR and Western Blot.

Then, transfecting cells with a plasmid encoding GFP under a synapsin promoter at DIV9 allowed the study of the morphology of individual neurons and dendrites in a given primary hippocampal neuron as it fulfils the whole neuron with green fluorescence. As a control for GFP transfection, we stained transfected primary neurons for MAP2, a neuron-specific cytoskeletal protein marker that specifically stains dendrites. Together, with the lower effect of the transfection compared to the whole immunostaining of MAP2, we can trace several isolated neurons to visualise their whole structure. Then, the morphology of these neurons was compared with that of primary neurons with either genetic deficiency or pharmacological blockade of P2X7R by Sholl analysis (Fig. 5).

Finally, when needed, high-performance liquid chromatography (HPLC) was used to quantify the release of adenine nucleotides (ATP, ADP, AMP) and adenosine (Ado) from the culture medium.

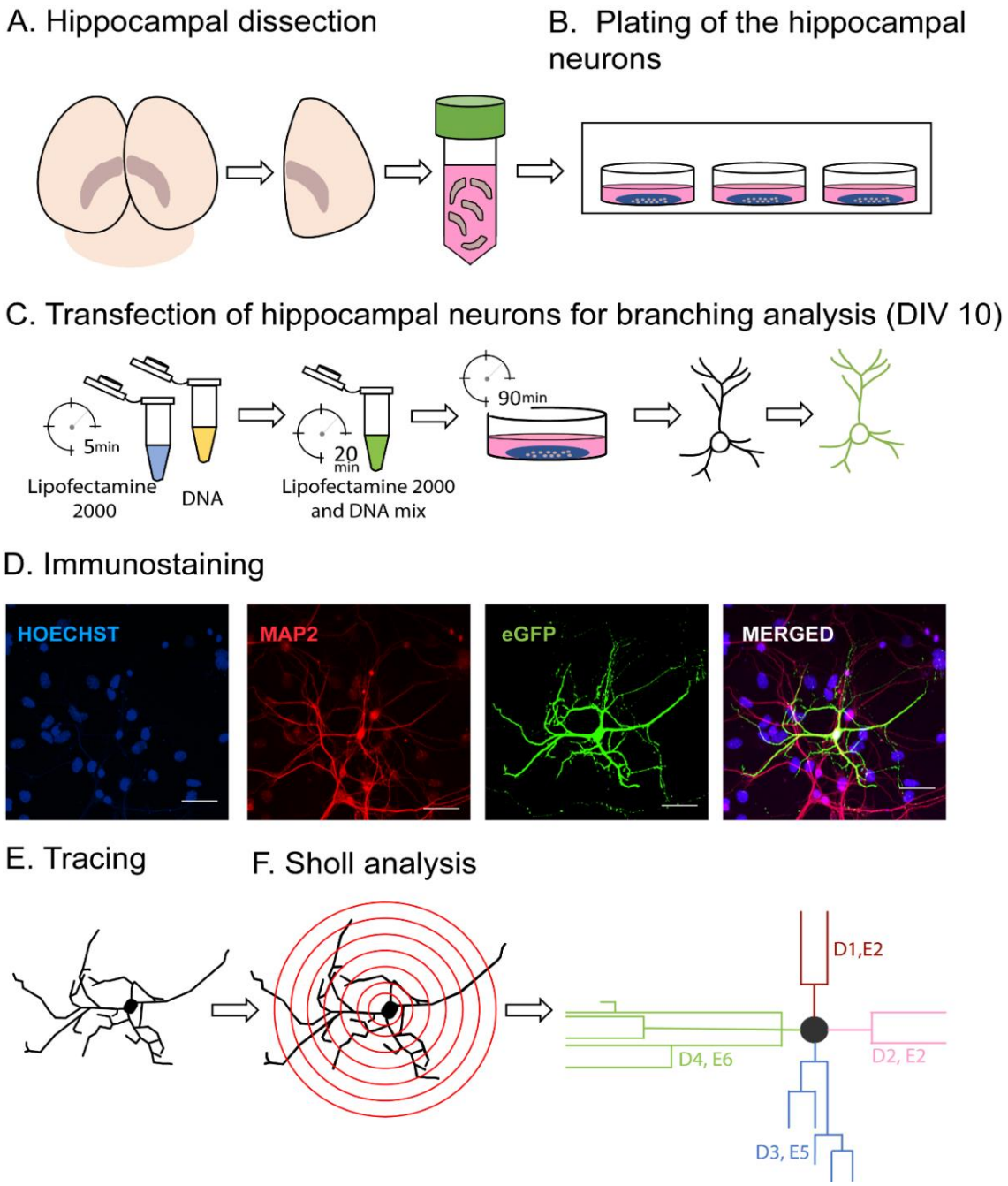

Figure 5. Scheme of the primary hippocampal neurons preparation and further morphological studies with Sholl analysis. Figure 1 from the protocol chapter book of Mut-Arbona and Sperlágh (2022) (139).

4.2.1. Primary cultures from E17.5–E18.5 control and P2X7 receptor KO mice embryos

Primary hippocampal cells were obtained as previously described (139). The culture dishes are coated with Poly-L-Lysine (100 ug/mL)/Laminine (1-2mg/cm2) overnight at 37°C at 5% CO2 in the air for a proper attachment and adhesion of the primary hippocampal cells.

For the dissection of the hippocampus, pregnant mice were euthanized by spinal dislocation per group. The E17.5-18.5 embryos hippocampi from 8-10 embryos/mum were dissected in a cold MEM medium in a petri dish under sterile conditions using a stereomicroscope within a cell culture hood. The craniums were carefully opened, and the meninges were removed. The hippocampus from the multiple embryos of the same genotype and treatment were pooled together for each experiment regardless of the gender. For all the conditions we replicated the hippocampal culture four times. Once the hippocampi were collected, chemical and mechanical dissociations were performed for optimal tissue dissociation. Trypsin-EDTA (0.5 mg/mL) was used in a solution with DNAse (0.05%) to protect the cells from chemical disaggregation. After 15 min at 37°C, the digestion was stopped with preheated FCS, and the mix was centrifuged. The supernatant was carefully removed while the healthy tissue remained on the pellet. Subsequently, the hippocampi were manually disaggregated by gently pipetting up with a 20-200 μL pipette. After the disaggregation, cells were filtered through a sterile mesh. Trypan blue solution was used at 1:1 dilution to identify the surviving cells, and cells were counted in a Neubauer chamber and plated at a density of 150000 cells/well at 1000 μL total volume. Neurons, once plated, were placed in the incubator at 37°C with 5% CO2. The day of plating was considered a day in vitro 1 (DIV1). When the confluence of the glial cells reached 90%, cytosine-arabinofuranoside (CAR, 10 μM; Sigma, #C6645) was added to the cultures to stop further proliferation and maintain a neuron-enriched culture with less than 10% of glial cells (140). The medium should be replaced for proper maintenance of the neuronal cultures. As neurons, especially when the astroglia is reduced, detach easily to the coverslip, the medium should be replaced carefully by replacing half the media volume from cells with a fresh medium. As so, On DIV6, one-third of the culture medium was replaced with MEM containing the abovementioned supplements. The cells were conserved in a cell culture incubator (37 °C in 5% CO2, 95% air atmosphere) until they were used for the experiments.

4.2.2. RNA isolation

Total RNA isolation was performed to measure the expression of P2X7R in the primary cultures by using an RNAse® Plus Mini Kit (Qiagen 74134, lot No. 169034695) according to the manufacturer's protocol. Briefly, cells were harvested and homogenized

with the lysis buffer, and the lysate was transferred to a gDNA eliminator spin column and centrifuged for 30 seconds at 14000rpm. 350uL of 70% ethanol was added and well mixed for further centrifugation for 15 seconds at 10000rpm. 7000uL of the mix was placed in an RNeasy spin column and centrifuged for 15 seconds at 100000rpm. 700uL of the washing buffer was added to the RNeasy spin column and centrifuged for 15 seconds at 100000rpm. Then, 500uL of the washing buffer was added for a second wash to the RNeasy spin column and centrifuged for 15 seconds at 100000rpm. Finally, 30uL of RNase-free water was added directly to the column and centrifuged for one minute at 14000rpm to elute the RNA, which was stored at -20°C. RNA integrity was checked by electrophoretic separation on 1% agarose gel. RNA concentrations were measured using Nanodrop 2000c Spectrophotometer (Thermo Fisher Scientific, Wilmington, DE, USA).

4.2.3 Real-time qPCR for P2X7R expression in primary cultures

Reverse transcription (RT) from 100 ng of total RNA into deoxyribonucleic acid (cDNA) was performed using the High-Capacity cDNA Archive Kit (Applied Biosystem, Foster City, CA, USA) according to the manufacturer's protocol. A total of 32 µl reagent mix was prepared and kept on ice. The content of the mixes is described in Table 1 while the conditions of thermal cycling are specified in Table 2.

Table 1. Reaction mix for RNA to cDNA transcription

Reagents	Volume (µl)
RNA sample (1µg/µl)	16 µl
10x Reverse Transcription (RT) Buffer	4 µl
deoxyribonucleotide triphosphate mix	1.6 µl
10x RT Random Primer	4 µl
MultiScribe Reverse Transcriptase	2 µl
Nuclease-free water	4.4 µl

Table 2. The protocol applied for cDNA synthesis

Step	Annealing	cDNA synthesis	Heat inactivation	Storage
Temperature	25°C	37°C	85°C	4°C
Time	10 min	120 min	2 min	∞

DOI:10.14753/SE.2023.2882

Based on the previously published primer sequences (141), the mRNA levels of P2X7R extracellular and intracellular sequences were measured by real-time quantitative polymerase chain reaction (RT-qPCR) (primer listed in Table 3). The housekeeping gene, GAPDH, was used for normalization to account for intra-well variability.

Table 3. Primers for the targeted genes

Target Gene	Forward Primer	Reverse Primer
P2X7R extracellular region	5′-GCACGAATTATGGCACCGTC-3′	5’-ACACCTGCCAGTCTGGATTCCT-3′
P2X7R intracellular region	5’-AGGATCCGGAAGGAGTT-3’	5′-TAGGGATACTTGAAGCCACT-3′
GAPDH	5′-TCACCACCATGGAGAGGGC-3′	5′-GGCATGGACTGTGGTCATGA-3′

The RT-qPCR reactions were performed using the SensiFast SYBR Green No-Rox kit (Bioline Reagents Limited, London, UK) performed in 96-well PCR plates according to the manufacturer’s protocol in 10 µl total volume (total of 2 µl/sample cDNA was amplified). PCR reactions were incubated at 95°C for 20 seconds (s) followed by 40 PCR cycles (95°C for 15s and 60°C for 15s) in a Quant Studio Real-Time PCR System (Applied Biosystems) (Table 4).

Table 4. The protocol applied for RT-qPCR

Step	Temperature	Time (s)	Cycles
Initial denaturation	95°C	20	Stage 1. Pre-step enzyme activates cDNA dissociate
Denaturation	95°C	1	Stage 2. Amplification
Annealing, extension	60°C	20	
Denaturation	95°C	15	Stage 3. Melt curve
Melt curve analysis	60°C→95°C, step: 0.5°C	15	

The RT-qPCR products of the P2X7 receptor were visualized by electrophoretic separation on 1% agarose gel (data not shown). Samples were measured in duplicates and mRNA expression levels were represented as $2^{-\Delta\Delta CT}$. The average cycle threshold (Ct) was obtained from quintuplets of each sample from 3 independent cultures. ΔCt means were normalized to parallel amplification of GAPDH as endogenous control. Fold changes for each sequence are represented and compared to the baseline (DIV1) after normalizing with GAPDH. Data were analysed with Applied biosystems relative Quantification (RC) powered by Thermofisher Cloud.

4.2.4 Western blotting

WT and P2X7R KO cells were lysed in radioimmunoprecipitation assay (RIPA) buffer containing 150 mM NaCl, 50 mM Tris-HCl (pH 7.4), 5 mM EDTA, 0.1% (w/v) SDS, 0.5% sodium deoxycholate and 1% Triton X-100 containing protease inhibitors (10 mg/ml leupeptin, pepstatin A, 4-(2-aminoethyl) benzenesulfonyl-fluoride and aprotinin) on the indicated days (DIV1 – DIV7). Total cell lysates were separated by sodium dodecyl sulfate–polyacrylamide gel electrophoresis. The protein was then transferred onto nitrocellulose membranes, nonspecific binding was blocked by incubation in 5% non-fat dry milk for 1 hour at room temperature and the membranes were incubated overnight with anti-P2X7R (Alomone Labs Alomone, RRID:AB_2040068) and anti-β-actin (Cell Signaling Technology Inc., RRID:AB_330288) primary antibodies at 1:1000. The membranes were incubated with horseradish peroxidase-conjugated secondary antibodies (Cell Signaling Technology Inc., Danvers, MA, USA) for 1 hour at room temperature and were developed using an ECL detection system (Thermo Scientific Pierce, Life Technologies). The protein band densities were analyzed by ImageJ software (NIH). The P2X7R protein band density was normalized to the density of the band representing total protein (the β-actin band).

4.2.5 Calcium imaging

Cells were plated at a density of 300000 cells/well. To study neuronal activity, neurons from DIV 4 were incubated with medium containing pluronic acid (F-127 P3000MP, 1 μM, previously warmed to 36°C) diluted 1:1 with Oregon Green 488 BAPTA-1 (OGB-488, Thermo Fisher, O6807, 5 μM) on DIV4. Thirty minutes later, the chamber was

loaded with crystals coated with the cells, and the dye-containing medium was replaced with fresh medium previously warmed to 36°C. Twenty minutes later, the spontaneous activity of the cells was recorded for 10 min with the N-STORM Super-Resolution System. The following parameters were used: channel intensity of 38% intensity, 30 ms/Hz, 12-bit (no binning), no delay between frames, 20x magnification. Later, the frames were analyzed with a NIS-Element AR microscope, and the fluorescence intensity change (ΔF/F) was calculated for 2 min after acute application of the agonist 2′(3′)-O-(4-benzoyl benzoyl) adenosine 5′-triphosphate triethylammonium salt (BzATP, Sigma–Aldrich, Missouri, US 1 mM). As a control, a calcium ionophore (Sigma, C7522-5MG, 1 mM) was acutely applied, and the fluorescence intensity change (ΔF/F) was calculated for each cell.

4.2.6 Quantification of nucleotides and nucleosides

The HPLC method was used to quantify the release of adenine nucleotides (ATP, ADP, AMP) and adenosine (Ado) from the culture medium. For this, 400 µl of medium from each well was transferred to a cold Eppendorf tube containing 10 µM theophylline (as an internal standard) solution in 0.1 M perchloric acid (total volume of 50 µl). Then, the sample was centrifuged (at 3510 g for 10 min at 0-4^{o}C) and the supernatant was collected and stored at -20^{o}C for further analysis. For the quantifying nucleotide content in the samples, the column-switching technique was coupled with Online Solid Phase Extraction. The separation step was performed by Shimadzu LC-20 AD Analytical System using UV (Agilent 1100 VW set at 253 nm) detection. The phenyl-hexyl packed (7.5 x 2.1 mm) column was used for online sample enrichment and, then, the separation was completed by coupling the analytical C-18 (150 × 2.1 mm) column. Following the Baranyi et al. protocol (142), the flow rate of the mobile phases was 350 or 450 µl/min , respectively, in a step gradient application [phase “A”: 10 mM potassium phosphate buffer with 0.25 mM EDTA; phase “B”: additional components such as 0.45 mM octane sulphonyl acid sodium salt, 8% acetonitrile (v/v), 2% methanol (v/v), pH 5.55]. The sample enrichment flow rate of buffer “A” was 300 µl/min during 4 min and the total runtime was 55 min. Concentrations were calculated by a two-point calibration curve internal standard method and data are expressed as pmol per ml:

$$\frac{\text{Area of nucleotide component} \times \text{f} \times \text{Sample Volume}}{\text{Injection Volumen} \times \text{Response factor of 1 pmol nucleotide standard}}$$

Being f the factor of Internal Standard (IS area in calibration/IS area in actual].

4.2.7. eGFP transfection

The plasmid pAVV-Syn-GFP (Addgene 58867, RRID:Addgene_58867), in which GFP is expressed under the control of the Synapsin promoter, was transfected into cells at DIV9 to allow clear visualization of the morphology of individual neurons following the manufacturer's indications (139). Lipofectamine 2000 reagent was used in cultured cells in a 24-well plate at a final volume of 2 µL / 490 µL Neurobasal medium/well. For this, 400 µL Neurobasal medium was replaced and kept at 37°C. In a new Eppendorf, the lipofectamine mix was prepared for each transfected well, where 2 µL of Lipofectamine 2000 was added to 45 µL of Neurobasal medium and incubate at RT for 5 minutes. In another Eppendorf, 0.8 µg of the plasmid pAVV-Syn-GFP was added to 45µL of Neurobasal medium and incubated for 5 minutes at RT. Then, the DNA mix was dropped gently into the lipofectamine solution and incubated at RT for 20 minutes. This mix was added to the well(s) selected for transfection gently, not to disturb the lipid-DNA complexes and the cells. The 24-well plate was placed in a 37 °C, 5% CO_2 incubator for 1h. Then, the transfection medium was replaced with the medium previously stored and retired to the incubator overnight at 37°C, with 5% CO_2. At DIV10, the transfection was checked under a fluorescent microscope and proceed to fix the cells with pre-warmed PFA solution for 14 minutes. Cells were washed gently three times with 1mL PBS and kept at 4°C for further experiments. For the study of the morphological differences in dendritic outgrowth, the strengthening of the transfection was performed with immunocytochemistry.

4.2.8. Immunocytochemistry and image acquisition

After PFA 4% fixation, the cells were permeabilized in phosphate-buffered saline (PBS)/0.2% Triton X-100 for 12 minutes at RT and washed with PBS three times. The blocking solution composed of 3% bovine serum albumin (BSA) in PBS was added to the cell for 30 min in RT. Then, the primary antibodies listed in Table 5 were added

accordingly, and incubated overnight at 4ºC, except for P2X7R, which was incubated for two nights.

Table 5. List of primary antibodies

Primary antibody	Concentration	Host	Reference
α-MAP2	1:1000	Mice	Sigma. Cat. #M9942; RRID:AB_477256
α-GFAP	1:1000	Guinea pig	SYSY. Cat. #173004; RRID:AB_10641162
α-P2X7R	1:100	Rabbit	Alomone. Cat. # APR-004; RRID:AB_2040068
α-GFP	1:1000	Chicken	Aves Lab. Cat. # GFP-1020; RRID:AB_10000240

Next, the primary antibody was washed out three times carefully with PBS. The correspondent fluorophore-conjugated secondary antibodies listed in Table 6 were added for 1,5 hours at RT. Nuclei were counterstained with a 1nM Hoechst solution (Invitrogen) before mounting. For mounting, the coverslips with the cells faced down on a slide a placed using a drop of ‘antifade’ mounting solution and let dry overnight in the dark. From the next day on, images were taken with Nikon C2+ confocal microscope setup connected to a Nikon Ni-E fully automatized microscope using the 20x objective. From 11 to 20 images were acquired for a z-stacks scan of 0.5–1 μm. For morphological analysis, images were reconstructed in z-stack to average intensity for Sholl analysis. Image acquisition was performed using NIS Elements 4.3 software (RRID:SCR_014329).

Table 6. List of secondary antibodies

Secondary antibody	Concentration	Reference
Goat anti-Mouse IgG (H+L) Highly Cross-Adsorbed Secondary Antibody, Alexa Fluor Plus 594	1:500	Invitrogen. Cat. # A32742; RRID:AB_2762825
Goat anti-Guinea Pig IgG (H+L) Highly Cross-Adsorbed Secondary Antibody, Alexa Fluor 647	1:500	Invitrogen. Cat. # A-21450 RRID:AB_2735091
Goat anti-Rabbit IgG (H+L) Highly Cross-Adsorbed Secondary Antibody, Alexa Fluor Plus 594	1:500	Invitrogen. Cat. # A32740; RRID:AB_2762824
Goat anti-Chicken IgY (H+L) Secondary Antibody, Alexa Fluor 488	1:500	Invitrogen. Cat.# A11039; RRID:AB_2534096

4.2.9. Sholl analysis

Using the Neurolucida tracing Software (MBF Bioscience), an individual transfected neuron was traced. For Sholl analysis, the trace was exported to Neurolucida explorer Software (MBF Bioscience). The software determines the number of intersections per radius for each trace starting at a radius of 5 μm from the centre of the neuronal soma and fixing the concentric shell distance between the circles at 2μm per shell. Moreover, with *Branched Structure Analysis* and *Neuron Summary* functions, further analysis of the branching can be studied, which includes several morphological analyses as the area of the cell body, number of dendrites, mean length and the number of endings and/or spines if needed. The sample size for every comparison is detailed in Table 7, corresponding to a blind selection of individual transfected neurons from four independent cultures per condition.

4.3. Hippocampal slice model

4.3.1. Immunostaining of Biocytin-Filled Cells

Hippocampal slices from CA1 and CA3 were prepared from 20- to 29-day-old WT and *P2rx7-/-* mice on the C57Bl/6J background previously filled with biocytin as described before (143) were used for morphological analysis for the understanding of the role of P2X7R in neuronal outgrowth in acute slices.

The mice were anesthetized with Forane (4 g/μL) and decapitated. The brains were quickly removed and cut into 300 μm transverse slices using a vibratome (Leica VT1200, Germany) in ice-cold cutting solution [in mM: 85 NaCl, 2.5 KCl, 0.5 CaCl, 1.25 NaH_2PO_4, 24 $NaHCO_3$, 25 glucose and 75 sucrose (pH 7.4, 290-300 mOsm)] bubbled with 95% O_2 and 5% CO_2. After 30 min of incubation at 34°C, the slices were stored at room temperature in artificial cerebrospinal fluid (ACSF) [in mM: 126 NaCl, 2.5 KCl, 2 $CaCl_2$, 2 $MgCl_2$, 1.25 NaH_2PO_4, 26 $NaHCO_3$ and 10 glucose (pH 7.4, 300-310 mOsm)] bubbled with 95% O_2 and 5% CO_2. Pyramidal cells were visualized using differential interference contrast (DIC) microscopy with an Olympus BX50WI microscope and a 40× water immersion objective (LUMPLFLN 40×WI, 0.8 NA; Olympus, Hamburg, Germany). Cells were patched using borosilicate glass pipettes with a resistance of 4-7 MΩ. Biocytin (Sigma Aldrich, B4261) was included at 8 mg/ml with the internal patch-solution after the electrophysiology experiments detailed in Mut-Arbona et al., (2023) (143). After 15 min, the recording pipette was quickly retracted from the cell to help maintain cell integrity for histology. After patch-pipette removal, cells were left for 10 min to allow excess extracellular biocytin to wash from the slice. Then, the slices were fixed overnight with 4% paraformaldehyde in phosphate buffer (PB, 100 mM, pH 7.4) at 4°C.

Slices were washed with 0.1 M PBS. Then, permeabilization of the cells was achieved with Tris-buffered saline (TBS). For the blocking solution, 5% normal goat serum (NGS; Vector Laboratories Inc., Burlingame, CA, USA) containing 0.03% Triton X-100 was added for 30 min. Then, slices were incubated with Alexa Fluor 564-conjugated streptavidin (S11227, Invitrogen) within 0.03% triton X-100 at a diluted ratio of 1: 500 (Life Technologies) for 4 hours at room temperature (RT). Slices were mounted onto gelatin-coated glass slides using Fluoroshield mounting medium (F6182-20ML, Sigma).

Images were taken with Nikon C2+ confocal microscope setup with a Nikon Ni-E fully automatized microscope using the 20x objective. From 11 to 20 images were acquired for a z-stacks scan of 0.5–1 μm. For morphological analysis, images were reconstructed in z-stack to average intensity for Sholl analysis. Image acquisition was performed using the NIS Elements 4.3 software.

4.3.2. Spine quantification

Spine density was studied in the biocytin-labelling slices for analysing synapsin strength. For this, 300 μm thick slices were demounted from the slide and washed three times and stored with PB(0.1mM). Then, slices were re-sectioned on ice embedded in agarose gel (2%) for further slicing in 50 μm with Vibratome (Leica VT1200s, Germany). In the Nikon C2 confocal microscope, images were acquired at 60x oil immersion objective (NA 1.4) and 0.07-pixel size was used. Z-stacks were acquired at an interval of 0.125 μm between steps. The original images were further deconvoluted by using Huygens Professional version 19.04 (Scientific Volume Imaging, The Netherlands, http://svi.nl) before quantification then the deconvoluted images were imported into Neurolucida software (MicroBrightField, VT, USA) to trace and quantify the total number of spines per 30 μm.

4.4. Cognitive performance in physiological conditions: experimental design

To study the consequences of the morphological deficits in hippocampal pyramidal neurons, mice were subjected to diverse tasks assessing cognitive functions related to the hippocampus and connections between this structure and the perirhinal and prefrontal cortices, i.e., the *what, where* and *when* components of episodic memory, in WT and KO mice according to the protocols described Cruz-Sanchez et al. (144) with minor modifications. The date of birth was designated postnatal day (P0). At P21, mice were weaned and housed in groups of same-sex 2–5 mice. All recognition tests were performed in a white squared plexiglass chamber (40x40x40). The mice were handled and habituated to the chamber from P20 to the testing day of each of the three recognition memory tasks. During the handling and habituation phase, the animals were handled for five minutes and then habituated to the empty chamber for five minutes. Males and females underwent different cognitive tests on P21, P24, P25 and P28. The mice were assigned randomly to experimental cohorts to prevent impairment of cognitive performance due to repeated testing. The first cohort underwent the object location (OL) task (P21) and temporal object recognition (TOR) task (P28), while the second cohort underwent only the novel object recognition (NOR) task (P24 and P25). All the objects used in the tests were built differently with Lego bricks, according to the needs of each trial.

DOI:10.14753/SE.2023.2882

4.5. Behavioural tests for physiological conditions in young animals

Tests were analysed with The Observer XT 12 (Noldus) by an experimenter blinded to the experimental conditions when mice interact directly by sniffing and/or pawing within 2 cm of the object by an experimenter blind to experimental conditions. Sitting on the object while sniffing the surrounding air or chewing the object was not considered exploration. In all the tests, there was an exclusion criterion where the mouse had to explore the familiar objects, which are maintained among tests, for at least 20 seconds to be included. The discrimination index was calculated in all the tests as a measure of novelty preference by dividing the time exploring the novel location/novel object/older object by the sum of time exploring both objects.

4.5.1. Object location task

For the sample phase, the mice explored two identical objects for 10 minutes and were subsequently placed into their cages for 1 hour. After the delay period, the mice underwent a 5 min test phase, in which one of the objects was relocated to an opposite novel location in a counterbalanced way (Fig. 6).

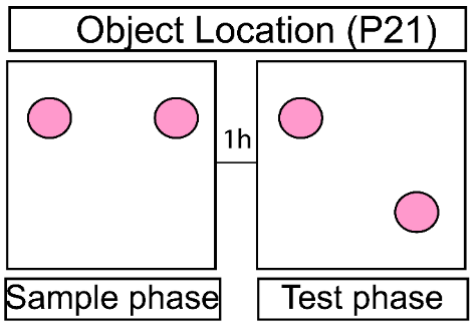

Figure 6. Scheme of the experiment.

4.5.2. Temporal order recognition task

TOR was divided in two sample phases followed by a one test phase. The sample phases involved exploring two different sets of identical objects for 10 min, separated by one-hour inter-phase interval. Following sample phase 2, after another one-hour inter-phase interval, mice underwent the test phase. During the 5 min test phase, mice explored one copy of the old object (object from sample phase 1) and one copy of the object from the sample phase 2in a counterbalanced way (Fig. 7).

DOI:10.14753/SE.2023.2882

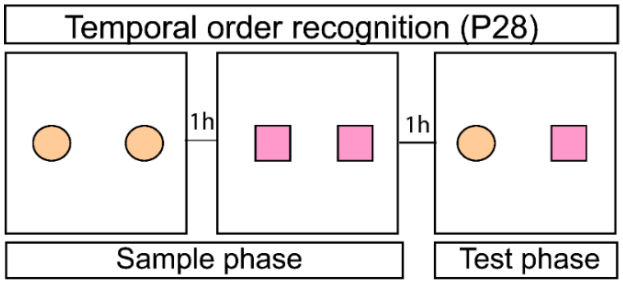

Figure 7. Scheme of the experiment.

4.5.3. Novel object recognition task

In the sample phase, the mice explored two identical objects until a criterion of total object exploration of 20 seconds was reached. Then, the animal was placed back into the home cage. Immediately (in less than 2 min), the mice underwent the test phase for 5 minutes with the familiar and a novel object. The animals were tested again at a longer delay (24h) in the same chamber in another test phase for 5 minutes with the familiar object and a novel object different from the previously used one. To avoid interference from a possible object preference, objects were counterbalanced between trials (Fig.8)

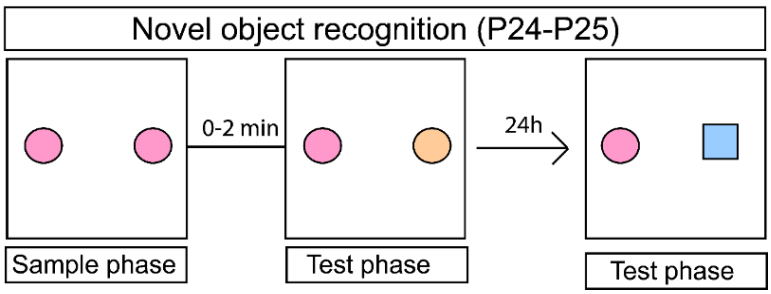

Figure 8. Scheme of the experiment.

4.6. Maternal immune activation model: experimental design

Maternal immune activation was used as a model for triggering schizophrenia-like behaviour in the offspring (145). Intraperitoneal poly(I:C) (PIC) injections during pregnancy activate antiviral pattern recognition receptors, such as TLR3 and PKR, in the mother and thereby activate the maternal immune system. Mothers were weighed 24 hours after the injection, with an anticipated decrease of 0.5g in mothers treated with PIC as an internal control of a proper PIC-induced inflammatory reaction. Compared to

control, PIC-treated mothers exhibited a higher incidence of spontaneous abortion or infanticide.

Morphological correlates of the disease were studied in *vitro* primary cultures following the same outline previously described from the hippocampus dissected from control and PIC-treated embryos. For the *in vitro* experiments, pregnant WT and KO mice were randomly assigned to different treatment groups and injected intraperitoneally with 10 mg/kg or 20 mg/kg PIC on E12.5. Control mice received saline injection (100 µl) at the same time point. PIC injection at embryonic day 12.5 was performed in mice corresponding to second trimester of the pregnancy in humans. Primary hippocampal cells were obtained from embryos of both genotypes from control and PIC-treated animals on E17.5–E18.5 and processed as described previously for morphological studies.

Then, possible inflammatory changes in the MIA model with the higher dose of PIC (20mg/kg) was measured. IL-1β levels were measured 24 hours after the saline and PIC injections in the fetal brain from E13.5 embryos with the quantitative analysis of IL-1β using enzyme-linked immunoassay sandwich technique (ELISA). For behavioural studies, offspring of either control or immune-activated animals were weaned into cages of 2-4 animals at P21. Behavioural experiments were performed on test-naive male mice at P60-P90, which correspond with approximately 15 to 20 years old patients, in the same order (open field, T maze, novel object recognition, social preference and prepulse inhibition test) by an experimenter blinded to the treatments (Fig. 9).

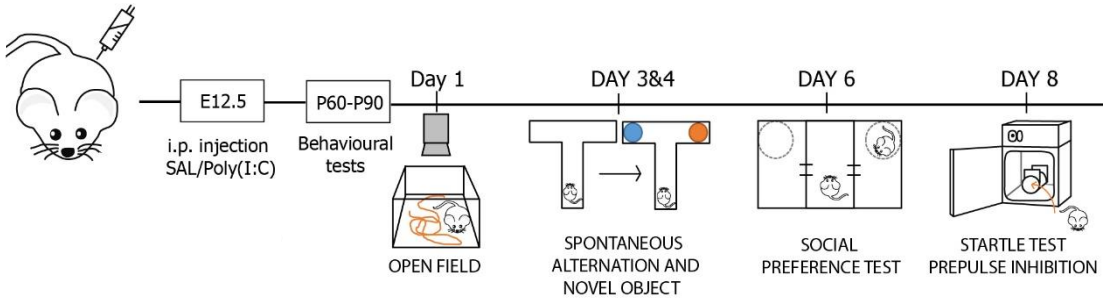

Figure 9. Battery of behavioural tests.

4.7. Quantitative analysis of IL-1β using enzyme-linked immunoassay sandwich technique (ELISA)

To measure the possible inflammatory changes in the MIA model IL-1β levels for E13.5 fetal brains were measured by The Quantikine® Mouse IL-1 beta Immunoassay, R&D Systems (Minneapolis, MN, United States). Fetal brains were collected 24h following intraperitoneal injection of PIC (20 mg/kg) or saline treatment from pregnant mice. For homogenization, samples were placed in lysis buffer (50 mM Tris HCL, 150 mM NaCl, 5 mM $CaCl_2$, 0,02%NaN_2, 1% Triton X-100, pH = 7,4) with 0.1% protease inhibitor double-diluted in PBS. After homogenization and centrifugation, brain homogenates were stored at −80 °C. IL-1β concentration was determined by mouse IL-1β-specific monoclonal antibody pre-coated microplates following the manufacturer's instructions. We determined the optical density with a microplate reader at 450 nm (Cytation™5 Cell Imaging Multi-Mode Reader). We calculated concentration values (pg/ml) using GraphPad (San Diego, CA, United States). For measuring total protein level in tissue samples, absorbance was measured at 560 nm. Fetal brain IL-1β concentrations were expressed in pg/mg protein.

4.8. Behavioural tests for neurodevelopmental schizophrenia

4.8.1. Open field

The open field was used for testing locomotor activity and exploration, neophobia and some aspects related to anxiety. The light was adjusted to dim light and mice were placed in the middle of a plexiglass white square box (40 x 40 cm), Ethovision XT 15 system (Noldus) connected to an overhead camera to the video track, recorded and tracked the locomotor activity for ten minutes. To avoid olfactory cues arena was wiped with 20% ethanol between trials. Both the total distance covered during the analysis (cm) and the velocity, were measured during the test.

4.8.2. Spontaneous alternation and novel object recognition

Spatial working memory and novel object recognition memory were tested according to the method described by Castañé and colleagues (146) with minor modifications. First, mice were habituated to a T-maze (one arm: 30x20 cm) for 10 min. Successful alternations were evaluated for the first five minutes.

Exploration of a novel environment is based on the motivation to map the environment for resources. Accordingly, a solid drive to explore the environment requires an adequate performance of the working memory to avoid redundant exploration and wasting valuable energy. Spontaneous alternation was defined as the enter of the animal to a different arm of the maze every time. Therefore, a mouse should enter one arm just after three consecutive arm entries for a successful performance. An arm entry occurs when all 4 paws of the mouse cross the threshold of the central zone and into the correspondent arm. The arms are named as follows: A (starting arm), B (left arm) and C (right arm). Both the total distance covered during the analysis (cm) and the velocity, were measured during the test. The percentage alternation was calculated:

$$\text{Spontaneous alternation \%} = \frac{\text{Number of espontaneous alternations}}{\text{Total numer of entries} - 1} \text{ x } 100$$

Twenty-four hours later, novel object recognition was tested as in the method as described (146). The novel object test is a recall task that is also used as a human test, but in rodents, the test is based on the natural motivation of mice to explore novelty. First, the animals explored two identical objects placed in the corner of both opposite sides (B and C). The animals were placed in the starting arm (A), equidistant to the two identical objects and were allowed to explore it for 10 minutes. This is called the training phase. Then, the animal is retired to its own cage for three minutes to study the performance in short working memory, while one of the identical objects was replaced with a novel object in its identical place (in a counterbalanced way). During the test session, the total time spent exploring novel and familiar objects was recorded by the Ethovision XT 15 system (Noldus) and measured for 10 min. All the objects used in the tests were built differently with Lego bricks, according to the needs of each trial.

The novel object recognition index was calculated as a percentage. Therefore, the time the test mouse spent interacting with the novel object (tn) was divided by the total time a test mouse spent with the novel and the familiar object (tf) as follows:

$$\text{Novel object recognition index } \big(\text{NOR } (\%)\big) = \frac{t_n}{t_n + t_f} \text{ x } 100$$

4.8.3. Social preference test

Social preference was performed according to the method described by Naviaux (147). The three-chamber plexiglass arena (60x40x33 cm) was divided into three compartments (20x40x33cm) with one wire cage (sniffing zones) placed in each side chamber. The location of the stranger mouse was alternated across trials. Ethovision XT 15 system (Noldus) connected with an overhead camera was used to video track lively and record the time the test mouse spent in each of the sniffing zones. First, there was a habituation phase of 5 minutes where the test animal freely explored the entire arena.

Then, the test animal was enclosed into the middle chamber of the arena by closing the other two side chambers. Then, a stranger mouse of the same age and sex was placed into a wire cage on one side of the chamber while the other wire cage remain empty. During the test phase, the doors opened, and the animal explored freely the whole arena for 10 minutes. Social preference is presented as the cumulative time (s) spent in every chamber that allowed the comparison between the time the test mouse spent in each of the sniffing zones determined in the software.

4.8.4. Acoustic Startle

Positive symptoms in schizophrenia are commonly associated with delusions and auditory hallucinations, which are rather unique in humans. In mouse models, they can be modelled and clustered mainly on locomotor hyperactivity and prepulse inhibition (PPI) disruptions. Indeed, a sensory gating deficit or PPI is described as the deficiency to inhibit response to the test stimulus and is used as an objective and relatively specific clinical biomarker of schizophrenia; therefore, it has high translational value. Baseline startle magnitude, prepulse inhibition (PPI), and habituation of startle were tested using startle chambers (San Diego Instruments). Five blocks were included in the session.

The startle response is a protective response to a sudden and intense stimulus that is reflected in a body inch for a mouse recorded by a movement sensitivity detector positioned in the middle of the startle chamber. For this, first, a five-minute acclimatization period was followed by five 120dB startle pulses (Block 1). The second block was composed of different intensities (80, 90, 100, 110, and 120 dB), randomly generated for testing the startle response. For the measurement of the PPI, three prepulse intensities (68, 71, and 77 dB) were preceded by 120dB startle pulses (Block 3). In the

fourth block, the interstimulus interval was tested by 73 dB prepulse preceding 120 dB pulses by 25, 50, 100, 200, or 500 m. Finally, the last block included five pulses of 120 dB to assess startle habituation, as in the first block.

In all experiments, the average startle magnitude over the record window (65 milliseconds (ms)) was used for all data analysis. Startle pulses were 40 ms in duration, prepulse was 20 ms in duration, and prepulse preceded the pulse by 100 ms (onset-onset). A 65 dB background was presented continuously throughout the session. The house light remained on throughout all testing sessions.

4.9. Phencyclidine model

Animals were randomized to different treatment groups with a sample of 8-12 and four groups/experiments were formed (2 genotypes/pharmacological treatments, PCP and/or Vehicle). Phencyclidine (PCP, 2 mg/kg) or its vehicle (Saline, 10 ml/kg) were injected intraperitoneally in a 10 ml/kg injection volume.

4.9.1 Social withdrawal test

Two months old male animals were single caged in a behavioural unit 24h before the experiments and randomized to different treatment groups with a sample of 6-12 and four groups/experiment (2 genotypes/pharmacological treatments). Forty-five minutes from the PCP injection, mice were exposed to the social withdrawal test, following the protocol of Kovanyi et al. (2016) (132). The test was performed in a circular open field (diameter: 38cm) and recorded for 10 minutes in dim light with the Ethovision XT 15 system (Noldus). The behavioural test was carried out between 8:30 a.m. and 1:00 p.m., by trained observers who were blind to the test groups. Two unfamiliar mice receiving the same pharmacological treatment were placed in the arena on opposite sides of the open field. The following behavioural variables were recorded: distance travelled, social interaction, ataxia and stationary stereotyped behaviour. Line crossings and social interactions were recorded for the whole duration of the test using a computer-based event recorder. Social investigations were defined as sniffing and nosing when the nose of the scored mouse touched (or was very close to) the body of the partner and following directed towards the partner.

Phencyclidine-induced stereotyped behaviour and ataxia were scored manually according to the protocol described in Nabeshima (148) and Sam-Dodd (149), respectively on whether the mice is static and performed circular head movements or head weaving and whether the mice walk in circles, respectively.

4.10. Drugs and treatments

The following drugs were used: JNJ47965567 (Tocris Bioscience), ITH15004 (personal contribution from Instituto Teófilo Hernando), ARL 67156 trisodium salt (Tocris Bioscience, 1283, Batch No. 16A/253182) and BzATP (Sigma–Aldrich, Missouri, US). Drugs were dissolved in sterile saline, except for JNJ47965567 and ITH15004, which were dissolved in 30% Captisol solution (sulfobutyl ether-7-cyclodextrin) and 5% DMSO, respectively. For the study of P2X7R in pathological conditions, Polyinosinic–polycytidylic potassium salt (Sigma-Aldrich, P9582-5MG, Batch No. 0000080809) was used in the MIA model freshly dissolved in the vehicle. For the PCP model of schizophrenia, PCP (Sigma–Aldrich Kft, Budapest, Hungary) was freshly dissolved in the vehicle (0.9% NaCl sterile).

4.11. Statistical analyses

Based on previous experience, one pregnant dam gives birth to an average of 10 pups; therefore, we calculated an ideal sample size before the breeding process as described in our previous study (136). Statistical analyses were performed using STATISTICA version 64 (StatSoft. Inc., Tulsa, OK, USA) and Graph Prism version 8.0.2 (GraphPad Software, San Diego, CA, USA). Data normality was tested using the Kolmogorov–Smirnov test and Shapiro–Wilk test. Possible outlier values were detected by the ROUT method (q=1%) (150), and therefore omitted from the analysis. Differences were analysed using the student's unpaired *t-test* for 2 groups, a one-way analysis of variance (ANOVA) followed by a post-hoc Kruskal–Wallis or Dunn's comparison test, and by a 2-way ANOVA followed by Bonferroni post-hoc test or Mann-Whitney *U*-test, as appropriate for multiple comparisons. The specific tests used are reported in the captions of the figures. All data are expressed as a mean ± standard error of the mean (S.E.M.) A p-value of less than 0.05 was considered statistically significant ($*p < 0.05$, $**p < 0.005$,

***$p < 0.0005$, **** $p < 0.0001$). All the statistical analysis and significances are summarized in Table 7&8.

5. Results

5.1. P2X7R in physiological conditions during development

5.1.1. P2X7R expression is decreased during development

RNA was collected each day *in vitro* for ten days to study P2X7R expression (Fig.7A). . The transcript level of the *P2rx7* gene was measured by RT-qPCR (Fig. 10B) and the results revealed changes in the average expression of both the intracellular and extracellular regions during the first days of culture (Fig. 10C). This could correspond to the growth of the neurons. Concerning the extracellular transcript, there was a significant increase in the average transcript level of the extracellular region on DIV4 that drops in later days (Fig. 10C, top). It was observed a similar tendency for the intracellular regions. Notably, the level of the intracellular region increased during the first days of culture, corresponding to the growth of the neurons, and transiently increased at DIV7, i.e., after the medium change, but was reduced immediately after and dropped below the initial level (Fig.10C, bottom).

Additionally, in correlation with the real-time PCR results, the expression of P2X7R protein demonstrates a transient increase; where P2X7R expression gradually increases from culture DIV 3, reaching a peak DIV 4 and subsequently declining until DIV 7 to a level below the detection limit (Fig. 10D). The specificity of the P2X7R antibody has been validated using cells harvested from wild type control and P2X7R-KO animals (Fig. 11).

To study the functional activity of the receptor in vitro, we performed calcium imaging at DIV4, when the expression of the receptor was higher. We observed that neurons from WT mice responded to BzATP (1 mM), an agonist of P2X7R, while the response of primary neurons from KO mice was negligible (Fig. 10E, top). As a control, we used a calcium ionophore (1 mM); neurons from both genotypes presented the same response to this compound (Fig.10E, bottom).

DOI:10.14753/SE.2023.2882

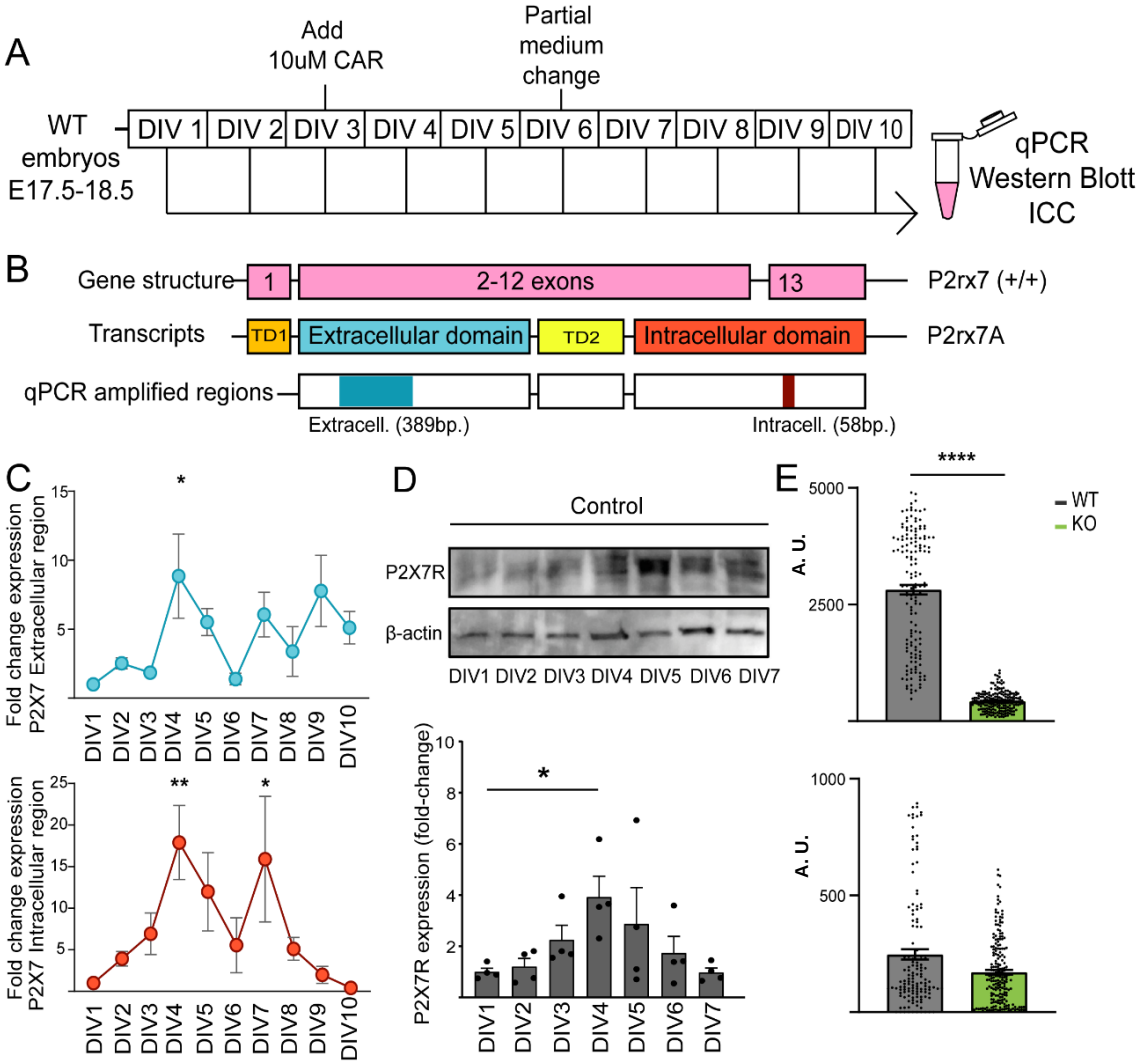

Figure 10. P2X7R expression decreases in cultivated neurons *in vitro* during development. (A) Experimental design. (B) Schematic representation of the P2rx7 gene in WT mouse lines, the principal splicing variant found in C57bl/6 line and the amplified regions in the qPCR. (C) P2X7R expression analysis by real-time qPCR from each day *in vitro* (DIV1) for the intracellular and extracellular sequences. Relative expressions were given as fold changes normalized to GAPDH. (D) Wild-type cells were cultured for a certain period of time as indicated, and the P2X7R protein expression was determined by immunoblotting. Graphs show the densitometric evaluation normalized to the total loaded protein. (E) Area under the curve (A.U.) for primary neurons at DIV 4 after BZATP (1mM) application. (top) and for WT and KO primary pyramidal cells at DIV 4 after calcium ionophore (1mM) acute application (bottom). *p<0.05, **p< 0.005. Figure 1A to H from the article of Mut-Arbona et al.,2023 (143).

DOI:10.14753/SE.2023.2882

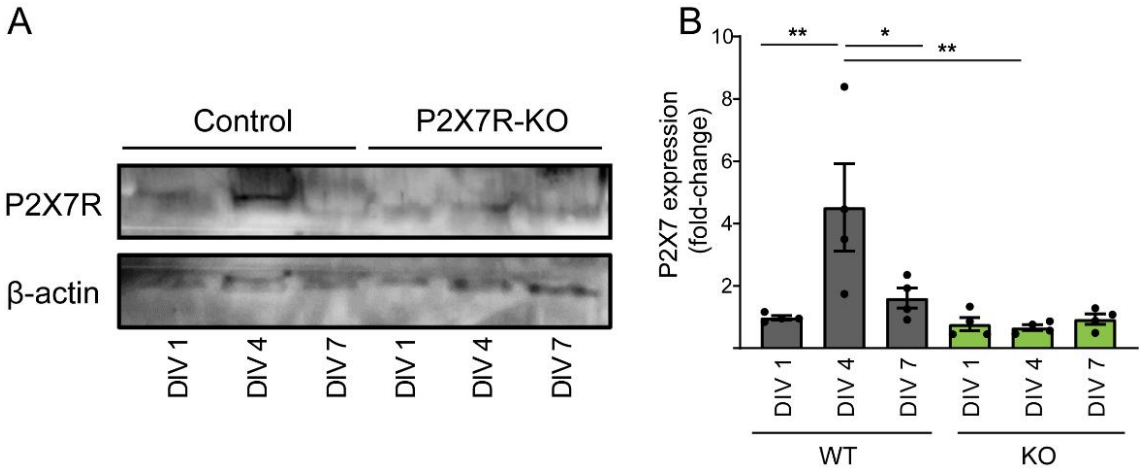

Figure 11. The specificity of the P2X7R antibody has been validated using cells harvested from wild type control and P2X7R-KO animals. (A) To validate the specificity of the P2X7R antibody, wild-type or KO cells were cultured for a certain period of time as indicated, and the P2X7R protein expression was determined by immunoblotting. (B) Graphs show the densitometric evaluation normalized to the total loaded protein. *p<0.05, **p< 0.005.

The presence of P2X7R was proved with an immunostaining in primary cultures in both WT and KO primary neurons at DIV10. The receptor was not present in KO neurons (Fig. 12A) as expected, while it was expressed on the WT neurons *in vitro* (Fig. 12B). To study the morphology of an individual neuron, we benefit from the lower effectivity of the transfection compared to the immunocytochemistry for the visualization and tracing. Particularly, the transfection of the plasmid encoding GFP was used for this purpose. Again, the P2X7R immunostaining showed a specific staining for a transfected neuron (Fig. 12C). Due to the CAR application, the astroglia population was considerably inhibited from DIV3 under these conditions to DIV10 where the immunostaining was performed (Fig. 12D).

DOI:10.14753/SE.2023.2882

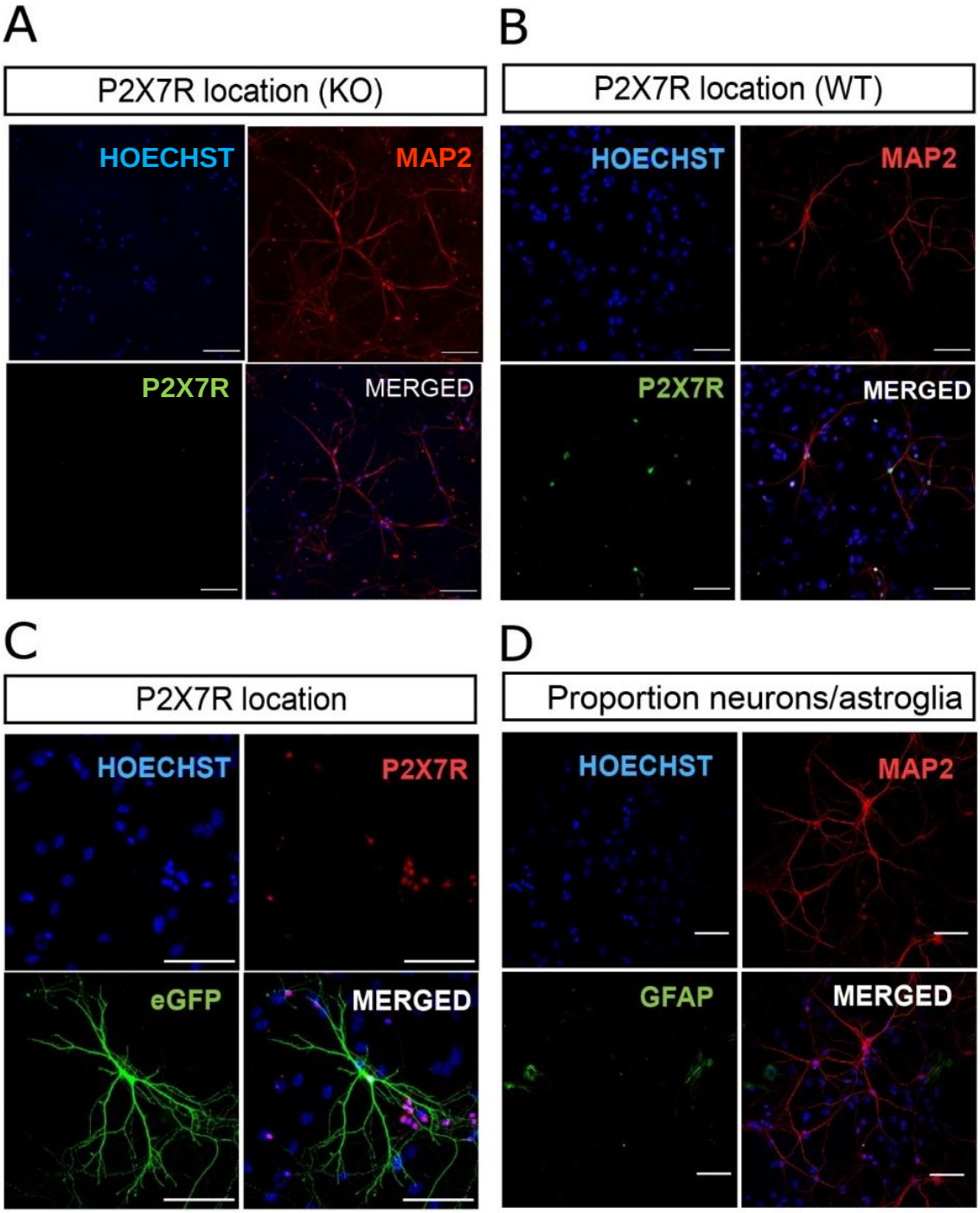

Figure 12. P2X7R expression in primary hippocampal neurons is located mainly in the soma. Immunostaining of neurons (MAP2) and P2X7R at DIV 10 for (A) KO primary neurons at DIV 10 and (B) WT primary neurons. (C) Immunostaining of neurons (MAP2) and P2X7R at DIV 10 for the transfected neurons (eGFP). (D) Immunostaining of neurons (MAP2) and astroglia (GFAP) showing the proportion of neurons and astroglia. Nuclei were counterstained with Hoechst. The scale bar is 200 μm. Figures 1I-J and 2B from the article of Mut-Arbona et al.,2023 (143).

5.1.2. P2X7R regulates dendritic outgrowth in primary hippocampal neurons

Primary pyramidal neurons from WT embryos at embryonic day 17.5-18.5 were compared with those from KO embryos (Fig. 13A) in addition to those isolated from WT embryos and treated with the P2X7R-specific antagonists, JNJ47965567 and ITH15004 (151) (Fig. 13A and B). While *P2rx7* was absent in neurons from *P2rx7* KO mice throughout development, P2X7R was only blocked in these cells after exposure to the antagonist, which was performed 4 hours after plating.

Co-localization for the GFP transfected primary hippocampal neurons with the neuron specific marker MAP2 can be observed validating the process of the transfection (Fig. 13B). This allows to visualise the whole structure of several isolated neurons and trace them (Fig. 13C). Sholl analysis showed that KO neurons present less dendritic outgrowth, i.e., had fewer branched neurons, than WT neurons (Fig. 13D). HPLC analyses revealed that adenine nucleotides (ATP, ADP, AMP) were present in the medium of mouse hippocampal neurons, and differences in the levels of ATP and other metabolites in the supernatant were found between neurons from mice of the two genotypes (Fig. 13E).

The cell body area, numbers of dendrites and dendritic endings, and the mean length of each neuron were also determined from Neurolucida analysis (Fig. 13F-I), validating the Sholl analysis results. Indeed, both the number of dendrites and the number of endings confirmed a decrease in complexity in the P2X7R deficient mice (Fig. 13G-H). Moreover, the shorter length of the KO neurons found in the Sholl analysis (Fig. 13D) was also observed when analysing the mean length of the sum of dendrites (Fig. 13I).

DOI:10.14753/SE.2023.2882

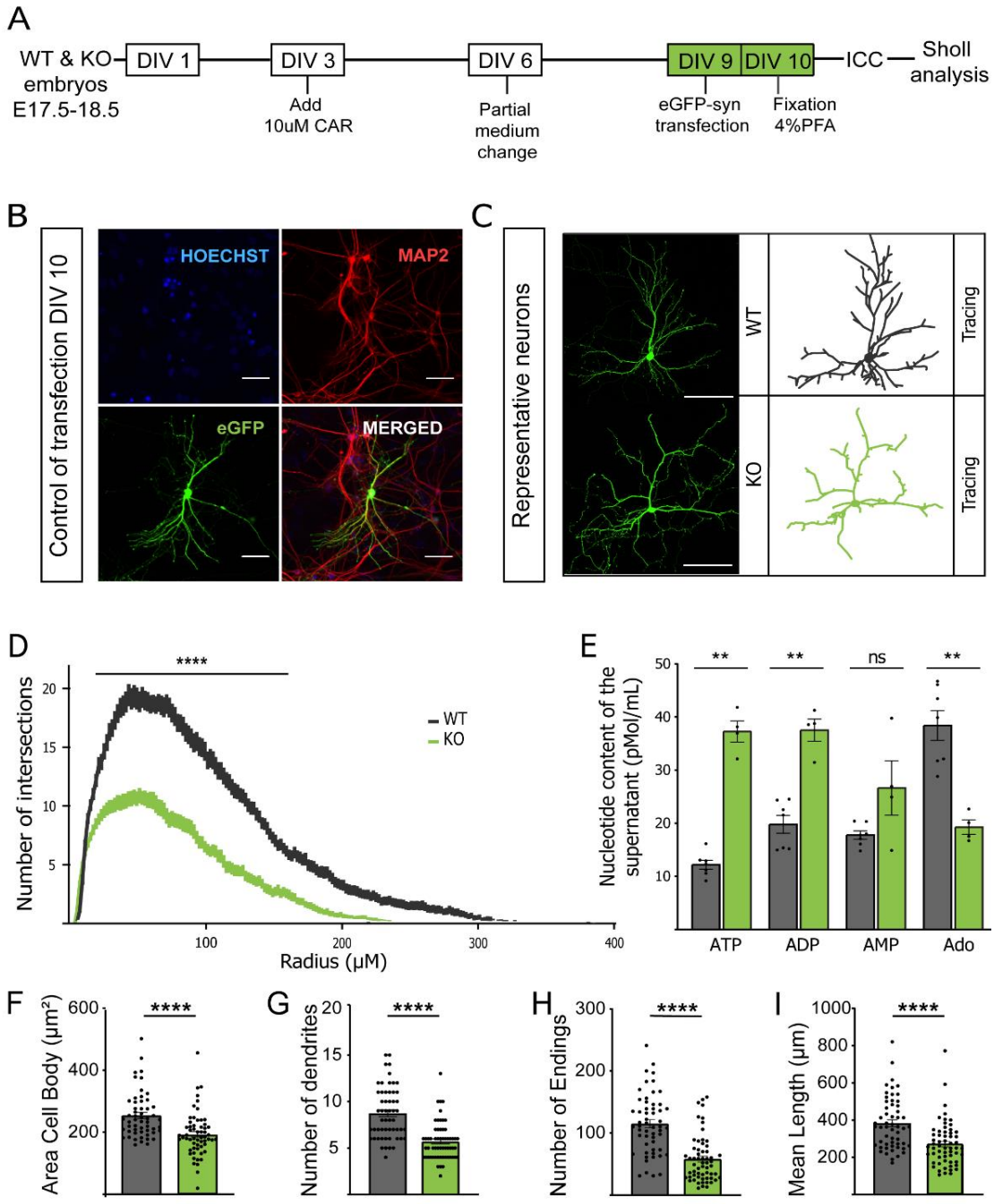

Figure 13. P2X7R deficiency elicits abnormal dendritic outgrowth in KO primary hippocampal neurons. (A) *In vitro* experimental design. (B) Control of the transfection with a neuronal marker (MAP2) and transfected control neuron (eGFP) at DIV 10. Nuclei were counterstained with Hoechst. The scale bar is 200 μm. (C) Representative hippocampal neurons from both genotypes transfected with GFP. The scale bar is 200 μm. (D) Sholl analysis presents the number of intersections versus the distance to the soma by Radius (μM). (E) Nucleotide concentrations of the supernatant obtained from WT and KO primary hippocampal neuron culture were measured by the HPLC technique. Quantification of (F) area cell body, (G) number of primary dendrites, (H) number of endings, (I) and mean length of the dendrites. For D-I, the (*) symbol indicates a statistically significant difference between WT and KO neurons. ** $p<0.005$, ****$p<0.0001$. Figure 2A,C-I from the article of Mut-Arbona et al.,2023 (143).

DOI:10.14753/SE.2023.2882

WT neurons treated with selective P2X7R antagonist JNJ47965567 (1 μM) and a recently developed P2X7R antagonist ITH15004 at 3μM (Fig. 14A-B) presented slightly less branched dendrites compared to control neurons, especially near the soma (Fig. 14C). Overall, in both genetically or pharmacologically blocked P2X7R, the neurons showed a healthy neuronal condition, albeit to the reduced number of intersections was observed in the antagonist-treated neurons (Fig. 14D-G) and KO (Fig. 13F-I), suggesting that the absence of P2X7R slowed the development of WT neurons and leads to a less developed dendritic tree.

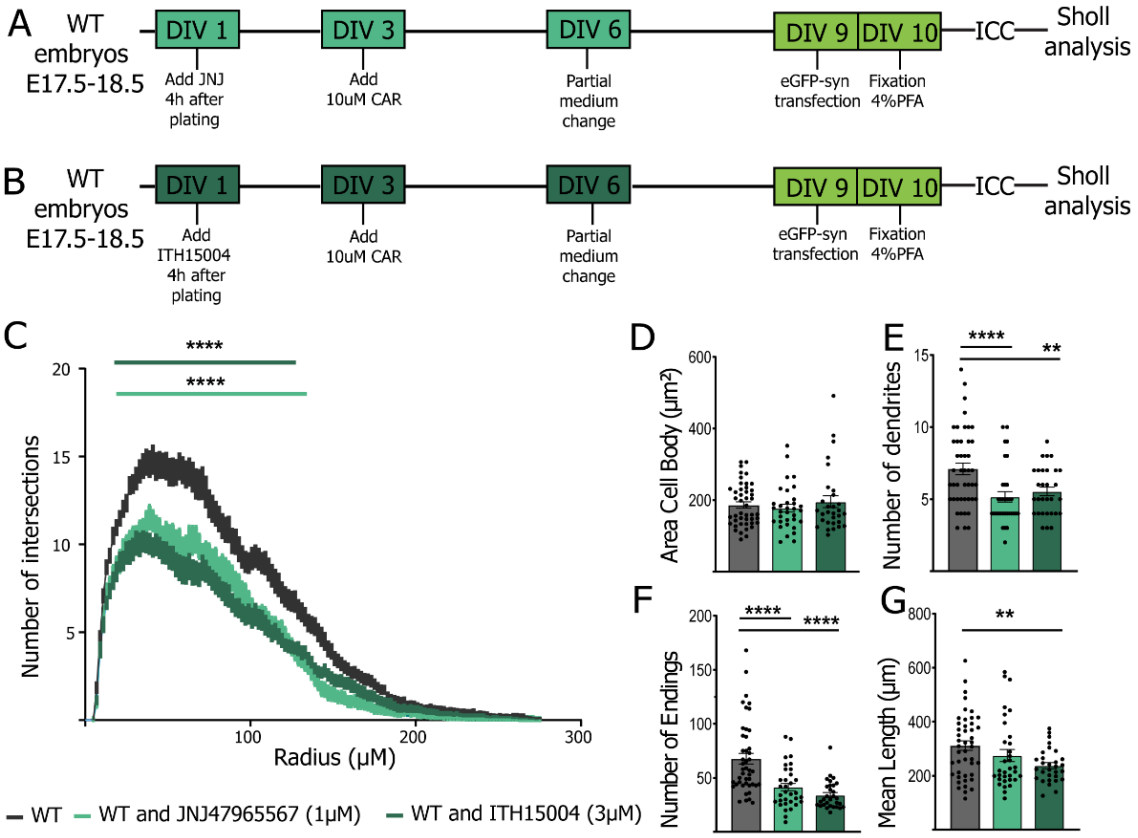

Figure 14. Pharmacological blockade of P2X7R elicits a disruption in dendritic outgrowth *in vitro*. (A) Scheme of the JNJ 47965567 (JNJ) application *in vitro*. (B) Scheme of the ITH15004 application *in vitro*. (C) Sholl analysis presents the number of intersections versus distance to soma. Quantification of area Cell Body, (D) number of primary dendrites, (E) number of endings, (F) means of the total dendrite length and (G) mean length of the dendrites. The (*) symbol indicates a statistically significant difference with the WT control for both groups. **p<0.005 ****, p<0.0001. Figure 3A-F from the article of Mut-Arbona et al.,2023 (143).

DOI:10.14753/SE.2023.2882

To understand how the endogenous purinergic signalling under physiological conditions influences the regulation of dendrite development, the extracellular ATP level was manipulated with an acute ARL 67156 (100U/mL) application (Fig. 15A). ARL 67156 is a specific inhibitor of NTPDase responsible for the metabolism of ATP in the medium (152). The acute treatment modified the morphology of the dendrites marginally, increasing their length and the complexity of the neurons themselves (Fig. 15B). When we analysed the ATP levels in the medium after the application of ARL 67156 (100 U/mL on DIV9) acutely, a significant increase in ATP, ADP and AMP levels were observed (Fig. 15C). To deepen into the Sholl analysis, the analysis was extended to the area of the cell body, the number of dendrites and endings, and the mean length (Fig. 15D-G). Only an increase in terminations (Fig. 15F) and mean length (Fig. 15G) were observed with the acute treatments concerning the control neurons not treated in the same culture. This finding indicates that both ATP and its metabolites influence maturation and dendritic outgrowth and that like P2X7R, other purinergic receptors might also participate in this regulation.

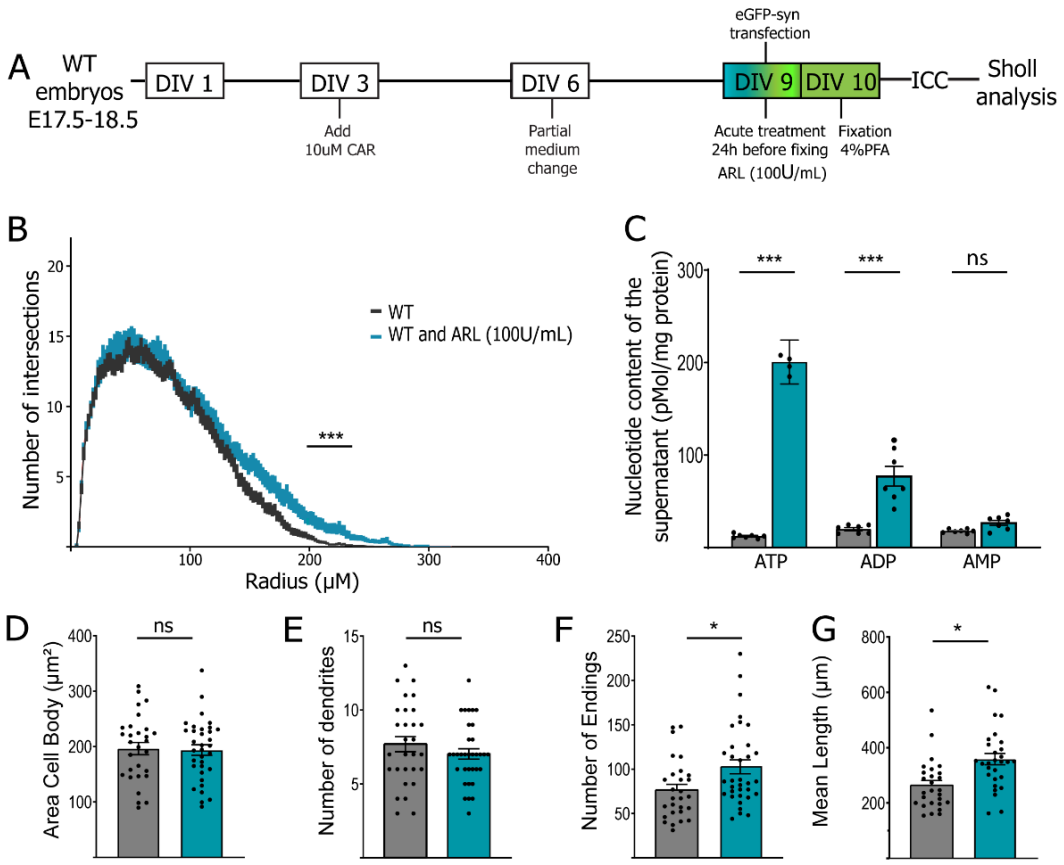

Figure 15. Figure legend in the next page.

Figure 15. Neurons acutely treated with ARL 67156 (100U/mL) present a marginal elongation in the endings of the dendrites (A) Scheme of the ARL 61756 (ARL) acute application 24h before the fixation for morphological analysis. (B) Sholl analysis presents the number of intersections versus the distance to the soma. Data are expressed as means ±SEM. (C) Measurement of nucleotide concentrations of the supernatant from WT and WT ARL-treated primary hippocampal neuron culture with HPLC technique. Quantification of (D) area cell body, (E) number of primary dendrites, (F) number of endings, (G) mean of the total dendrite length. The (*) symbol indicates a statistically significant difference between WT and WT treated with ARL. *<p0.05, *** p<0.0005. Figure 3G-M from the article of Mut-Arbona et al.,2023 (143).

5.1.3. P2X7R regulates dendritic outgrowth in pyramidal hippocampal neurons in slice

By using a more complex model system *in vitro,* reflecting the hippocampal neuronal architecture and trisynaptic network, the pyramidal neurons from the CA1 (Fig. 16A-F) and CA3 (Fig. 16G-L) regions of acute hippocampal slices were studied at postnatal day (PN) 20-29 from both genotypes. Therefore, we could confirm the morphological correlates that we observed in cultures regulated by the endogenous activation of P2X7R. Although this study was performed at a later stage of brain development, differences between WT and KO are apparent in CA1 neurons (Fig. 16A) and confirmed by Sholl analysis (Fig. 16B). Precisely, the length of the dendrites was significantly undersized in KO CA1 neurons as well as the number of endings (Fig. 16E&F). Interestingly, we found a region-specificity as these differences were not found in CA3 pyramidal neurons (Fig. 16G-L).

Following, to understand whether the dendritic morphology change could alter the synapse strength, the spine number was also analysed. The observed decrease in spines in KO (Fig. 16M-N) could indeed correspond to a possible weaker synapse strength due to the less spine density. We can conclude that P2X7R depletion led to abnormal dendritic arborisation in pyramidal hippocampal neurons affecting the synapsis in the CA1 region of the hippocampus.

DOI:10.14753/SE.2023.2882

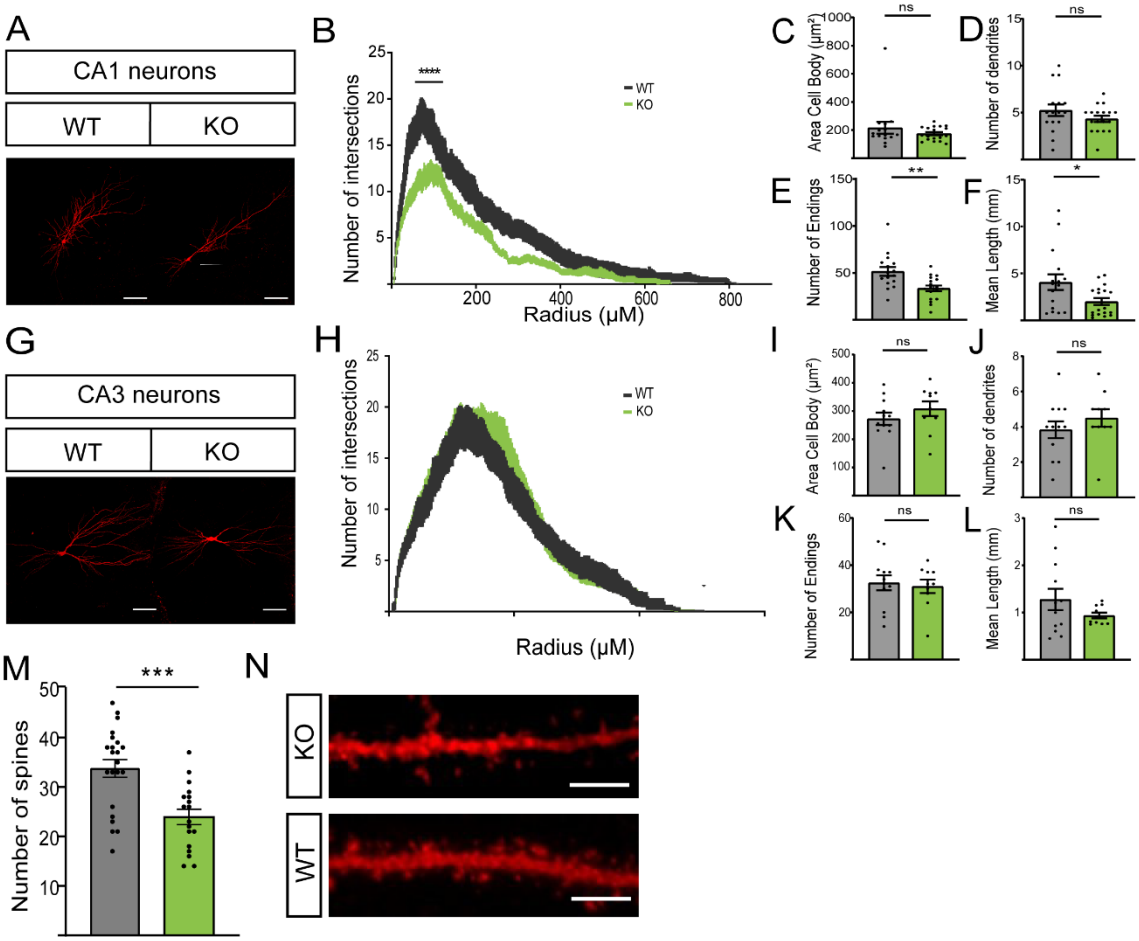

Figure 16. P2X7R influences the dendritic outgrowth in pyramidal hippocampal cells in a region-specific manner. (A) Representative P20-29 pyramidal hippocampal neurons from mice CA1 hippocampal slices for both genotypes. (B) Sholl analysis presents the number of intersections versus the distance to the soma from CA1 WT and KO pyramidal neurons. Quantification of (C) area cell body, (D) number of primary dendrites, (E) number of endings and (F) mean length of the dendrites. (G) Representative P20-29 pyramidal hippocampal neurons from mice CA3 hippocampal slices for both genotypes. (H) Sholl analysis presents the number of intersections versus the distance to the soma from CA3 WT and KO pyramidal neurons. Quantification of (I) area cell body, (J) number of primary dendrites, (K) number of endings and (L) mean length of the dendrites. (M) Number of spines between genotypes from CA1 pyramidal hippocampal neurons. The (*) symbol indicates a statistically significant difference between WT and KO neurons. *p< 0.05, ***p< 0.0005 and ****p< 0.0001. (P) Representative segments for spine counting for both genotypes. Scale bar 50μm. Figures 4A-L and 5I-J from the article of Mut-Arbona et al.,2023 (143).

Deficits in object location, novel object recognition and temporal object recognition were observed in KO mice animals (Fig. 17B, D, F and H) while the total object exploration duration was not significant among genotypes in the different test phases (Fig. 17A, C, E and G), indicating that P2X7R-deficient mice might undergo a

delayed neuronal maturation process. Moreover, KO mice seem to present a neophobic behaviour towards the new object in NOR within the next 24 hours (Fig. 17H), which could be linked with a higher anxiety than the WT animals.

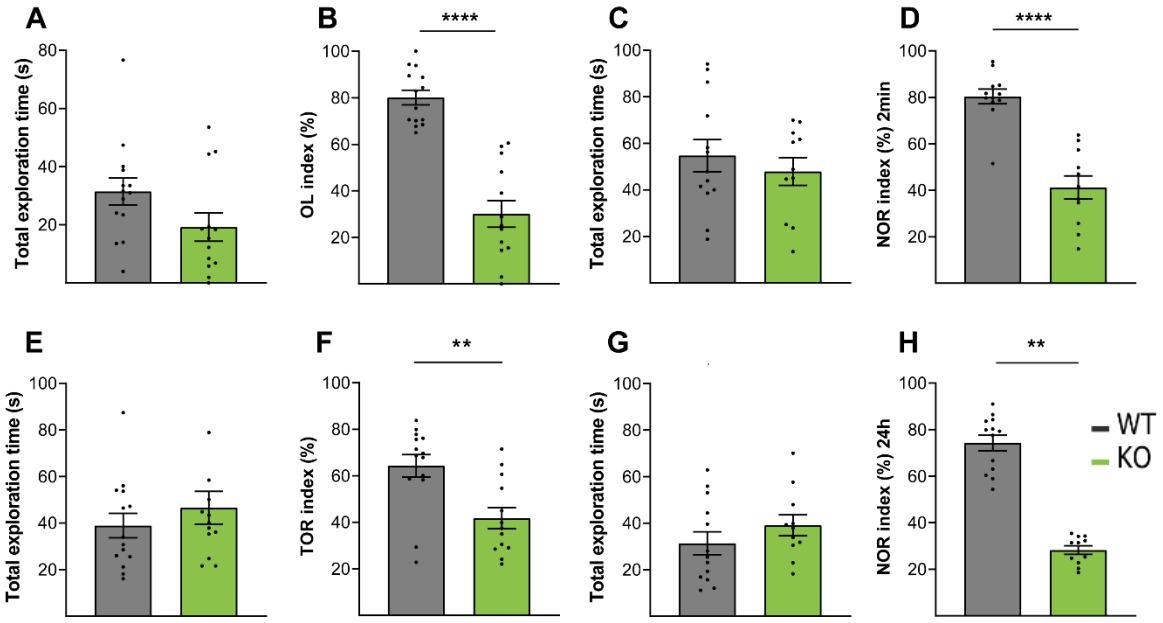

Figure 17. P2X7R is involved in cognitive performance at younger animals. Different aspects for episodic memory were analysed such as object location (OL), novel object recognition (NOR) or temporal object recognition (TOR). (A) Duration (seconds) of total object exploration for OL. (B) Object location index. (C) Duration (seconds) of total object exploration for NOR. (D) Novel object recognition 2 min from the sample phase. (E) Duration (seconds) of total object exploration for TOR. (F) Temporal object recognition index. (G) Duration (seconds) of total object exploration for NOR within a longer delay of 24h. (H) Novel object recognition within a longer delay of 24h. The (*) symbol indicates a statistically significant difference between WT and KO. **p<0.005, ****p<0.0001. Figure 4M-S from the article of Mut-Arbona et al.,2023 (143).

5.2. P2X7R in pathological conditions

5.2.1. P2X7 receptor in a phencyclidine induced mouse model of Schizophrenia. Genetic overexpression of P2X7R exacerbates schizophrenic-like behaviour in rodents

A low dose of phencyclidine (PCP) (2mg/kg i.p.) was used acutely in both C57Bl/6J P2rx7+/+ (WT) and a heterozygous C57Bl/6J P2rx7+/gfp (Tg/+) mouse line overexpressing the P2X7-EGFP protein (138). The behaviour was recorded and analysed as previously described (132) (Fig. 18A). Basal levels of locomotion, social behaviour, stereotypy, and ataxia were not affected by genotype but differences in behaviour and stereotypy were observed in both genotypes treated with PCP (Fig. 18B-E). In controls, acute PCP treatment showed its predicted effects: a decrease in social interaction in

treated WT animals (Fig. 18C) along with a robust increase in stereotypical behaviour (Fig. 18D). Still, the locomotor activity (Fig. 18B) was not significantly affected by the PCP injection, neither the ataxia was triggered. Overall, Tg/+ mice are more affected by the treatment. The schizophrenia-like phenotype was exacerbated in overexpressing animals, which apart from social withdrawal and stereotypical behaviour, also showed hyperlocomotion and traits related to ataxia (Fig. 18B-E).

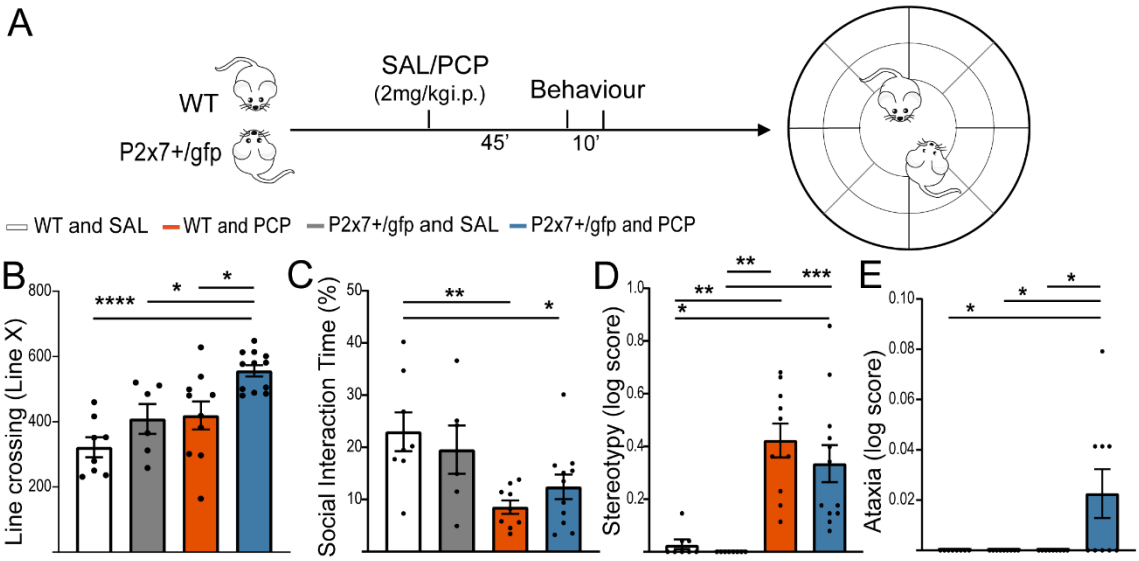

Figure 18. Overexpression of P2X7R exacerbates the acute phencyclidine (PCP) psychotomimetic effects. (A) Scheme of the experiment. Different aspects of PCP induced behaviour were analysed, such as (B) hyper locomotor activity, (C) time of social interaction, (D) stereotype behaviour and (E) ataxia. The (*) symbol indicates a statistically significant difference between P2x7+/gfp and WT exposed to Saline or PCP. *p<0.05, **<p0.005, ***p<0.0005 ****, p<0.0001. Figure 8A to C from the article of Calovi et al (2020) (153).

5.2.2. P2X7R in a maternal immune activation model of schizophrenia

5.2.2.1. P2X7R endogenous activation mediates dendritic outgrowth regulation in a neurodevelopmental model of schizophrenia

Morphological alternations in dendrites could be a correlate of cognitive deficits in psychiatric disorders, such as schizophrenia and ASD. To test this concept, we constructed a model of MIA-induced schizophrenia model as described by Horváth and colleagues with modifications (136). E17.5–E18.5 control and P2X7R KO mouse embryos from pregnant mice that received intraperitoneal injection of saline or different

doses of PIC (10-20 mg/kg) on E12.5 were dissected, and morphological analysis was performed.

To examine whether ATP level and its metabolites are affected by the treatments; and if they influence the maturation and dendritic outgrowth in pathological conditions, culture medium from saline and PIC treated embryos were analysed with HPLC (Fig. 19A). After saline treatment, there was no significant increase in ATP levels compared to cell media derived from control cultures. Contrariwise, ATP levels increased significantly in a dose-dependent manner after both doses of PIC compared to control mice. Interestingly, in the case of the other metabolites such as ADP, AMP and adenosine, a higher significant difference was observed at the lower dose of PIC treatment. These findings might point to a cell-autonomous ATP release mediated by the inflammation in the pregnancy, resulting in a considerably higher extracellular ATP level compared with the cultures derived from saline-treated or naïve mouse pups. Likewise, the extracellular breakdown of nucleotides is also compromised, resulting in altered extracellular ADP, AMP and adenosine levels.

To analyse whether the increased extracellular ATP level affects neuronal morphology and, thus, contributes to the susceptibility to develop cognitive symptoms in young adulthood, Sholl analysis was performed with primary hippocampal neurons subjected to naïve, saline or both PIC treatments (Fig. 19B-D). Sholl analysis revealed dose-dependent changes in the dendritic morphology of primary hippocampal neurons from WT mice (Fig. 19B). These differences were confirmed with area cell body (Fig. 19C), number of dendrites (Fig. 19D), number of endings (Fig. 19E) and mean length (Fig. 19F). Interestingly, some disturbances are also observed in saline-treated neurons compared with the controls, such as the number of dendrites (Fig. 19D) or the number of endings (Fig. 19E), which might be caused by stress during the process of injection. In conclusion, these findings indicate that, while P2X7R contributes to normal dendritic outgrowth of pyramidal neurons under physiological conditions, a pathological increase of ATP during MIA compromises normal neuronal development.

DOI:10.14753/SE.2023.2882

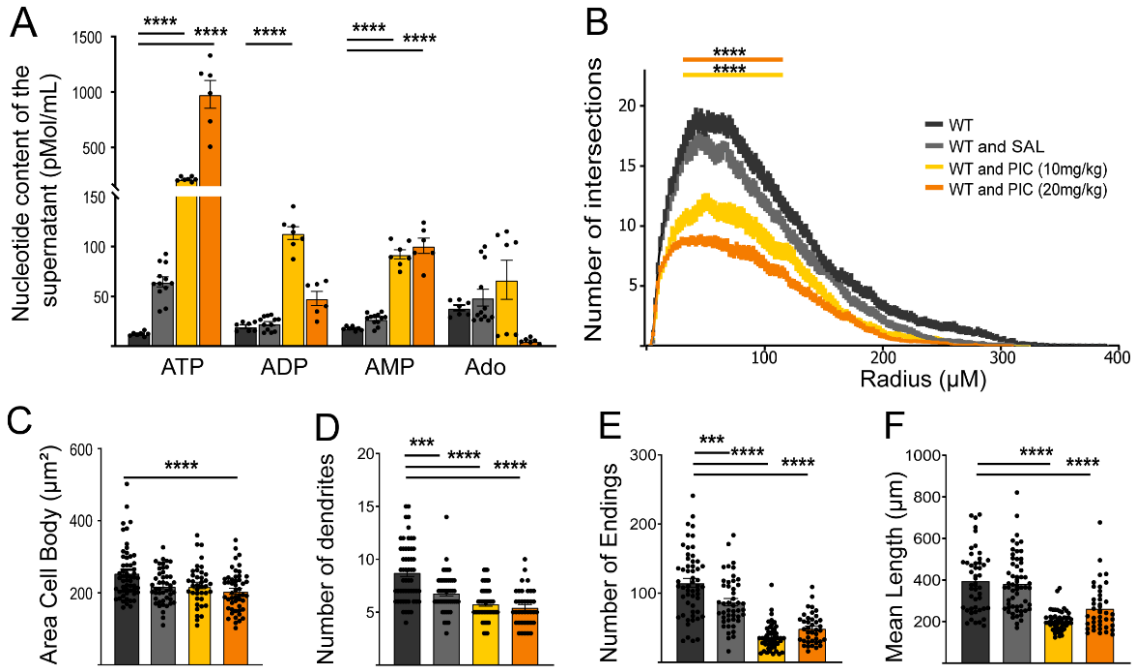

Figure 19. MIA affects dendritic outgrowth in a neurodevelopmental disease model of schizophrenia. (A) Measurement of nucleotide concentrations of the supernatant from primary hippocampal neuron cultures with HPLC technique. (B) Sholl analysis presents the number of intersections versus the distance to the soma from WT and WT treated with Saline or PIC at different doses. Quantification of (C) area cell body, (D) number of primary dendrites, (E) number of endings and (F) mean length of the dendrites for WT at different treatments. The (*) symbol indicates a statistically significant difference between WT and WT exposed to Saline o PIC. *p<0.05, ***p<0.0005, **** p<0.0001. Figure 6A, C-F and K from the article of Mut-Arbona et al.,2023 (143).

HPLC analysis was also performed in a culture medium from saline and PIC treated KO embryos following the same MIA protocol. Briefly, E17.5–E18.5 KO mice embryos of pregnant mouse dams receiving intraperitoneal saline and different doses of PIC (10-20 mg/kg) at E12.5, were dissected and analysed. Here, both 10mg/kg and 20mg/kg PIC increased identically the ATP level in the medium (Fig. 20A). Contrary to the previous analysis, WT in ADP and AMP quantification, the medium levels were significantly decreased in KO cultures after both treatment doses of PIC, respectively. Only adenosine release showed a significant increase in the medium for both dosages. These data indicate that ATP and its breakdown metabolites release are partly P2X7R-mediated cell-autonomous. The imbalance in extracellular purine levels might shed some light on the observed changes in the development of dendritic arborisation, which are not identical to those detected in the absence of pathological signals and could lead to long term changes in offspring behaviour.

Moreover, the observed dendritic deficits in WT-treated pyramidal neurons in the Sholl analysis were not present in KO primary hippocampal neurons in any condition (Fig. 20B) nor other Neurolucida analyses (Fig. 20C-F). Therefore, we can conclude that P2X7R seems necessary to transduce the MIA phenotype and disrupted dendritogenesis related to SCZ or autistic-like phenotypes already detected in young adult offspring.

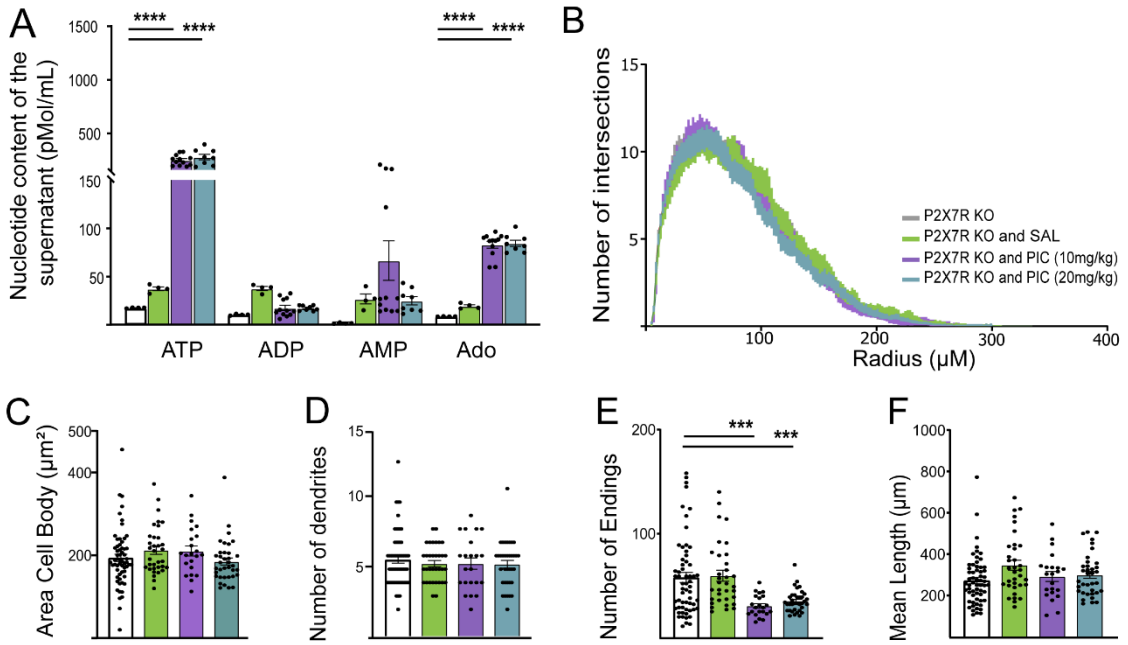

Figure 20. Endogenous P2X7R activation is needed to transduce dendritic deficits in an MIA neurodevelopmental disease model. (A) Measurement of nucleotide concentrations of the supernatant from KO primary hippocampal neuron cultures with HPLC technique (B) Sholl analysis presents the number of intersections versus the distance to the soma from KO and KO treated with Saline or PIC at different doses. Quantification of (C) area cell body, (D) number of primary dendrites, (E) number of endings and (F) mean length of the dendrites for KO at different treatments. The (*) symbol indicates a statistically significant difference between KO and KO exposed to Saline o PIC. ***p<0.0005 ****, p<0.0001. Figure 6B, G-J and L from the article of Mut-Arbona et al.,2023 (143).

5.2.2.2. PIC induces elevated IL-1β in control mice treated with PIC but not in genetically P2X7R deficient mice

In response to pro-inflammatory stimuli such as bacterial lipopolysaccharide or viral RNA sequence (PIC), TLR receptors lead to the transcription of inflammatory cytokine precursors such as pro-IL-1β. The activation of P2X7R due to this inflammatory event comes with forming an active NLRP3 inflammasome. The assembly of inflammasome complexes induces caspase-1 activation, responsible for initiating pro-inflammatory

cytokine production (154). Thus, pro-IL-1β synthesized as an inactive precursor is ready to be released to the extracellular space by caspase-1 as a biologically active form after cleavage (155). Therefore, MIA-induced time-dependent changes on IL-1 β may be an important hallmark for this particular model while playing an important role in P2X7-mediated long-term impact on brain development. Inflammatory changes in IL-1β levels were measured in the MIA model with the higher dose of PIC 24-hours later to the injection in fetal brain from E13.5 embryos with the quantitative analysis of IL-1β using enzyme-linked immunoassay sandwich technique (ELISA) (Fig. 21A). PIC induced elevation in the level of IL-1β in fetal tissue samples of WT mice while genetic deletion of P2X7s prevented significant IL-1β elevation by PIC (Fig. 21B).

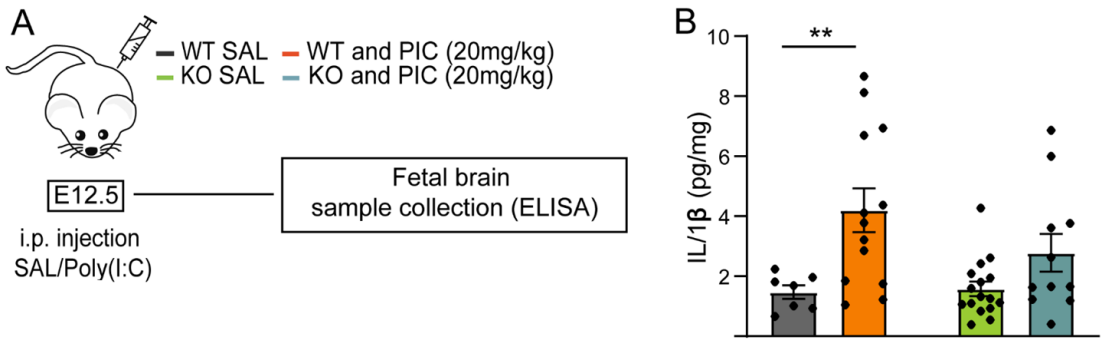

Figure 21. PIC induced elevation in the level of IL-1β in fetal tissue samples of WT mice. Genetic inhibition of P2X7s prevented significant IL-1β elevation by PIC instead. (A) Scheme of the experiment. (B) PIC induced elevation in IL-1β concentrations 24 h after MIA induction in fetal brain samples of WT mice, while this effect was not observed in samples from KO fetal brains. Values measured are expressed in picograms per mg of total protein. **p < 0.005. Figure 7A-B from the article of Mut-Arbona et al.,2023 (143).

5.2.2.3. Endogenous activation of P2X7R partly drives schizophrenic-like behaviour in mice

To comprehend the whole spectrum of the disease, positive, cognitive and negative symptoms were examined. Concerning the positive symptoms, different parameters were tested with open field exploration and sensorimotor performance (acoustic startle reflex and PPI) (Fig. 22). Cognition (spatial working memory, novel object recognition) were tested in young adult female and male mice mixed exposed to MIA (Fig. 23). Negative symptoms were also studied by analysing the sociability with the three-chamber social

preference test (Fig. 24). All the behavioural tests were examined between P60 and P90 in the offspring of WT and KO pregnant mice treated at E12.5 with 20mg/kg PIC.

5.2.2.4. P2X7R drives PIC induced positive-like schizophrenic symptoms in mice

The open field was performed as the first test in the battery of behavioural tests to study locomotor activity, and acoustic startle reflex and PPI were tested one week later (Fig. 22A). While locomotor activity was not affected regarding genotype nor by MIA (Fig. 22B-C), PPI showed some disruptions (Fig. 22D-E). In this protocol, the startle reflex is measured after a loud acoustic stimulus before the main pulse (120dB). For PPI, this was described in this protocol as a reduction of a response to a stimulus. Impairment in PPI was observed at a 20mg/kg dose of PIC in WT animals, and these deficits were not replicated in KO animals with the same treatment (Fig. 22E). Therefore, it can be concluded that P2X7R presence is needed to transduce the PPI deficits related to the positive symptoms observed in humans.

DOI:10.14753/SE.2023.2882

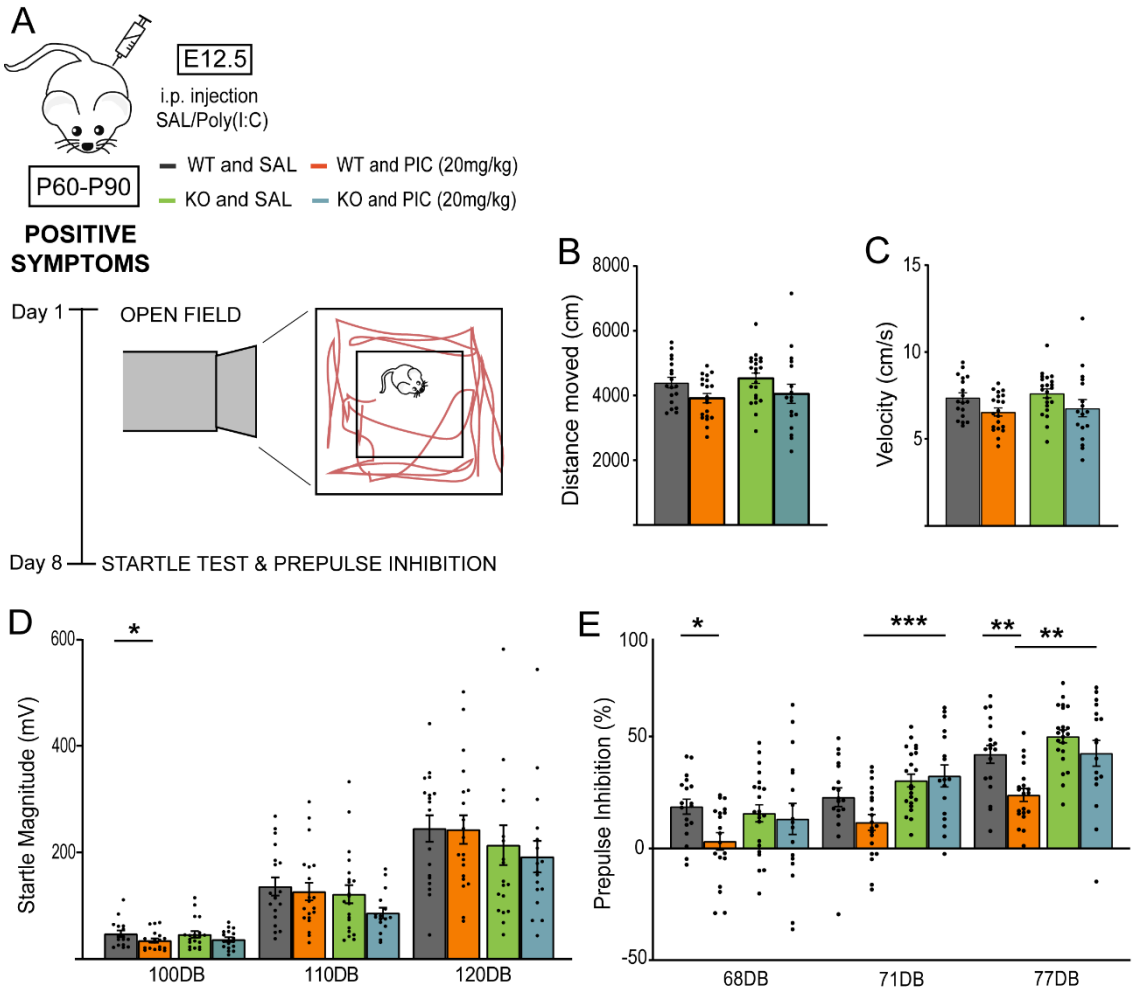

Figure 22. endogenous activation of P2X7R prompts PPI disruptions in mice MIA model. (A) Overview of the experimental protocol. Quantification of (B) Total distance moved (cm) and (C) Velocity (cm/s) are not affected in the open field for WT animals and WT PIC-treated animals. (D) Startle response in WT and WT-PIC treated animals is not affected. (E) Prepulse inhibition is disturbed in WT PIC treated animals. The (*) symbol indicates a statistically significant difference between WT and WT-treated female and male mice. *p<0.05; **, p<0.005. Figure 7C-D and H-I from the article of Mut-Arbona et al.,2023 (143).

5.2.2.5. P2X7R drives PIC induced cognitive deficits in working memory mice

To analyse the cognitive symptoms of schizophrenia in mice, spatial and recognition memory were tested in T-maze spontaneous alternation and novel object recognition test, respectively (Fig. 23A). Interestingly, deficits in working memory in T-maze and novel object recognition, were observed in WT PIC-treated animals, but no difference was observed in the KO-treated cohorts (Fig. 23B-C). Therefore, in this MIA protocol, Endogenous activation of P2X7R is sufficient to elicit cognitive symptoms (deficits in T-

maze and novel object recognition) related to schizophrenic behaviours in male and female offspring.

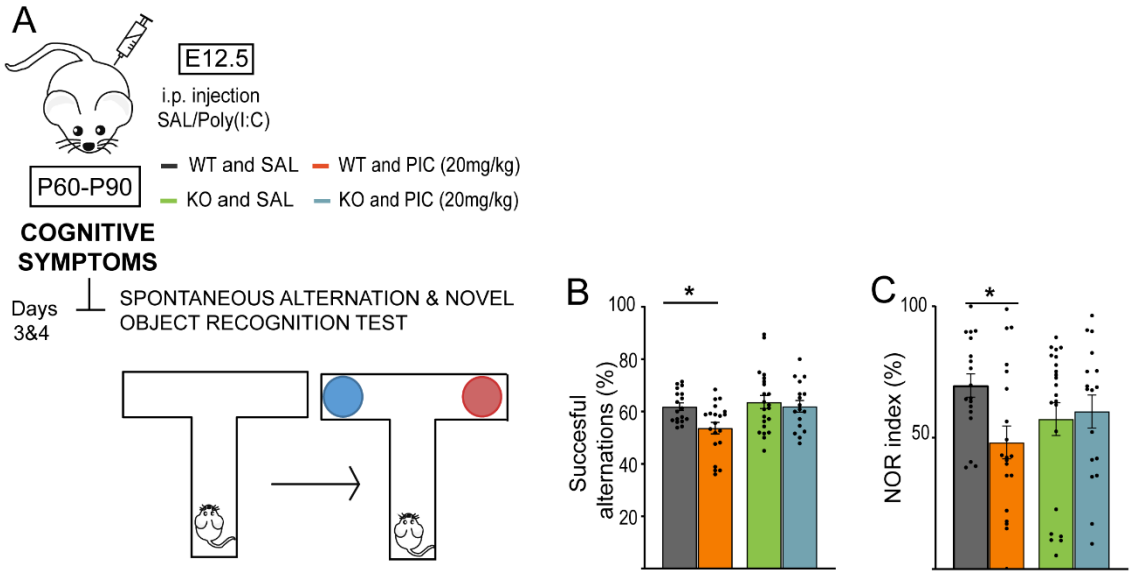

Figure 23. endogenous activation of P2X7R prompts cognitive impairment in the MIA model. (A) Overview of the experimental protocol. Quantification of (B) spontaneous alternation (%) and **(E)** Novel object recognition (NOR index (%)) in the T-maze shows deficits in performance in WT-treated animals. The (*) symbol indicates a statistically significant difference between WT and WT-treated female and male mice. *p<0.05; **, p<0.005. Figure 7E-F from the article of Mut-Arbona et al.,2023 (143).

5.2.2.6. MIA fails to reproduce social withdrawal in mice

There were no significant MIA-induced changes in the cumulative duration spent in the intruder chamber in either genotype in a three-chamber sociability test. Moreover, we observed how independently of their genotype, there is a preference to stay with the intruder in any condition (Fig. 24B). Therefore, we can conclude that social deficits could not be replicated with this model.

DOI:10.14753/SE.2023.2882

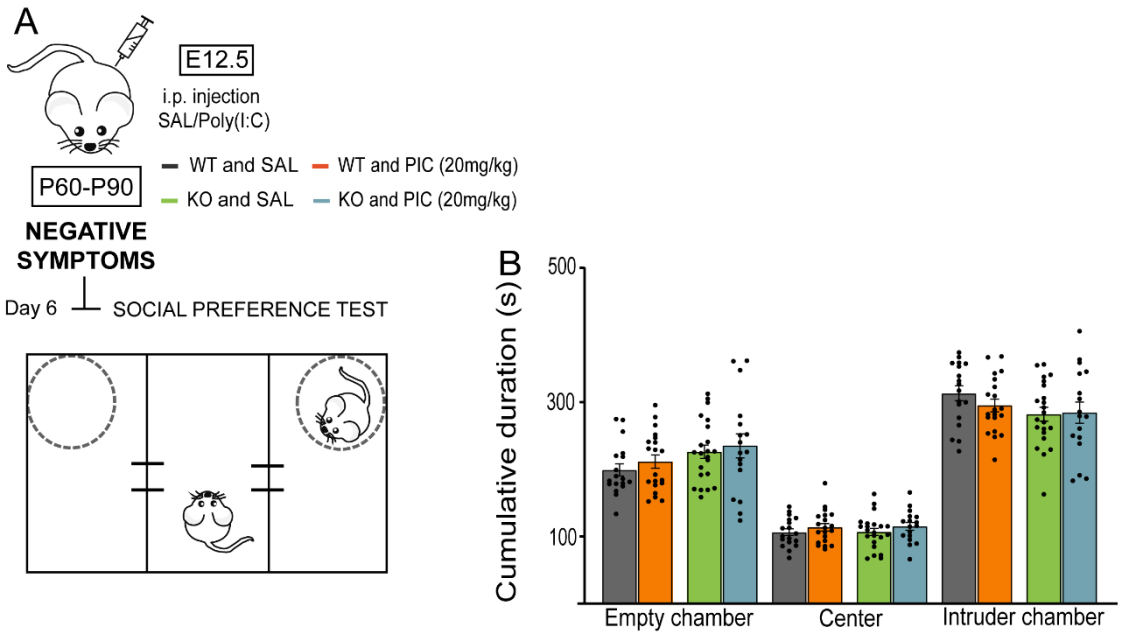

Figure 24. endogenous activation of P2X7R did not elicit social withdrawal in mice. (A) Overview of the experimental protocol. Quantification of (B) cumulative duration (s) in each chamber in a three-chamber sociability test. Figure 7G from the article of Mut-Arbona et al.,2023 (143).

DOI:10.14753/SE.2023.2882

Table 7. Statistical results

Experiment		Statistical analysis	Interaction value	p-value	Post-hoc	p-value	n
qPCR	Fig. 10C	Ordinary one-way ANOVA	F (9, 39) = 2.616	0.0181	Sidak's multiple comparisons test		3,5,3,5,6,6,4, 5,5,7
		Ordinary one-way ANOVA	F (9, 39) = 3.284	0.0046	**DIV1 vs. Div4** Sidak's multiple comparisons test **DIV1 vs. Div4** **DIV1 vs. Div7**	0.0449 0.0088 0.0458	5,5,3,5,6,6,4, 5,5,5
Western Blot	Fig. 10D	Ordinary one-way ANOVA	F (6, 21) = 2.367	0.0665	Dunnett's multiple comparisons test		4,4
					DIV1 vs DIV4	0.0407	
	Fig. 11	Ordinary one-way ANOVA	F (5, 18) = 6.048	0.0019	Tukey's multiple comparisons test		4,4,4,4,4,4
					DIV1WT vs DIV4WT **DIV4WT vs DIV7WT** **DIV4WT vs DIV4KO**	0.0065 0.0305 0.0039	
Calcium Imaging	Fig. 10E	Mann-Whitney		<0.0001			150,196
		Mann-Whitney					135, 196
Sholl analysis	Fig. 13D	Two-way ANOVA	F (191, 21696) = 25.33	<0.0001	Bonferroni's multiple comparisons test		55,60
					from Radius 15 um to 193um	<0.0001	
	Fig 13F	Mann-Whitney		<0.0001			55,60
	Fig. 13G	Unpaired t-test		<0.0001			55,60
	Fig. 13H	Unpaired t-test		<0.0001			55,60
	Fig. 13I	Unpaired t-test		<0.0001			55,60
HPLC	Fig. 13E	Two-way ANOVA	F (1, 36) = 125.4	<0.0001	Sidak's multiple comparisons test		4,7
					ATP **ADP** **AMP** **Ado**	<0.0001 <0.0001 0.0558 <0.0001	
Sholl analysis	Fig. 14B	Two-way ANOVA	F (292, 15835) = 4.231	<0.0001	Bonferroni's multiple comparisons test		45,33,35
					WT vs. ITH15005 from Radius 17 um to 119 um	<0.0001	
					WT vs. JNJ Radius 21 um to 143 um	<0.0001	
	Fig. 14C	Ordinary one-way ANOVA	F (2, 105) = 0.5159	0.5984			45,33,35
	Fig. 14D	Ordinary one-way ANOVA	F (2, 105) = 8.158	0.0005	Sidak's multiple comparisons test		45,33,35
					WT vs. ITH15005 **WT vs. JNJ**	0.0085 0.0006	
	Fig. 14E	Ordinary one-way ANOVA	F (2, 105) = 19.31	<0.0001	Sidak's multiple comparisons test		45,33,35
					WT vs. ITH15005 **WT vs. JNJ**	<0.0001 <0.0001	
	Fig. 14F	Ordinary one-way ANOVA	F (2, 105) = 4.194	0.0177	Sidak's multiple comparisons test		45,33,35
					WT vs. ITH15005	0.0096	

Experiment		Statistical analysis	Interaction value	p-value	Post-hoc	p-value	n
Sholl analysis	Fig. 15B	Two-way ANOVA	F (157, 9954) = 1,252	0,0184	Bonferroni's multiple comparisons test **Radius 151 um to 159 um**	0,0025	30,35
	Fig. 15C	Unpaired t-test		0,8527			30,35
	Fig. 15D	Unpaired t-test		0,2820			30,35
	Fig. 15E	Unpaired t-test		0,0140			30,35
	Fig. 15F	Unpaired t-test		0,0009			30,35
Sholl analysis	Fig.16B	Two-way ANOVA	F (407, 12648) = 2.156	<0.0001	Bonferroni's multiple comparisons test **from Radius 17 um to 85 um**	<0.0001	16,17
	Fig.16C	Mann-Whitney		0.6048			16,17
	Fig.16D	Mann-Whitney		0.2768			16,17
	Fig.16E	Mann-Whitney		0.002			16,17
	Fig.16F	Mann-Whitney		0.0326			16,17
	Fig.16H	Two-way ANOVA	F (250, 5020) = 0.2482	>0.9999			12,10
	Fig.16I	Mann-Whitney		0.2614			12,10
	Fig.16J	Mann-Whitney		0.3066			12,10
	Fig.16K	Mann-Whitney		0.8085			12,10
	Fig.16L	Mann-Whitney		0.7354			12,10
Synaptic strength	Fig. 16M	Unpaired t-test		0.0003			22,18
Sholl Analysis PIC	Fig. 19B	Two-way ANOVA	F (654, 40058) = 13.92	<0.0001	Bonferroni's multiple comparisons test **WT vs. SAL from Radius 23 um to 105 um** **WT vs. 10 from Radius 13 um to 201** **WT vs. 20 from Radius 13 um to 223 um**		55,46,39,50
	Fig. 19A	Two-way ANOVA	F (444, 22052) = 0.5251	>0.9999			55,46,39,50
	Fig. 19C	Ordinary one-way ANOVA	F (3, 186) = 6.703	0.0003	Sidak's multiple comparisons test **WT vs. SAL** **WT vs. 10** **WT vs. 20**		55,46,39,50
	Fig. 19D	Ordinary one-way ANOVA	F (3, 185) = 25.29	<0.0001	Sidak's multiple comparisons test **WT vs. SAL** **WT vs. 10** **WT vs. 20**	0.0002	55,46,39,50
	Fig. 19E	Ordinary one-way ANOVA	F (3, 186) = 55.76	<0.0001	Sidak's multiple comparisons test **WT vs. SAL** **WT vs. 10** **WT vs. 20**		55,46,39,50

Experiment		Statistical analysis	Interaction value	p-value	Post-hoc	p-value	n
Sholl Analysis PIC	Fig. 20F	Ordinary one-way ANOVA	F (3, 186) = 29.50	<0.0001	Sidak's multiple comparisons test **KO vs. SAL** **KO vs. 10** **KO vs. 20**		55,46,39,50
	Fig. 20C	Ordinary one-way ANOVA	F (3, 148) = 1.568	P=0.1997			
	Fig. 20D	Ordinary one-way ANOVA	F (3, 148) = 0.3550	P=0.7856			
	Fig. 20E	Ordinary one-way ANOVA	F (3, 148) = 9.464	P<0.0001	Sidak's multiple comparisons test **KO vs. 10** **KO vs. 20**		
	Fig. 20F	Ordinary one-way ANOVA	F (3, 148) = 2.802	P=0.0420			
HPLC	Fig. 19A	Two-way ANOVA	F (9, 112) = 72.10	<0.0001	Sidak's multiple comparisons test **ATP WT vs. 20** **ATP WT vs. 10** **ADP WT vs. 10**	 <0.0001 <0.0001 0.0166	7,12,7,6
	Fig. 20A	Two-way ANOVA	F (9, 96) = 18.84	<0.0001	Sidak's multiple comparisons test **ATP KO vs. 20** **ATP KO vs. 10** **ADP KO vs. SAL** **AMP KO vs. 10** **ADO KO vs. 20** **ADO KO vs. 10**	 <0.0001 <0.0001 0.0056 0.0062 0.0008 0.0004	4,4,12,8
ELISA	Fig. 21B	Two-way ANOVA			Sidak's multiple comparisons test		7, 13, 16,11
		Interaction	F (1, 43) = 1,897	0,1755	**WT SAL vs WT PIC**	0,0050	
		Treatment	F (1, 43) = 1,393	0,2444			
		Genotype	F (1, 43) = 12,58	0,0010			

DOI:10.14753/SE.2023.2882

Table 8. Behavioural statistical analysis

Experiment & Fig.		Statistical analysis	F-interaction value	p-value	Post-hoc	p-value	n
Object location recognition	Fig. 17A	Unpaired t-test		0.0664			14,13
		No sex differences: Two-way ANOVA [F (1, 23) = 0.6508, p=0.4281]					
	Fig. 17B	Unpaired t-test		<0.0001			
Novel object Recognition	Fig. 17C&G	Unpaired t-test		0.4665			13,13
		Unpaired t-test		0.2647			
		No sex differences: Two-way ANOVA [F (1, 21) = 0.2054, p=0.655]					
	Fig. 17D&H	Mann-Whitney test		<0.0001			
		No sex differences: Two-way ANOVA [F (1, 22) = 0.2653, p=0.6117]					
		Mann-Whitney		<0.0001			
Temporal object recognition	Fig. 17E	Unpaired t-test		0.3855			14,13
		No sex differences: Two-way ANOVA [F (1, 23) = 0.5439, p=0.4683]					
	Fig. 17F	Mann-Whitney		0.0047			
PCP model	Fig. 18B	Two-way ANOVA			Sidak's multiple comparisons test		8,6,10, 12
		Interaction	F (1, 32) = 0.5370	0.4690	**WT Sal vs P2x7r+/gfp PCP**	<0.0001	
		Genotype	F (1, 32) = 10.50	0.0028	**WT PCP vs P2x7r+/gfp PCP**	0.0186	
		Treatment	F (1, 32) = 12.54	0.0012	**P2x7r+/gfp Sal vs P2x7r+/gfp PCP**	0.0353	
	Fig. 18C	Two-way ANOVA			Sidak's multiple comparisons test		8,6,10, 12
		Interaction	F (1, 30) = 1.515	0.2279	**WT Sal vs WT PCP**	0.0043	
		Genotype	F (1, 30) = 0.005544	0.9411	**WT Sal vs P2x7r+/gfp PCP**	0.0349	
		Treatment	F (1, 30) = 13.12	0.0011			
	Fig. 18D	Two-way ANOVA			Sidak's multiple comparisons test		8,6,10, 12
		Interaction	F (1, 34) = 0.2652	0.6099	**WT Sal vs WT PCP**	0.0002	
		Genotype	F (1, 34) = 1.020	0.3197	**WT Sal vs P2x7r+/gfp PCP**	0.0033	
		Treatment	F (1, 34) = 39.73	<0.0001	**WT PCP vs P2x7r+/gfp Sal**	<0.0001	
					P2x7r+/gfp Sal vs P2x7r+/gfp PCP	0.0012	
	Fig. 18E	Two-way ANOVA			Sidak's multiple comparisons test		8,6,10, 12
		Interaction	F (1, 31) = 5.067	0.0316	**WT Sal vs P2x7r+/gfp PCP**	0.0222	
		Genotype	F (1, 31) = 5.067	0.0316	**WT PCP vs P2x7r+/gfp PCP**	0.0173	
		Treatment	F (1, 31) = 5.067	0.0316	**P2x7r+/gfp Sal vs P2x7r+/gfp PCP**	0.0173	

DOI:10.14753/SE.2023.2882

Experiment & Fig.	Statistical analysis	F-interaction value	p-value	Post-hoc	p-value	n
Open field	No sex differences: Two-way ANOVA [F (1, 23) = 0.5439, p=0.4683]					19,22, 20,17
	Fig. 22B Two-way ANOVA					
	Interaction	F (1, 74) = 0.02201	0.8825			
	Treatment	F (1, 74) = 5.489	0.0218			
	Genotype	F (1, 74) = 0.7304	0.3955			
	Fig. 22C No sex differences: Three-way ANOVA [F(1, 69) = 3.254, p=0.0756]					
	Two-way ANOVA					19,22, 20,17
	Interaction	F (1, 74) = 0.04155	0.839			
	Treatment	F (1, 74) = 6.155	0.0154			
	Genotype	F (1, 74) = 0.7932	0.376			
T-maze and Novel object recognition	No sex differences: Three-way ANOVA [F (1, 69) = 2.074 p=0.1544]					19,22, 20,17
	Fig. 23B Two-way ANOVA			Sidak's multiple comparisons test		
	Interaction	F (1, 73) = 2.295	0.1341	**WT vs. 20**	0.0224	
	Treatment	F (1, 73) = 4.477	0.0378			
	Genotype	F (1, 73) = 5.774	0.0188			
	No sex differences: Three-way ANOVA [F (1, 69) = 1.564, p=0.2153]					19,22, 20,17
	Fig. 23C Two-way ANOVA			Sidak's multiple comparisons test		
	Interaction	F (1, 74) = 4.179	0.0445	**WT vs. 20**	0.0251	
	Treatment	F (1, 74) = 2.419	0.1241			
	Genotype	F (1, 74) = 0.002605	0.9594			
Three chamber social test	No sex differences: Three-way ANOVA [F (1, 69) = 0.4612 P=0.4993]					19,22, 20,17
	Fig. 24B Two-way ANOVA					
	Interaction	F (1, 74) = 0.05707	0.8118			
	Treatment	F (1, 74) = 0.003845	0.9507			
	Genotype	F (1, 74) = 1.082	0.3016			
Startle acoustic test	Fig. 22D No sex differences: Three-way ANOVA [F (1, 63) = 0.4812, p=0.4904]					18,22, 20,17
	startle 100DB Two-way ANOVA			Sidak's multiple comparisons test		
	Interaction	F (1, 73) = 0.3223	0.572	**WT vs. 20**	0.0309	
	Treatment	F (1, 73) = 8.677	0.0043			
	Genotype	F (1, 73) = 0.7274	0.3965			
	No sex differences: Three-way ANOVA [F (1, 63) = 0.04105, p=0.8401]					18,22, 20,17
	startle 110DB Two-way ANOVA					
	Interaction	F (1, 73) = 0.1835	0.6696			
	Treatment	F (1, 73) = 2.264	0.1367			
	Genotype	F (1, 73) = 0.5829	0.4476			
	No sex differences: Three-way ANOVA [F (1, 63) = 1.181, p=0.2814]					18,22, 20,17
	startle 120DB Interaction	F (1, 73) = 0.05067	0.8225			
	Treatment	F (1, 73) = 2.309	0.133			
	Genotype	F (1, 73) = 0.5806	0.4485			

DOI:10.14753/SE.2023.2882

Experiment & Fig.	Statistical analysis	F-interaction value	p-value	Post-hoc	p-value	n
PPI	Fig. 22E					18,22, 20,17
	68B	No sex differences: Three-way ANOVA [F (1, 63) = 1.777, p=0.1874]				
	Two-way ANOVA			Sidak's multiple comparisons test		
	Interaction	F (1, 73) = 2.447	0.122	**WT vs. 20**	0.026	
	Treatment	F (1, 73) = 4.173	0.0447			
	Genotype	F (1, 73) = 1.694	0.1971			
	71DB	No sex differences: Three-way ANOVA [F (1, 63) = 0.5386, p=0.4657]				
	Two-way ANOVA			Sidak's multiple comparisons test		
	Interaction	F (1, 73) = 1.725	0.1932	**WT20 vs KO20**	0.0009	
	Treatment	F (1, 73) = 0.6170	0.4347			
	Genotype	F (1, 73) = 15.78	0.0002			
	77DB	No sex differences: Three-way ANOVA [F (1, 63) = 0.002469, p=0.9605]				
	Two-way ANOVA			Sidak's multiple comparisons test		
	Interaction	F (1, 74) = 1.449	0.2325	**WT vs. 20**	0.0054	
	Treatment	F (1, 74) = 10.04	0.0022	**WT20 vs KO20**	0.0026	
	Genotype	F (1, 74) = 13.30	0.0005			

6. Discussion

6.1. P2X7R is needed in neurodevelopmental maturation in physiological conditions

The main results of the thesis are the reported changes in dendritic outgrowth and synaptic strength in pyramidal hippocampal neurons from P2X7R-deficient mice, affecting normal cognitive performance on young KO animals. Moreover, it was observed that both ATP and its metabolites influence maturation and dendritic outgrowth and that, like P2X7R, other purinergic receptors might also participate in this regulation. Therefore, at the initial stages of purinergic system development, a high degree of complexity (enzyme and receptor diversity, multiple roles) is expected, although the systems mature over development to adulthood. Especially during the development of the brain, extracellular ATP and nucleotides and nucleosides are higher as they need to regulate many neural processes. Progressively, a switch occurs when ATP signals "danger" in the adult brain, a marker for pathology and neuroinflammation. These results emphasize the complexity of the purinergic system observed in the responses of P2X7R to ATP and the dual role in physiology and pathology in an individual's life course. Also, it might be hypothesised that ATP levels within a neuronal system may regulate both conditions due to its integrated roles as an intracellular second messenger in biology.

6.1.1. P2X7R is highly expressed at the early stages of development influencing the proper development of dendrites

P2X7R is well-known for its pleiotropic effects as a gateway to various neuronal pathologies and neuroinflammation. Therefore, it is a therapeutic target for CNS diseases in adults and during ageing (156,157). However, its role in early neuronal development is still unclear, although it is expressed in the embryonic brain early at E14 (158) and is involved in neuronal growth and differentiation regulation (159). Some *in vitro* studies in primary hippocampal neurons have pointed out similar regulatory effects of P2X7R on axonal growth (61).

Purinergic signalling gained some attention regarding its direct involvement in neurodevelopmental processes in prenatal life and its role in neurodevelopmental psychiatric disorders has also been proposed. P2X7R expression in neural stem cells and immature neurons during the embryonic period was recently reviewed (160). It has been demonstrated that the receptor is upregulated during embryonic stem cell proliferation

and that activity is suppressed during neuronal differentiation, showing that it plays a specific role in the initiation of proliferation and differentiation in earlier stages (51). In another study in neuronal precursor cells, among other receptors, P2X7R downregulation also accompanied neuronal differentiation (161).

Here, the decrease in P2X7R expression during development in the *in vitro* culture systems explains the low expression of this receptor in adulthood. These data indicate that P2X7R may initially mediate neuronal maturation and then be switched off or internalized, allowing it to respond to stimuli under pathologically high extracellular ATP levels in adulthood. However, in cell cultures, especially using immortalized cell lines, the expression and function of different receptors and signalling pathways might be the subject of change by the culturing procedure. Indeed, a recent study in human derived pluripotent cells showed that the P2X7R is localized on the cell membrane of microglia and NPCs but the presence of P2X7R was present in the fraction containing the intracellular proteins (IC) in the case of neuronal cells (58). In this results, P2X7R is present in both intracellular and extracellular regions of the primary hippocampal neurons, being higher at the first days *in vitro*.

For the first time, a morphological difference in dendritic outgrowth in primary hippocampal neurons in P2X7R-deficient mice is reported. These findings might shed some light on the receptor's *in vitro* time-dependent expression and behaviour as a modulator of induced dendritic outgrowth in hippocampal pyramidal cells under physiological conditions. Moreover, findings have been reconfirmed in a concentration-dependent manner in wild-type neurons co-cultured with specific P2X7R antagonists. Both JNJ47965567 and the recently synthesised ITH15004 antagonists showed the same effect *in vitro*. As well, the study of the new antagonists in physiological conditions will be important to understand the mechanism of action of the drug on the receptor permitting further *in vitro* and *in vivo* studies in CNS diseases for the development of potential clinical targets.

The expression of P2X7R in hippocampal astrocytes and its further stimulation was shown to indirectly influence the functionality of neurons (133). To exclude the contribution of astroglia, we treated our cells with an inhibitor of astroglia proliferation, which decreased the population of astroglia to approximately less than 10%. However, we still cannot rule out the indirect effect of signaling molecules derived from residual

astrocytes on neuronal morphology, mainly when the expression of the receptor fluctuated after CAR application.

When ARL 67156, a specific inhibitor of NTPDase, was applied, extracellular ATP and ADP levels were elevated. In line with previous results, this treatment elicited a stimulatory effect on dendritic outgrowth, increasing the number of endings. This finding suggests that in culture systems, ATP, ADP and their breakdown products in the medium regulated the growth of dendrites through other non-P2X7-Rs, counterbalancing the action of endogenous ATP on P2X7Rs. Indeed, ATP regulates the proliferation and migration of embryonic rat-derived neural stem and precursor cells by activating various purinergic receptors in addition to P2X7R (161).

Another suggested role for P2X7R is as a mediator of phagocytosis and as a scavenger receptor in the CNS (162). P2X7Rs show high expression during earlier stages of neurogenesis on human neural precursor cells and neuroblasts with high phagocytic activity towards apoptotic neuronal cells (163). Phagocytosis in the early stages of embryonic life could potentially be the principal role of P2X7Rs without ATP activation, influencing the maturation process of induced branching in primary neurons from the hippocampus.

Nevertheless, it seems that the role of P2X7R on differentiation and proliferation might depend on the cell type. While the upregulation of the receptors seems to contribute to the maintenance of the proliferation in mouse embryonic stem cells itself (51), P2X7R activation in primary astroglia produce a growth arrest (164). Interestingly, it is a fundamental principle of neocortical and hippocampal development is that neurogenesis and astrogenesis are temporally segregated processes (165). In previous studies, the down-regulation of the receptor expression at P19 embryonal carcinoma cells by RNA interference affected neuronal differentiation and phenotype specification, thus resulting in decreased cell proliferation and GFAP expression. These results suggested the need for functional P2X7 receptors in the process of gliogenesis (44).

Together with these results, P2X7R might be expressed differentially during neural differentiation depending on the cell fate lineage and whether it is needed for neurogenesis or gliogenesis. Therefore, it can be hypothesized whether it is firstly highly expressed in neuron precursors and during neurogenesis until the process of proliferation and neuronal maturation ends. This note might also explain why the P2X7R is still present

in adult niches for neurogenesis in adulthood. On the other hand, however, the opposite occurs in astroglia, where P2X7R is expressed higher later in development during gliogenesis. Undoubtedly, all these data indicate the importance of purinergic signalling for cell fate determination, early embryogenesis and brain development.

Ultimately, based on these results, the transient expression of P2X7 receptors in the early stages of development might indicate that purinergic signalling has some refined functional implications in the embryonic stages rather than in the adult CNS. The results are a shred of direct evidence that P2X7R directly impacts neuronal outgrowth, maturation and differentiation. It is also likely that ATP and other metabolites, under-regulated release, play a significant role in these processes inducing multiple signalling pathways, creating a synergy between growth factors, cytokines, purines/pyrimidines and, ultimately, purinergic receptors, where P2X7R is proved to have a functional role. Future directions would be to study the purinergic system in development as a dynamic and interactive signalling system, as studying a single element might provide a biased interpretation of the results.

6.1.2. Morphological and synaptic deficits are cell-specific in the hippocampus and affect proper cognitive performance in KO mice

P2X7R-positive neurons were found in hippocampal pyramidal cell layers among other areas in the rat brain using P2X7R mRNAs isotopic in situ hybridisation (166), in a humanized mouse *P2RX7* knock-in model (167) and recently in human excitatory but not inhibitory neurons by single-nucleus RNA-sequencing (168). In hippocampal slices functional expression of P2X7Rs has also been demonstrated (55). The results *in vitro* are also substantiated in hippocampal slices, a model system where neuronal architecture and the trisynaptic structure of the hippocampal network is preserved. The morphology in late development in acutely prepared hippocampal slices of P20-26 mice from both genotypes was also analysed. Firstly, they displayed less complex dendritic arborisation in the absence of P2X7R reconfirming results obtained in the primary culture. Then, the synaptic strength seems also to be compromised as the spine density of the pyramidal cells from CA1 region is substantially decreased. Additionally, we found a region specificity in P2X7R showing morphological deficits in pyramidal neurons from CA1 region but not in CA3 region-specificity in pyramidal neurons. These differences might

suggest a diversity of roles in different cell types or areas in the brain for this receptor, which needs further investigation. These differences indicate a novel role of P2X7R during the development and maturation of this cell type.

Regarding the biological correlates of these results, behavioural analysis elucidates the morphological correlates with recognition and episodic memory engagement related to different brain regions such as perirhinal and prefrontal cortex, but especially hippocampus. These novel tests assess the what, where and when components of episodic memory (144). While the time of exploration doesn't differ in both genotypes, a crucial decrease is observed in performance for the three tests: OL, NOR and TOR, which can correspond to the deficits observed in pyramidal neurons in slices. Interestingly, these deficits in cognitive performance are counterbalanced in the adults, as no significant differences were observed in the young adults in NOR. It is possible that task emergence, which is dependent on the maturation of associated brain regions, is delayed in P2X7R-deficient mice.

6.2. P2X7R endogenous activation is needed for transducing a schizophrenic-like phenotype

Here, it was demonstrated that dendritic outgrowth is compromised in a model of MIA-induced schizophrenia in a manner mediated by P2X7R. Dendritic deficits reflected on subsequent impairment of cognitive function in young adult offspring in this model and positive-like symptoms. Negative symptoms and hyperlocomotion were exacerbated in an overexpressing-P2X7R mice in an acute mouse model of PCP in the young adults, instead. Overall, the results corroborate the contribution of P2X7R to the pathogenesis of schizophrenia in different mouse models.

Using summary statistics from recent meta-analysis genome-wide association studies in SCZ patients is identified significant enrichment of SCZ risk heritability in excitatory and inhibitory neurons. P2X7R has been indicated as a strong candidate gene, driving a schizophrenia association signal. Besides the lack of functionally relevant polymorphisms identified in the proposed P2X7R candidate gene region, it corroborates our findings that neuroimmune mechanisms during SCZ pathogenesis and the relation in the apparent neuronal dysregulation with P2X7R function in human SCZ patients (130). It has previously demonstrated the pivotal role of P2X7R in the MIA mouse of autism

(136), using a MIA protocol. Interestingly, time, immunoactivator and the designed dose are crucial for developing different alterations in cytokine levels and behavior paradigms during young adulthood (169,170,106). Likewise, P2X7R involvement was recently reported in the phencyclidine (PCP) induced acute and subchronic models of schizophrenia (10,132,171,172). Supporting our data, a similar impairment in dendritic outgrowth has also been observed subjected to prenatal PIC treatment with the involvement of the TLR3 receptor, a receptor upstream from the P2X7-NLRP3 inflammatory pathway (173).

6.2.1. Deficits in dendritic morphology are a good correlate for the cognitive symptoms present in schizophrenic patients

Deficiencies in dendrite morphology are thought to be relevant to diverse neurological disorders related to intellectual disabilities and cognitive deficits, for example, in ASD, Rett syndrome and Down syndrome (174). Neurons in some regions of the brain affected in schizophrenia show reduced dendritic length (175) and other alterations of dendritic morphology of pyramidal cells (176,177) suggesting an abnormal dendritic outgrowth in schizophrenic patients (178).

On the other hand, here we also showed for the first time that the dendritic outgrowth is compromised in a model of MIA-induced schizophrenia in a manner mediated by P2X7R. The morphological deficits in pyramidal cells have been proposed as an important marker of cognitive deficits in neurological disorders (179,180). The study of the dendritic deficits in pathological conditions in our disease model with the subsequent deficit in cognitive behaviour test in young adult offspring could correlate with the human pathophysiology. Indeed, deficits in primary basilar dendrites from layers II and V of the medial prefrontal cortex are observed in schizophrenic patients (181).

Here, we report a correlation between morphological and behavioural hallmarks in a mouse model of neurodevelopmental disorder. These deficits were not observed in P2X7R-deficient mice, indicating a dual and opposing role for P2X7R during normal neuronal development and in neurodevelopmental psychiatric disorders. In our experiments, the endogenous activation of the receptor seemed necessary to transduce MIA led to the development of a schizophrenic phenotype in offspring since PIC treatment did not decrease dendritic outgrowth or induce behavioural symptoms in mice

with genetic P2X7Rs deficiency. Notably, deficits in the dendritic outgrowth of neurons derived from naïve or saline-treated KO mice were observed in these experiments, but maternal PIC treatment did not elicit further deficits. Nevertheless, the exact mechanism whereby P2X7R activation during MIA leads to deficits in dendritic morphology and subsequent behavioural alterations requires further investigation.

6.2.2. P2X7R endogenous activation elicits hyperlocomotion and social withdrawal in a PCP model of schizophrenia

Previous studies have addressed the role of P2X7R in PCP models of schizophrenia, as genetic deletion or pharmacological inhibition of P2X7R signalling reduces schizophrenia-like behavioural alterations (132). Here, we show how the PCP influences positive and negative symptoms in mice are partly modulated by P2X7R functional expression. For the first time, the overexpression of the receptor in P2rx7tg/+ young-adult animals with acute PCP was tested, which complemented the results obtained with the inhibition of the receptor. Thus, heterozygous animals displayed exacerbated behaviour, showing positive-like symptoms.

In this acute model, there is a clear increase in hyperactivity and stereotypical behaviour in P2X7R-overexpressing animals with PCP but also with basal overexpressing animals. However, the social deficits were not so pronounced in our experiment. Recently, it has been investigated the long-term behavioural and histological differences between acute and subchronic models of PCP in adult C57BL/6J mice. It turned out that subchronic but not acute models induce working memory deficits which relates with more complex changes in activity patterns (146). It has been shown in this acute PCP model an increase in stained c-fos neurons mainly in the medial prefrontal cortex subregions, more precisely in the layer V of infralimbic and prelimbic areas (153). These results correspond with the already established implication of the prefrontal cortex on the pathogenesis of schizophrenia (182). Here, the hyperactivation of the receptor might affect the excitability of the mPFC circuitry.

6.2.3. P2X7R endogenous activation elicits cognitive and positive symptoms of schizophrenia but not social withdrawal in MIA

Neurodevelopmental disruption in the early stages of pregnancy influences an individual's susceptibility to psychiatric disorders in later stages of postnatal life (183). However, the time window between the insult and its consequence might depend on events during brain development. As neurogenesis starts in mice around gestation day 12.5 (184), we could connect disruptions in this embryonic day, such as an inflammation event, with cognitive deficits observed in the young adult mice. Although other events occurring during and after pre-and postnatal development might obscure the interpretation of the behavioural results, the MIA model is considered a relevant tool for the study of schizophrenia (185).

PIC has a sex-dependent effect on the gene expression and protein levels of pro-inflammatory cytokines in the hippocampus when administered intracerebroventricularly (186), which highlights the importance of the use of both sexes in the study of neuroinflammatory diseases. However, these results do not translate into the behavioural alterations observed in our model of MIA. Interestingly, in a MIA model, PIC treatment was found to induce a sex-dependent decrease in the number of Purkinje cells in the cerebellum in adolescence and social deficits were observed specifically in adolescent males (187). In contrast, these deficits are not observed in our young adults. Factors such as the batch and source of PIC (170), the caging system (188), or even the time point of the study in mice can elicit higher variability across different studies, making it harder to find a robust phenotype. Researchers have argued that high variability when modelling psychiatric disorders could be related to sex differences (189), but, generally, only male rodents are used. Recently, more studies have focused on the affection of MIA in females (171). However, no statistical differences between the two sexes were observed in this model (Table 8). Even with the high variability among the treated animals, there are significant alterations in their behaviour reminiscent of positive (PPI alternations) and cognitive (deficits in working memory) symptoms of schizophrenia. These findings in behaviour correspond with morphological deficits in the pyramidal neurons from the hippocampus *in vitro* and cognitive impairments observed in WT-treated animals but not KO-animals.

Environmental factors can also be important in the study of neurodevelopmental diseases. Therefore, a priming/multi-hit model using an inflammatory reaction as a primer susceptibility factor followed by a second stressor during the juvenile period should be used to increase the validity of the study of these multifactorial disorders such as SCZ and ASD. Interestingly, P2X7R KO mice present a basal anti-depressive phenotype when exposed to the tail suspension test and an attenuated anhedonia response in the sucrose preference test (190,191). Notably, it has been suggested that some tricyclic antidepressants reduce NLRP3, caspase-1, IL-1β and IL-18 in patients' blood samples, suggesting that, in some way, antidepressants modulate the activation and release of inflammatory components (192). Then, if neuroinflammation exacerbates a stress reaction thus, the KO mice exposed to MIA might be less vulnerable to stressors during their lifetime and, therefore, less vulnerable to developing an SCZ phenotype in young adulthood.

In conclusion, an exacerbated inflammatory reaction in pathological conditions is critical for developing a compromised nervous system. The role of P2X7R in initiating a neuroinflammatory reaction is required for modulating both behavioural and structural changes in the brain in mood and psychiatric disorders. However, the mechanism by which P2X7R is endogenously activated under these conditions and whether the behavioural changes elicited are different among different models and treatments need to be further examined.

DOI:10.14753/SE.2023.2882

7. Conclusions

The following conclusions can be drawn from the studies performed regarding the physiological studies:

1. Higher transient expression of P2X7R is necessary for normal dendritic outgrowth during neuronal development, proliferation, and maturation, and its downregulation after the first stages of development relegates the receptor to pathological conditions in the adulthood.
2. Morphological and synaptic deficits are cell-specific in the hippocampus.
3. Behavioural deficits related to cognitive performance are present at the youngest stages but not in the adulthood, showing a slower maturation process in P2X7R-deficient mice.

The following conclusions can be drawn from the studies performed regarding pathological studies:

1. In a PCP model, P2X7R endogenous activation elicits social withdrawal performance and hyperactivity.
2. Endogenous activation of the receptor in a MIA model compromises dendritic outgrowth *in vitro* and might contribute to developmental and cognitive behavioural deficits in a mouse model of schizophrenia instead.
3. Neuroinflammation in mice during the second trimester of pregnancy partially reproduces the symptoms of schizophrenia observed in young patients, possibly mediated by the endogenous activation of P2X7R during the inflammatory insult. Therefore, this highlights the translational potential of P2X7R as a therapeutic target for schizophrenia.

Therefore, P2X7R has different regulatory functions depending on the stage of maturation (development or young adulthood) and whether receptor activation occurs. Additionally, activated P2X7R appears to have a pivotal role during pathological inflammatory events in immune activation models such as the MIA model, driving schizophrenia-like behaviours.

DOI:10.14753/SE.2023.2882

8. Summary

Higher extracellular ATP operates as a "danger" molecule under pathological conditions through purinergic receptors, including the ionotropic P2X7 receptor (P2X7R). Its endogenous activation is associated with neurodevelopmental disorders; however, its function during early embryonic stages remains largely unclear.

The main objective was to determine the role of P2X7Rs in regulating neuronal outgrowth. For this purpose, dendritic branching was established as a marker for correct brain development, whilst abnormal dendritic branching is a hallmark of certain neurodevelopmental disorders, such as schizophrenia. Sholl analysis was performed for wild-type and P2X7R genetically deficient and pharmacologically inhibited primary murine hippocampal neurons and acute hippocampal slices. Following a downregulation in the brain that relegates the receptor to a pathological condition, the transient expression of P2X7R during development impacted the proper development of the CNS and cognitive performance.

Therefore, the morphological investigations were extended to a maternal immune activation (MIA) in vitro model for schizophrenia (SCZ) and subsequently to the MIA-induced behavioural deficits in young adult mice. As a result, either gene deficiency or pharmacological blockage of P2X7R leads to branching deficits in physiological conditions. On the other hand, the pathological activation of the receptor also leads to deficits in dendritic outgrowth in wild-type but not knockout primary neurons exposed to maternal immune activation. Finally, only wild-type treated mice displayed schizophrenia-like behavioural and cognitive deficits. In another acute PCP model of SCZ, the overexpression of P2X7R showed exacerbated stereotypy and locomotor activity, showing the receptor's role in the disease's evolution.

In conclusion, P2X7R has different physiological and pathological functions, and its fine-tuned activity impacts the correct CNS functionality and behaviour. It is demonstrated that its endogenous activation has a pivotal role during pathological inflammatory events (i.e., when it is activated in an immune activation model like MIA during pregnancy or during an acute effect of PCP treatment, driving schizophrenia-like behaviours).

DOI:10.14753/SE.2023.2882

8. Összefoglalás

A magasabb extracelluláris ATP patológiás körülmények között "veszélyes" molekulaként működik a purinerg receptorokon, köztük az ionotróp P2X7 receptoron (P2X7R) keresztül. Endogén aktivációja idegrendszeri fejlődési rendellenességekkel hozható összefüggésbe; azonban a korai embrionális stádiumokban betöltött funkciója még mindig nagyrészt tisztázatlan.

A fő cél az volt, hogy meghatározzuk a P2X7R-ek szerepét a neuronok növekedésének szabályozásában. Ebből a célból a dendritikus elágazást a helyes agyfejlődés markereként határoztuk meg, míg a rendellenes dendritikus elágazás bizonyos neurofejlődési rendellenességek, például a skizofrénia jellemzője. Sholl-analízist végeztünk vad típusú és P2X7R genetikailag hiányos és farmakológiailag gátolt primer egér hippokampusz neuronokon és akut hippokampusz szeleteken. A receptort patológiás állapotba helyező agyi downregulációt követően a P2X7R átmeneti expressziója a fejlődés során befolyásolta a CNS megfelelő fejlődését és a kognitív teljesítményt.

Következtetésképpen a morfológiai vizsgálatokat kiterjesztettük a szkizofrénia (SCZ) anyai immunaktiváció (MIA) in vitro modelljére, majd a MIA által kiváltott viselkedési hiányosságokra fiatal felnőtt egerekben. Ennek eredményeként mint a génhiány, mint a P2X7R farmakológiai blokkolása elágazási hiányosságokhoz vezetett fiziológiás körülmények között. Másrészt a receptor patológiás aktivációja szintén a dendritikus elágazás hiányosságaihoz vezetett a vad típusú, de nem knockout primer neuronokban, amelyek anyai immunaktivációnak vannak kitéve. Végül, csak a vad típusú kezelt egerek mutattak skizofréniához hasonló viselkedési és kognitív deficitet. Az SCZ egy másik, akut PCP modelljében a P2X7R túlzott expressziója súlyosbodott sztereotípiát és mozgásszervi aktivitást mutatott, ami bizonyítja a receptornak a betegség kialakulásában betöltött szerepét.

Összefoglalva, a P2X7R különböző fiziológiai és patológiai funkciókkal rendelkezik, finomhangolt aktivitása befolyásolja a megfelelő CNS-funkcionalitást és viselkedést. Kimutattuk, hogy endogén aktivációja kulcsfontosságú szerepet játszik a patológiás gyulladásos események során (azaz amikor immunaktivációs modellben aktiválódik, mint a MIA a terhesség alatt, vagy a PCP-kezelés akut hatása alatt, ami skizofréniaszerű viselkedést vált ki).

9. Bibliography

1. Burnstock G. Purinergic signalling: From discovery to current developments. Experimental Physiology. 2014;99(1):16–34.

2. Linden J, Koch-Nolte F, Dahl G. Purine Release, Metabolism, and Signaling in the Inflammatory Response. Annual Review of Immunology. 2019;37:325–47.

3. Junger WG. Immune cell regulation by autocrine purinergic signalling. Nature Reviews Immunology. 2011 Feb 18;11(3):201–12.

4. Burnstock G, Verkhratsky A. Evolutionary origins of the purinergic signalling system. Acta Physiologica. 2009 Apr;195(4):415–47.

5. Khakh BS, North RA. Neuromodulation by extracellular ATP and P2X receptors in the CNS. Neuron. 2012 Oct 4;76(1):51–69.

6. Chang CP, Wu KC, Lin CY, Chern Y. Emerging roles of dysregulated adenosine homeostasis in brain disorders with a specific focus on neurodegenerative diseases. Journal of Biomedical Science. 2021 Oct 11;28(1):70.

7. Verderio C, Matteoli M. ATP in neuron-glia bidirectional signalling. Brain Research Reviews. 2011 Jan 7;66(1–2):106–14.

8. Neary JT, Kang Y, Shi YF. Cell cycle regulation of astrocytes by extracellular nucleotides and fibroblast growth factor-2. Purinergic Signalling. 2005 Dec;1(4):329–36.

9. Yamazaki Y, Fujii S. Extracellular ATP modulates synaptic plasticity induced by activation of metabotropic glutamate receptors in the hippocampus. Biomedical Research (Japan). 2015;36(1):1–9.

10. Calovi S, Mut-Arbona P, Sperlágh B. Microglia and the Purinergic Signaling System. Neuroscience. 2019 Dec 21;405:137–47.

11. Franco R, Lillo A, Rivas-Santisteban R, Reyes-Resina I, Navarro G. Microglial adenosine receptors: From preconditioning to modulating the M1/M2 balance in

activated cells. Cells [Internet]. 2021 [cited 2022 Aug 2];10(5). Available from: https://doi.org/10.3390/cells10051124

12. Negro S, Bergamin E, Rodella U, Duregotti E, Scorzeto M, Jalink K, et al. ATP released by injured neurons activates schwann cells. Frontiers in Cellular Neuroscience. 2016;10(MAY):134.

13. Zimmermann H. Nucleotide signaling in nervous system development. Pflugers Archiv European Journal of Physiology. 2006 Aug;452(5):573–88.

14. Burnstock G, Ulrich H. Purinergic signaling in embryonic and stem cell development. Cellular and Molecular Life Sciences. 2011;68(8):1369–94.

15. Cavaliere F, Donno C, D'Ambrosi N. Purinergic signaling: A common pathway for neural and mesenchymal stem cell maintenance and differentiation. Frontiers in Cellular Neuroscience. 2015 Jun 2;9(JUNE):211.

16. Tierney AL, Nelson CA. Brain Development and the Role of Experience in the Early Years. Zero to three. 2009 Nov 1;30(2):9–13.

17. Weissman TA, Riquelme PA, Ivic L, Flint AC, Kriegstein AR. Calcium waves propagate through radial glial cells and modulate proliferation in the developing neocortex. Neuron. 2004 Sep 2;43(5):647–61.

18. Götz M, Huttner WB. The cell biology of neurogenesis. Nature Reviews Molecular Cell Biology. 2005 Nov;6(10):777–88.

19. Pearson RA, Dale N, Llaudet E, Mobbs P. ATP released via gap junction hemichannels from the pigment epithelium regulates neural retinal progenitor proliferation. Neuron. 2005 Jun 2;46(5):731–44.

20. Schwindt TT, Trujillo CA, Negraes PD, Lameu C, Ulrich H. Directed differentiation of neural progenitors into neurons is accompanied by altered expression of P2X purinergic receptors. Journal of Molecular Neuroscience. 2011 Jul;44(3):141–6.

21. del Puerto A, Wandosell F, Garrido JJ. Neuronal and glial purinergic receptors functions in neuron development and brain disease. Frontiers in Cellular Neuroscience [Internet]. 2013 [cited 2022 May 11];(OCT). Available from: www.frontiersin.org

22. Shukla V, Zimmermann H, Wang L, Kettenmann H, Raab S, Hammer K, et al. Functional expression of the ecto-ATPase NTPDase2 and of nucleotide receptors by neuronal progenitor cells in the adult murine hippocampus. Journal of Neuroscience Research. 2005 Jun 1;80(5):600–10.

23. Hogg RC, Chipperfield H, Whyte KA, Stafford MR, Hansen MA, Cool SM, et al. Functional maturation of isolated neural progenitor cells from the adult rat hippocampus. European Journal of Neuroscience. 2004 May;19(9):2410–20.

24. McCarthy AE, Yoshioka C, Mansoor SE. Full-Length P2X7 Structures Reveal How Palmitoylation Prevents Channel Desensitization. Cell. 2019 Oct 17;179(3):659-670.e13.

25. Habermacher C, Dunning K, Chataigneau T, Grutter T. Molecular structure and function of P2X receptors. Neuropharmacology. 2016 May 1;104:18–30.

26. Di Virgilio F, Giuliani AL, Vultaggio-Poma V, Falzoni S, Sarti AC. Non-nucleotide agonists triggering P2X7 receptor activation and pore formation. Frontiers in Pharmacology. 2018 Feb 1;9(FEB):39.

27. Donnelly-Roberts DL, Namovic MT, Han P, Jarvis MF. Mammalian P2X7 receptor pharmacology: Comparison of recombinant mouse, rat and human P2X7 receptors. British Journal of Pharmacology. 2009;157(7):1203–14.

28. North RA. Molecular physiology of P2X receptors. Physiological Reviews. 2002;82(4):1013–67.

29. Di Virgilio F, Schmalzing G, Markwardt F. The Elusive P2X7 Macropore. Trends in Cell Biology. 2018 May;28(5):392–404.

30. Franchi L, Eigenbrod T, Muñoz-Planillo R, Nuñez G. The inflammasome: A caspase-1-activation platform that regulates immune responses and disease pathogenesis. Nature Immunology. 2009;10(3):241–7.

31. Calzaferri F, Ruiz-Ruiz C, de Diego AMG, de Pascual R, Méndez-López I, Cano-Abad MF, et al. The purinergic P2X7 receptor as a potential drug target to combat neuroinflammation in neurodegenerative diseases. Medicinal Research Reviews. 2020 Nov 1;40(6):2427–65.

32. Sperlágh B, Illes P. P2X7 receptor: An emerging target in central nervous system diseases. Trends in Pharmacological Sciences. 2014;35(10):537–47.

33. Skaper SD, Debetto P, Giusti P. The P2X 7 purinergic receptor: from physiology to neurological disorders. The FASEB Journal. 2010 Feb 1;24(2):337–45.

34. Tewari M, Seth P. Emerging role of P2X7 receptors in CNS health and disease. Ageing Research Reviews. 2015 Nov 1;24:328–42.

35. Cheung KK, Chan WY, Burnstock G. Expression of P2X purinoceptors during rat brain development and their inhibitory role on motor axon outgrowth in neural tube explant cultures. Neuroscience. 2005;133(4):937–45.

36. Back MJ, Lee HK, Lee JH, Fu Z, Son MW, Choi SZ, et al. P2X1 Receptor-Mediated Ca^{2+} Influx Triggered by DA-9801 Potentiates Nerve Growth Factor-Induced Neurite Outgrowth. ACS Chem Neurosci. 2016 Nov 16;7(11):1488–98.

37. Blanchard C, Boué-Grabot E, Massé K. Comparative Embryonic Spatio-Temporal Expression Profile Map of the Xenopus P2X Receptor Family. Front Cell Neurosci. 2019 Jul 26;13:340.

38. Massé K, Dale N. Purines as potential morphogens during embryonic development. Purinergic Signalling. 2012 Sep;8(3):503–21.

39. Cheung KK, Burnstock G. Localization of P2X3 receptors and coexpression with P2X2 receptors during rat embryonic neurogenesis. J Comp Neurol. 2002 Feb 18;443(4):368–82.

40. Guo W, Zhang Z, Liu X, Burnstock G, Xiang Z, He C. Developmental expression of P2X5 receptors in the mouse prenatal central and peripheral nervous systems. Purinergic Signalling. 2013 Jun;9(2):239–48.

41. Solini A, Santini E, Chimenti D, Chiozzi P, Pratesi F, Cuccato S, et al. Multiple P2X receptors are involved in the modulation of apoptosis in human mesangial cells: Evidence for a role of P2X4. American Journal of Physiology - Renal Physiology [Internet]. 2007 [cited 2022 Dec 9];292(5). Available from: https://pubmed.ncbi.nlm.nih.gov/17264311/

42. Leeson HC, Kasherman MA, Chan-Ling T, Lovelace MD, Brownlie JC, Toppinen KM, et al. P2X7 Receptors Regulate Phagocytosis and Proliferation in Adult Hippocampal and SVZ Neural Progenitor Cells: Implications for Inflammation in Neurogenesis. Stem Cells. 2018;36(11):1764–77.

43. Kuang XJ, Zhang CY, Yan BY, Cai WZ, Lu CL, Xie LJ, et al. P2X2 receptors in pyramidal neurons are critical for regulating vulnerability to chronic stress. Theranostics. 2022;12(8):3703–18.

44. Yuahasi KK, Demasi MA, Tamajusuku ASK, Lenz G, Sogayar MC, Fornazari M, et al. Regulation of neurogenesis and gliogenesis of retinoic acid-induced P19 embryonal carcinoma cells by P2X2 and P2X7 receptors studied by RNA interference. International Journal of Developmental Neuroscience. 2012 Apr 1;30(2):91–7.

45. Young A, Machacek DW, Dhara SK, Macleish PR, Benveniste M, Dodla MC, et al. Ion channels and ionotropic receptors in human embryonic stem cell derived neural progenitors. Neuroscience. 2011 Sep 29;192:793–805.

46. Heine C, Wegner A, Grosche J, Allgaier C, Illes P, Franke H. P2 receptor expression in the dopaminergic system of the rat brain during development. Neuroscience. 2007 Oct 12;149(1):165–81.

47. Khaira S, Pouton C, Haynes J. P2X2, P2X4 and P2Y1 receptors elevate intracellular Ca2+ in mouse embryonic stem cell-derived GABAergic neurons. Br J Pharmacol. 2009 Dec;158(8):1922–31.

48. Trujillo CA, Negraes PD, Schwindt TT, Lameu C, Carromeu C, Muotri AR, et al. Kinin-B2 receptor activity determines the differentiation fate of neural stem cells. J Biol Chem. 2012 Dec 28;287(53):44046–61.

49. Oliveira SLB, Trujillo CA, Negraes PD, Ulrich H. Effects of ATP and NGF on Proliferation and Migration of Neural Precursor Cells. Neurochemical Research. 2015 Sep 1;40(9):1849–57.

50. Kashfi S, Peymani M, Ghaedi K, Baharvand H, Nasr-Esfahani MH, Javan M. Purinergic Receptor Expression and Potential Association with Human Embryonic Stem Cell-Derived Oligodendrocyte Progenitor Cell Development. Cell J. 2017 Oct;19(3):386–402.

51. Glaser T, De Oliveira SLB, Cheffer A, Beco R, Martins P, Fornazari M, et al. Modulation of mouse embryonic stem cell proliferation and neural differentiation by the P2X7 receptor. Pruszak J, editor. PLoS ONE. 2014 May 5;9(5):e96281.

52. Messemer N, Kunert C, Grohmann M, Sobottka H, Nieber K, Zimmermann H, et al. P2X7 receptors at adult neural progenitor cells of the mouse subventricular zone. Neuropharmacology. 2013 Oct;73:122–37.

53. Resende RR, Majumder P, Gomes KN, Britto LRG, Ulrich H. P19 embryonal carcinoma cells as in vitro model for studying purinergic receptor expression and modulation of N-methyl-d-aspartate-glutamate and acetylcholine receptors during neuronal differentiation. Neuroscience. 2007 May 25;146(3):1169–81.

54. Mut-Arbona P, Sperlágh B. P2 receptor-mediated signaling in the physiological and pathological brain: From development to aging and disease. Neuropharmacology. 2023 Aug 1;233:109541.

55. Sperlágh B, Köfalvi A, Deuchars J, Atkinson L, Milligan CJ, Buckley NJ, et al. Involvement of P2X7 receptors in the regulation of neurotransmitter release in the rat hippocampus. Journal of Neurochemistry. 2002;81(6):1196–211.

56. Campos RC, Parfitt GM, Polese CE, Coutinho-Silva R, Morrone FB, Barros DM. Pharmacological blockage and P2X7 deletion hinder aversive memories: Reversion in an enriched environment. Neuroscience. 2014 Nov 7;280:220–30.

57. Zheng B, Lai R, Li J, Zuo Z. Critical role of P2X7 receptors in the neuroinflammation and cognitive dysfunction after surgery. Brain, Behavior, and Immunity. 2017 Mar 1;61:365–74.

58. Francistiová L, Vörös K, Lovász Z, Dinnyés A, Kobolák J. Detection and Functional Evaluation of the P2X7 Receptor in hiPSC Derived Neurons and Microglia-Like Cells. Frontiers in Molecular Neuroscience. 2022 Jan 12;14:351.

59. Díez-Zaera M, Díaz-Hernández JI, Hernández-Álvarez E, Zimmermann H, Díaz-Hernández M, Miras-Portugal MT. Tissue-nonspecific alkaline phosphatase promotes axonal growth of hippocampal neurons. Molecular Biology of the Cell. 2011;22(7):1014–24.

60. Kanellopoulos JM, Delarasse C. Pleiotropic Roles of P2X7 in the Central Nervous System. Frontiers in Cellular Neuroscience. 2019;13(September):1–18.

61. Díaz-Hernandez M, del Puerto A, Díaz-Hernandez JI, Diez-Zaera M, Lucas JJ, Garrido JJ, et al. Inhibition of the ATP-gated P2X7 receptor promotes axonal growth and branching in cultured hippocampal neurons. Journal of Cell Science. 2008 Nov 15;121(22):3717–28.

62. Anccasi RM, Ornelas IM, Cossenza M, Persechini PM, Ventura ALM. ATP induces the death of developing avian retinal neurons in culture via activation of P2X7 and glutamate receptors. Purinergic Signalling. 2013 Mar 1;9(1):15–29.

63. Oliveira Á, Illes P, Ulrich H. Purinergic receptors in embryonic and adult neurogenesis. Neuropharmacology. 2016 May 1;104:272–81.

64. Tsao HK, Chiu PH, Sun SH. PKC-dependent ERK phosphorylation is essential for P2X7 receptor-mediated neuronal differentiation of neural progenitor cells. Cell Death and Disease [Internet]. 2013 Aug [cited 2022 May 19];4(8). Available from: https://pubmed.ncbi.nlm.nih.gov/23907465/

65. Tang Y, Illes P. Regulation of adult neural progenitor cell functions by purinergic signaling. GLIA. 2017 Feb 1;65(2):213–30.

66. Leeson H, Chan-Ling T, Lovelace M, Brownlie J, Gu B, Weible M. P2X7 receptor signaling during adult hippocampal neurogenesis. Neural Regeneration Research. 2019 Oct 1;14(10):1684–94.

67. Sperry L, Sperry J. Schizophrenia spectrum and other psychotic disorders. In: Psychopathology and psychotherapy: DSM-5 diagnosis, case conceptualization, and treatment, 3rd ed. New York, NY, US: Routledge/Taylor & Francis Group; 2015. p. 177–204.

68. Lewis DA, Gonzalez-Burgos G. Pathophysiologically based treatment interventions in schizophrenia. Nature Medicine. 2006;12(9):1016–22.

69. Hugdahl K. Auditory hallucinations: A review of the ERC "VOICE" project. World Journal of Psychiatry. 2015;5(2):193.

70. McCutcheon RA, Abi-Dargham A, Howes OD. Schizophrenia, Dopamine and the Striatum: From Biology to Symptoms. Trends in Neurosciences. 2019 Mar 1;42(3):205–20.

71. Moseley P, Fernyhough C, Ellison A. Auditory verbal hallucinations as atypical inner speech monitoring, and the potential of neurostimulation as a treatment option. Neuroscience and Biobehavioral Reviews. 2013 Dec;37(10):2794–805.

72. Brisch R, Saniotis A, Wolf R, Bielau H, Bernstein HG, Steiner J, et al. Corrigendum to The role of dopamine in schizophrenia from a neurobiological and evolutionary perspective: Old fashioned, but still in vogue [Front Psychiatry 5, 47] DOI:10.3389/fpsyt.2014.00047. Frontiers in Psychiatry. 2014 Jan 1;5(AUG):47.

73. Bowie CR, Harvey PD. Cognitive deficits and functional outcome in schizophrenia. Neuropsychiatric Disease and Treatment. 2006;2(4):531–6.

74. Chai WJ, Abd Hamid AI, Abdullah JM. Working memory from the psychological and neurosciences perspectives: A review. Frontiers in Psychology. 2018 Mar 27;9(MAR):401.

75. Lesh TA, Niendam TA, Minzenberg MJ, Carter CS. Cognitive control deficits in schizophrenia: Mechanisms and meaning. Neuropsychopharmacology. 2011 Jan;36(1):316–38.

76. Avery MC, Krichmar JL. Improper activation of D1 and D2 receptors leads to excess noise in prefrontal cortex. Frontiers in Computational Neuroscience. 2015 Mar 11;9(MAR):31.

77. Lynch MR. Schizophrenia and the D1 receptor: Focus on negative symptoms. Progress in Neuropsychopharmacology and Biological Psychiatry. 1992;16(6):797–832.

78. Haddad PM, Correll CU. The acute efficacy of antipsychotics in schizophrenia: a review of recent meta-analyses. Therapeutic Advances in Psychopharmacology. 2018 Nov;8(11):303–18.

79. Blair DT, Dauner A. Extrapyramidal symptoms are serious side-effects of antipsychotic and other drugs. Nurse Practitioner. 1992;17(11):56–67.

80. Hattori S, Kishida I, Suda A, Miyauchi M, Shiraishi Y, Fujibayashi M, et al. Effects of four atypical antipsychotics on autonomic nervous system activity in schizophrenia. Schizophrenia Research. 2018 Mar 1;193:134–8.

81. Stiedl O, Pappa E, Konradsson-Geuken Å, Ögren SO. The role of the serotonin receptor subtypes 5-HT1A and 5-HT7 and its interaction in emotional learning and memory. Frontiers in Pharmacology. 2015;6(Aug).

82. Citrome L. Cariprazine for acute and maintenance treatment of adults with schizophrenia: an evidence-based review and place in therapy. Neuropsychiatr Dis Treat. 2018 Oct 5;14:2563–77.

83. Bajouco M, Mota D. Cariprazine on Psychosis: Beyond Schizophrenia – A Case Series. Neuropsychiatr Dis Treat. 2022 Jul 5;18:1351–62.

84. Solmi M, Murru A, Pacchiarotti I, Undurraga J, Veronese N, Fornaro M, et al. Safety, tolerability, and risks associated with first-and second-generation antipsychotics: A state-of-the-art clinical review. Therapeutics and Clinical Risk Management. 2017;13:757–77.

85. Jones C, Watson D, Fone K. Animal models of schizophrenia. British Journal of Pharmacology. 2011 Oct;164(4):1162–94.

86. McCutcheon RA, Krystal JH, Howes OD. Dopamine and glutamate in schizophrenia: biology, symptoms and treatment. World Psychiatry. 2020;19(1):15–33.

87. Chaperon F, Müller W, Auberson YP, Tricklebank MD, Neijt HC. Substitution for PCP, disruption of prepulse inhibition and hyperactivity induced by N-methyl-D-aspartate receptor antagonists: Preferential involvement of the NR2B rather than NR2A subunit. In: Behavioural Pharmacology [Internet]. Behav Pharmacol; 2003 [cited 2022 Aug 2]. p. 477–87. Available from: https://pubmed.ncbi.nlm.nih.gov/14501261/

88. Curzon P, Decker MW. Effects of phencyclidine (PCP) and (+)MK-801 on sensorimotor gating in CD-1 mice. Progress in Neuro-Psychopharmacology and Biological Psychiatry. 1998 Jan 1;22(1):129–46.

89. Lee PR, Brady DL, Shapiro RA, Dorsa DM, Koenig JI. Social interaction deficits caused by chronic phencyclidine administration are reversed by oxytocin. Neuropsychopharmacology. 2005 Mar 30;30(10):1883–94.

90. Brigman JL, Ihne J, Saksida LM, Bussey TJ, Holmes A. Effects of subchronic phencyclidine (PCP) treatment on social behaviors, and operant discrimination and

reversal learning in C57BL/6J mice. Frontiers in Behavioral Neuroscience [Internet]. 2009 Feb 23 [cited 2022 Aug 2];3(FEB). Available from: /pmc/articles/PMC2649201/

91. Noda A, Noda Y, Kamei H, Ichihara K, Mamiya T, Nagai T, et al. Phencyclidine impairs latent learning in mice: Interaction between glutamatergic systems and sigma1 receptors. Neuropsychopharmacology. 2001;24(4):451–60.

92. Lisman JE, Coyle JT, Green RW, Javitt DC, Benes FM, Heckers S, et al. Circuit-based framework for understanding neurotransmitter and risk gene interactions in schizophrenia. Trends in Neurosciences. 2008 May;31(5):234–42.

93. Ellaithy A, Younkin J, González-Maeso J, Logothetis DE. Positive allosteric modulators of metabotropic glutamate 2 receptors in schizophrenia treatment. Trends in Neurosciences. 2015 Aug 1;38(8):506–16.

94. Gonzalez-Burgos G, Cho RY, Lewis DA. Alterations in cortical network oscillations and parvalbumin neurons in schizophrenia. Biological Psychiatry. 2015 Jun 15;77(12):1031–40.

95. Moghaddam B, Adams BW. Reversal of phencyclidine effects by a group II metabotropic glutamate receptor agonist in rats. Science. 1998 Aug 28;281(5381):1349–52.

96. Selemon LD, Zecevic N. Schizophrenia: A tale of two critical periods for prefrontal cortical development. Translational Psychiatry. 2015 Aug 18;5(8):e623–e623.

97. Adams-Chapman I. Insults to the developing brain and impact on neurodevelopmental outcome. Journal of Communication Disorders. 2009 Jul;42(4):256–62.

98. Meyer U, Feldon J, Schedlowski M, Yee BK. Towards an immuno-precipitated neurodevelopmental animal model of schizophrenia. Neuroscience & Biobehavioral Reviews. 2005 Jan;29(6):913–47.

99. Solek CM, Farooqi N, Verly M, Lim TK, Ruthazer ES. Maternal immune activation in neurodevelopmental disorders. Developmental Dynamics. 2018 Apr;247(4):588–619.

100. Shi L, Fatemi SH, Sidwell RW, Patterson PH. Maternal influenza infection causes marked behavioral and pharmacological changes in the offspring. Journal of Neuroscience. 2003 Jan 1;23(1):297–302.

101. Feigenson KA, Kusnecov AW, Silverstein SM. Inflammation and the two-hit hypothesis of schizophrenia. Neuroscience and Biobehavioral Reviews. 2014;38:72–93.

102. Bergdolt L, Dunaevsky A. Brain changes in a maternal immune activation model of neurodevelopmental brain disorders. Progress in Neurobiology. 2019 Apr 1;175:1–19.

103. Patterson PH. Immune involvement in schizophrenia and autism: Etiology, pathology and animal models. Behavioural Brain Research. 2009 Dec 7;204(2):313–21.

104. Hu W, Jain A, Gao Y, Dozmorov IM, Mandraju R, Wakeland EK, et al. Differential outcome of TRIF-mediated signaling in TLR4 and TLR3 induced DC maturation. Proceedings of the National Academy of Sciences of the United States of America. 2015 Nov 10;112(45):13994–9.

105. Fitzgerald KA, Rowe DC, Barnes BJ, Caffrey DR, Visintin A, Latz E, et al. LPS-TLR4 signaling to IRF-3/7 and NF-κB involves the toll adapters TRAM and TRIF. Journal of Experimental Medicine. 2003 Oct 6;198(7):1043–55.

106. Bao M, Hofsink N, Plösch T. LPS vs. Poly I:C Model: Comparison of Long-Term Effects of Bacterial and Viral Maternal Immune Activation (MIA) on the Offspring. American Journal of Physiology - Regulatory Integrative and Comparative Physiology [Internet]. 2022 Feb 1 [cited 2022 Apr 7];322(2). Available from: https://journals.physiology.org/doi/full/10.1152/ajpregu.00087.2021

107. Choi GB, Yim YS, Wong H, Kim S, Kim H, Kim SV, et al. The maternal interleukin-17a pathway in mice promotes autism-like phenotypes in offspring. Science. 2016 Feb 26;351(6276):933–9.

108. Shin Yim Y, Park A, Berrios J, Lafourcade M, Pascual LM, Soares N, et al. Reversing behavioural abnormalities in mice exposed to maternal inflammation. Nature. 2017 Sep 28;549(7673):482–7.

109. Reemst K, Noctor SC, Lucassen PJ, Hol EM. The Indispensable Roles of Microglia and Astrocytes during Brain Development. Frontiers in Human Neuroscience [Internet]. 2016 [cited 2023 Jan 20];10. Available from: https://www.frontiersin.org/articles/10.3389/fnhum.2016.00566

110. Menassa DA, Gomez-Nicola D. Microglial Dynamics During Human Brain Development. Front Immunol. 2018 May 24;9:1014.

111. Chini M, Hanganu-Opatz IL. Prefrontal Cortex Development in Health and Disease: Lessons from Rodents and Humans. Trends in Neurosciences. 2021 Mar 1;44(3):227–40.

112. Müller N. Inflammation in schizophrenia: Pathogenetic aspects and therapeutic considerations. Schizophrenia Bulletin. 2018 Aug 20;44(5):973–82.

113. Khandaker GM, Dantzer R. Is there a role for immune-to-brain communication in schizophrenia? Psychopharmacology. 2016 May 1;233(9):1559–73.

114. Wang AK, Miller BJ. Meta-analysis of Cerebrospinal Fluid Cytokine and Tryptophan Catabolite Alterations in Psychiatric Patients: Comparisons between Schizophrenia, Bipolar Disorder, and Depression. Schizophrenia Bulletin. 2018 Jan 1;44(1):75–83.

115. DiSabato DJ, Quan N, Godbout JP. Neuroinflammation: the devil is in the details. Journal of Neurochemistry. 2016;139:136–53.

116. Bourgognon JM, Cavanagh J. The role of cytokines in modulating learning and memory and brain plasticity. Brain and Neuroscience Advances. 2020 Dec 18;4:239821282097980.

117. Donzis EJ, Tronson NC. Modulation of learning and memory by cytokines: Signaling mechanisms and long term consequences. Neurobiology of Learning and Memory. 2014 Nov 1;115:68–77.

118. Di Benedetto S, Müller L, Wenger E, Düzel S, Pawelec G. Contribution of neuroinflammation and immunity to brain aging and the mitigating effects of physical and cognitive interventions. Neuroscience and Biobehavioral Reviews. 2017 Apr 1;75:114–28.

119. Won E, Kim YK. Neuroinflammation-associated alterations of the brain as potential neural biomarkers in anxiety disorders. International Journal of Molecular Sciences. 2020 Sep 2;21(18):1–19.

120. Dantzer R, O'Connor JC, Freund GG, Johnson RW, Kelley KW. From inflammation to sickness and depression: When the immune system subjugates the brain. Nature Reviews Neuroscience. 2008 Jan;9(1):46–56.

121. Bauer ME, Teixeira AL. Neuroinflammation in Mood Disorders: Role of Regulatory Immune Cells. NeuroImmunoModulation. 2021 Aug 1;28(3):99–107.

122. Illes P, Verkhratsky A, Tang Y. Pathological ATPergic Signaling in Major Depression and Bipolar Disorder. Frontiers in Molecular Neuroscience. 2020 Jan 31;12:331.

123. Iwata M, Ota KT, Li XY, Sakaue F, Li N, Dutheil S, et al. Psychological stress activates the inflammasome via release of adenosine triphosphate and stimulation of the purinergic type 2X7 receptor. Biological Psychiatry. 2016 Jul 1;80(1):12–22.

124. Csölle C, Andó RD, Kittel Á, Gölöncsér F, Baranyi M, Soproni K, et al. The absence of P2X7 receptors (P2rx7) on non-haematopoietic cells leads to selective alteration in mood-related behaviour with dysregulated gene expression and stress reactivity

in mice. International Journal of Neuropsychopharmacology. 2013 Feb;16(1):213–33.

125. Gölöncsér F, Baranyi M, Balázsfi D, Demeter K, Haller J, Freund TFF, et al. Regulation of hippocampal 5-HT release by P2X7 receptors in response to optogenetic stimulation of median raphe terminals of mice. Frontiers in Molecular Neuroscience. 2017;10.

126. McGuffin P, Knight J, Breen G, Brewster S, Boyd PR, Craddock N, et al. Whole genome linkage scan of recurrent depressive disorder from the depression network study. Human Molecular Genetics. 2005 Nov 15;14(22):3337–45.

127. Vereczkei A, Abdul-Rahman O, Halmai Z, Nagy G, Szekely A, Somogyi A, et al. Association of purinergic receptor P2RX7 gene polymorphisms with depression symptoms. Progress in Neuro-Psychopharmacology and Biological Psychiatry. 2019 Jun 8;92:207–16.

128. Kristof Z, Eszlari N, Sutori S, Gal Z, Torok D, Baksa D, et al. P2RX7 gene variation mediates the effect of childhood adversity and recent stress on the severity of depressive symptoms. PLoS ONE. 2021 Jun 1;16(6 June):e0252766.

129. Sprooten E, Gupta CN, Knowles EEM, Mckay DR, Mathias SR, Curran JE, et al. Genome-wide significant linkage of schizophrenia-related neuroanatomical trait to 12q24. American Journal of Medical Genetics, Part B: Neuropsychiatric Genetics. 2015 Dec 1;168(8):678–86.

130. Trubetskoy V, Pardiñas AF, Qi T, Panagiotaropoulou G, Awasthi S, Bigdeli TB, et al. Mapping genomic loci implicates genes and synaptic biology in schizophrenia Check for updates. Nature [Internet]. 2022 [cited 2022 Apr 26];604. Available from: https://doi.org/10.1038/s41586-022-04434-5

131. Boks MP, He Y, Schubart CD, Gastel W van, Elkrief L, Huguet G, et al. Cannabinoids and psychotic symptoms: A potential role for a genetic variant in the P2X purinoceptor 7 (P2RX7) gene. Brain, Behavior, and Immunity. 2020 Aug 1;88:573–81.

132. Koványi B, Csölle C, Calovi S, Hanuska A, Kató E, Köles L, et al. The role of P2X7 receptors in a rodent PCP-induced schizophrenia model. Scientific Reports. 2016 Nov 8;6(1):1–16.

133. Huang H, Zheng S, Chen M, Xie L, Li Z, Guo M, et al. The potential of the P2X7 receptor as a therapeutic target in a sub-chronic PCP-induced rodent model of schizophrenia. Journal of Chemical Neuroanatomy [Internet]. 2021 Oct 1 [cited 2022 Apr 26];116. Available from: https://pubmed.ncbi.nlm.nih.gov/34147620/

134. Hempel C, Nörenberg W, Sobottka H, Urban N, Nicke A, Fischer W, et al. The phenothiazine-class antipsychotic drugs prochlorperazine and trifluoperazine are potent allosteric modulators of the human P2X7 receptor. Neuropharmacology. 2013;75:365–79.

135. Beamer E, Kovács G, Sperlágh B. ATP released from astrocytes modulates action potential threshold and spontaneous excitatory postsynaptic currents in the neonatal rat prefrontal cortex. Brain Research Bulletin. 2017 Oct 1;135:129–42.

136. Horváth G, Otrokocsi L, Beko K, Baranyi M, Kittel Á, Fritz-Ruenes PA, et al. P2X7 Receptors Drive Poly(I:C) Induced Autism-like Behavior in Mice. The Journal of Neuroscience. 2019 Mar 27;39(13):2542 LP – 2561.

137. Szabó D, Tod P, Gölöncsér F, Román V, Lendvai B, Otrokocsi L, et al. Maternal P2X7 receptor inhibition prevents autism-like phenotype in male mouse offspring through the NLRP3-IL-1β pathway. Brain, Behavior, and Immunity. 2022 Mar 1;101:318–32.

138. Kaczmarek-Hajek K, Zhang J, Kopp R, Grosche A, Rissiek B, Saul A, et al. Re-evaluation of neuronal P2X7 expression using novel mouse models and a P2X7-specific nanobody. eLife. 2018 Aug 3;7.

139. Mut-Arbona P, Sperlagh B. Analysis of P2X7-Induced Neuronal Branching. Methods in Molecular Biology. 2022;2510.

140. Gao H. Generation of Neuron-enriched Cultures (Method 1). Bio-Protocol. 2011;1(21).

141. Sánchez-Nogueiro J, Marín-García P, Miras-Portugal MT. Characterization of a functional P2X7-like receptor in cerebellar granule neurons from P2X7 knockout mice. FEBS Letters. 2005 Jul 4;579(17):3783–8.

142. Baranyi M, Milusheva E, Vizi ES, Sperlágh B. Chromatographic analysis of dopamine metabolism in a Parkinsonian model. Journal of Chromatography A. 2006 Jul 7;1120(1–2):13–20.

143. Mut-Arbona P, Huang L, Baranyi M, Tod P, Iring A, Calzaferri F, et al. Dual Role of the P2X7 Receptor in Dendritic Outgrowth during Physiological and Pathological Brain Development. J Neurosci. 2023 Feb 15;43(7):1125–42.

144. Cruz-Sanchez A, Dematagoda S, Ahmed R, Mohanathaas S, Odenwald N, Arruda-Carvalho M. Developmental onset distinguishes three types of spontaneous recognition memory in mice. Scientific Reports [Internet]. 2020 Dec 1 [cited 2022 Jul 5];10(1). Available from: https://pubmed.ncbi.nlm.nih.gov/32606443/

145. Vigli D, Palombelli G, Fanelli S, Calamandrei G, Canese R, Mosca L, et al. Maternal Immune Activation in Mice Only Partially Recapitulates the Autism Spectrum Disorders Symptomatology. Neuroscience. 2020;445:109–19.

146. Castañé A, Santana N, Artigas F. PCP-based mice models of schizophrenia: Differential behavioral, neurochemical and cellular effects of acute and subchronic treatments. Psychopharmacology. 2015 Nov 1;232(21–22):4085–97.

147. Naviaux RK, Zolkipli Z, Wang L, Nakayama T, Naviaux JC, Le TP, et al. Antipurinergic Therapy Corrects the Autism-Like Features in the Poly(IC) Mouse Model. PLoS ONE. 2013;8(3).

148. Nabeshima T, Ishikawa K, Yamaguchi K, Furukawa H, Kameyama T. Phencyclidine-induced head-weaving observed in mice after ritanserin treatment. European Journal of Pharmacology. 1987 Jul 9;139(2):171–8.

149. Sams-Dodd F. Automation of the social interaction test by a video-tracking system: behavioural effects of repeated phencyclidine treatment. Journal of Neuroscience Methods. 1995;59(2):157–67.

150. Motulsky HJ, Brown RE. Detecting outliers when fitting data with nonlinear regression - A new method based on robust nonlinear regression and the false discovery rate. BMC Bioinformatics [Internet]. 2006 Mar 9 [cited 2022 Jan 13];7. Available from: https://pubmed.ncbi.nlm.nih.gov/16526949/

151. Calzaferri F, Narros-Fernández P, De Pascual R, De Diego AMG, Nicke A, Egea J, et al. Synthesis and Pharmacological Evaluation of Novel Non-nucleotide Purine Derivatives as P2X7 Antagonists for the Treatment of Neuroinflammation. Journal of Medicinal Chemistry. 2021 Feb 25;64(4):2272–90.

152. Lévesque SA, Lavoie ÉG, Lecka J, Bigonnesse F, Sévigny J. Specificity of the ecto-ATPase inhibitor ARL 67156 on human and mouse ectonucleotidases. British Journal of Pharmacology. 2007 Aug 8;152(1):141–50.

153. Calovi S, Mut-Arbona P, Tod P, Iring A, Nicke A, Mato S, et al. P2X7 Receptor-Dependent Layer-Specific Changes in Neuron-Microglia Reactivity in the Prefrontal Cortex of a Phencyclidine Induced Mouse Model of Schizophrenia. Frontiers in Molecular Neuroscience. 2020 Nov 11;13:202.

154. Ogura Y, Sutterwala FS, Flavell RA. The Inflammasome: First Line of the Immune Response to Cell Stress. Cell. 2006 Aug 25;126(4):659–62.

155. Dinarello CA. A signal for the caspase-1 inflammasome free of TLR. Immunity. 2007 Apr;26(4):383–5.

156. Andrejew R, Oliveira-Giacomelli Á, Ribeiro DE, Glaser T, Arnaud-Sampaio VF, Lameu C, et al. The P2X7 Receptor: Central Hub of Brain Diseases. Frontiers in Molecular Neuroscience. 2020 Jul 31;13:124.

157. Teresa Miras-Portugal PM, Sebastián-Serrano Á, De Diego García L, Díaz-Hernández M. Neuronal P2X7 receptor: Involvement in neuronal physiology and. Journal of Neuroscience. 2017 Jul 26;37(30):7063–72.

158. Cheung AFP, Pollen AA, Tavare A, Deproto J, Molnár Z. Comparative aspects of cortical neurogenesis in vertebrates. In: Journal of Anatomy. 2007. p. 164–76.

159. Ribeiro DE, Glaser T, Oliveira-Giacomelli Á, Ulrich H. Purinergic receptors in neurogenic processes. Brain research bulletin. 2019 Sep;151:3–11.

160. Fumagalli M, Lecca D, Abbracchio MP, Ceruti S. Pathophysiological role of purines and pyrimidines in neurodevelopment: Unveiling new pharmacological approaches to congenital brain diseases. Frontiers in Pharmacology. 2017;8(DEC).

161. Oliveira SLB, Trujillo CA, Negraes PD, Ulrich H. Effects of ATP and NGF on Proliferation and Migration of Neural Precursor Cells. Neurochemical Research. 2015 Sep 1;40(9):1849–57.

162. Ou A, Gu BJ, Wiley JS. The scavenger activity of the human P2X7 receptor differs from P2X7 pore function by insensitivity to antagonists, genetic variation and sodium concentration: Relevance to inflammatory brain diseases. Biochimica et Biophysica Acta - Molecular Basis of Disease. 2018;1864(4):1051–9.

163. Lovelace MD, Gu BJ, Eamegdool SS, Weible MW, Wiley JS, Allen DG, et al. P2X7 receptors mediate innate phagocytosis by human neural precursor cells and neuroblasts. Stem Cells. 2015 Feb 1;33(2):526–41.

164. Neary JT, Shi YF, Kang Y, Tran MD. Opposing effects of P2X7 and P2Y purine/pyrimidine-preferring receptors on proliferation of astrocytes induced by fibroblast growth factor-2: Implications for CNS development, injury, and repair. Journal of Neuroscience Research. 2008;86(14):3096–105.

165. Bond AM, Berg DA, Lee S, Garcia-Epelboim AS, Adusumilli VS, Ming GL, et al. Differential timing and coordination of neurogenesis and astrogenesis in developing mouse hippocampal subregions. Brain Sciences. 2020 Nov 26;10(12):1–14.

166. Yu Y, Ugawa S, Ueda T, Ishida Y, Inoue K, Kyaw Nyunt A, et al. Cellular localization of P2X7 receptor mRNA in the rat brain. Brain Research. 2008 Feb 15;1194:45–55.

167. Metzger MW, Walser SM, Aprile-Garcia F, Dedic N, Chen A, Holsboer F, et al. Genetically dissecting P2rx7 expression within the central nervous system using conditional humanized mice. Purinergic Signalling. 2017;13(2):153–70.

168. Hodge RD, Bakken TE, Miller JA, Smith KA, Barkan ER, Graybuck LT, et al. Conserved cell types with divergent features in human versus mouse cortex. Nature 2019 573:7772. 2019 Aug 21;573(7772):61–8.

169. Reisinger S, Khan D, Kong E, Berger A, Pollak A, Pollak DD. The Poly(I:C)-induced maternal immune activation model in preclinical neuropsychiatric drug discovery. 2015;149:213–26.

170. Kowash HM, Potter HG, Edye ME, Prinssen EP, Bandinelli S, Neill JC, et al. Poly(I:C) source, molecular weight and endotoxin contamination affect dam and prenatal outcomes, implications for models of maternal immune activation. Brain, Behavior, and Immunity. 2019 Nov 1;82:160–6.

171. Su Y, Lian J, Hodgson J, Zhang W, Deng C. Prenatal Poly I:C Challenge Affects Behaviors and Neurotransmission via Elevated Neuroinflammation Responses in Female Juvenile Rats. International Journal of Neuropsychopharmacology. 2022;25(2):160–71.

172. Huang L, Otrokocsi L, Sperlágh B. Role of P2 receptors in normal brain development and in neurodevelopmental psychiatric disorders. Brain Research Bulletin. 2019 Sep 1;151:55–64.

173. Chen C, Liu H, Hsueh Y. TLR 3 downregulates expression of schizophrenia gene Disc1 via MYD 88 to control neuronal morphology. EMBO reports. 2017 Jan;18(1):169–83.

174. Moser HW. Dendritic anomalies in disorders associated with mental retardation. Developmental Neuropsychology. 1999 Dec;16(3):369–71.

175. Kalus P, Muller TJ, Zuschratter W, Senitz D. The dendritic architecture of prefrontal pyramidal neurons in schizophrenic patients. NeuroReport. 2000 Nov 9;11(16):3621–5.

176. Shelton MA, Newman JT, Gu H, Sampson AR, Fish KN, MacDonald ML, et al. Loss of Microtubule-Associated Protein 2 Immunoreactivity Linked to Dendritic Spine Loss in Schizophrenia. Biological Psychiatry. 2015 Sep 15;78(6):374–85.

177. Moyer CE, Shelton MA, Sweet RA. Dendritic spine alterations in schizophrenia. Neuroscience Letters. 2015;601:46–53.

178. Grubisha MJ, Sun T, Eisenman L, Erickson SL, Chou SY, Helmer CD, et al. A Kalirin missense mutation enhances dendritic RhoA signaling and leads to regression of cortical dendritic arbors across development. Proceedings of the National Academy of Sciences of the United States of America [Internet]. 2021 [cited 2022 Jan 12];118(49). Available from: http://www.pnas.org/lookup/

179. Morrison JH, Baxter MG. The ageing cortical synapse: Hallmarks and implications for cognitive decline. Nature Reviews Neuroscience. 2012 Apr;13(4):240–50.

180. Allard S, Scardochio T, Cuello AC, Ribeiro-da-Silva A. Correlation of cognitive performance and morphological changes in neocortical pyramidal neurons in aging. Neurobiology of Aging. 2012 Jul;33(7):1466–80.

181. Broadbelt K, Byne W, Jones LB. Evidence for a decrease in basilar dendrites of pyramidal cells in schizophrenic medial prefrontal cortex. Schizophrenia Research. 2002;58(1):75–81.

182. Goldman-Rakic PS. The relevance of the dopamine- D1 receptor in the cognitive symptoms of schizophrenia. Neuropsychopharmacology. 1999;21(6):S170–80.

183. Bayer TA, Falkai P, Maier W. Genetic and non-genetic vulnerability factors in schizophrenia: The basis of the 'Two hit hypothesis'. Journal of Psychiatric Research. 1999;33(6):543–8.

184. Haddad FL, Patel SV, Schmid S. Maternal Immune Activation by Poly I:C as a preclinical Model for Neurodevelopmental Disorders: A focus on Autism and Schizophrenia. Neuroscience and Biobehavioral Reviews. 2020;113:546–67.

185. Meyer U, Feldon J. To poly(I:C) or not to poly(I:C): Advancing preclinical schizophrenia research through the use of prenatal immune activation models. Neuropharmacology. 2012 Mar;62(3):1308–21.

186. Posillico CK, Garcia-Hernandez RE, Tronson NC. Sex differences and similarities in the neuroimmune response to central administration of poly I:C. Journal of Neuroinflammation. 2021 Dec 1;18(1):1–17.

187. Haida O, Al Sagheer T, Balbous A, Francheteau M, Matas E, Soria F, et al. Sex-dependent behavioral deficits and neuropathology in a maternal immune activation model of autism. Translational Psychiatry. 2019 Mar 28;9(1):1–12.

188. Mueller FS, Polesel M, Richetto J, Meyer U, Weber-Stadlbauer U. Mouse models of maternal immune activation: Mind your caging system! Brain, Behavior, and Immunity. 2018 Oct 1;73:643–60.

189. Kokras N, Dalla C. Sex differences in animal models of psychiatric disorders. British journal of pharmacology. 2014;171(20):4595–619.

190. Basso AM, Bratcher NA, Harris RR, Jarvis MF, Decker MW, Rueter LE. Behavioral profile of P2X7 receptor knockout mice in animal models of depression and anxiety: Relevance for neuropsychiatric disorders. Behavioural Brain Research. 2009 Mar 2;198(1):83–90.

191. Csölle C, Baranyi M, Zsilla G, Kittel Á, Gölöncsér F, Illes P, et al. Neurochemical Changes in the Mouse Hippocampus Underlying the Antidepressant Effect of Genetic Deletion of P2X7 Receptors. PLoS ONE. 2013 Jun 21;8(6):e66547.

192. Alcocer-Gómez E, de Miguel M, Casas-Barquero N, Núñez-Vasco J, Sánchez-Alcazar JA, Fernández-Rodríguez A, et al. NLRP3 inflammasome is activated in mononuclear blood cells from patients with major depressive disorder. Brain, Behavior, and Immunity. 2014 Feb;36:111–7.

10. Bibliography of the candidate's publications

10.1. Publications used for the thesis

1. Mut-Arbona Paula, Huang Lumei, Baranyi Mária, Tod Pál, Iring András, Calzaferri Francesco, de los Ríos Cristobal, Sperlágh Beáta (2023) Dual Role of the P2X7 Receptor in Dendritic Outgrowth during Physiological and Pathological Brain Development. JOURNAL OF NEUROSCIENCE 43: 7 pp. 1125-1142.

IF: 6,709

2. Calovi S, Mut-Arbona P, Tod P, Iring A, Nicke A, Mato S, Vizi ES, Tønnesen J, Sperlagh B (2020) P2X7 Receptor-Dependent Layer-Specific Changes in Neuron-Microglia Reactivity in the Prefrontal Cortex of a Phencyclidine Induced Mouse Model of Schizophrenia. FRONTIERS IN MOLECULAR NEUROSCIENCE 13 Paper: 566251, 23 p.

IF: 5,639

3. Mut-Arbona P, Sperlágh B (2023) P2 receptor-mediated signaling in the physiological and pathological brain: From development to aging and disease. NEUROPHARMACOLOGY 233 Paper: 109541, 17 p.

IF: 5,273

4. Mut-Arbona Paula, Sperlágh Beáta (2022) Analysis of P2X7-Induced Neuronal Branching. In: Nicke, Annette (eds.) The P2X7 Receptor: Methods and Protocols
New York City, United States of America: Springer US (2022) pp. 341-353. Paper: Chapter 19, (Chapter in Book)

IF:1.37

10.2. Additional publications

1. Calovi Stefano, Mut-Arbona Paula, Sperlágh Beáta (2019) Microglia and the Purinergic Signaling System. NEUROSCIENCE 405 pp. 137-147.

IF: 3,056

2. Kristóf Zsüliet, Baranyi Mária, Tod Pál, Mut-Arbona Paula, Demeter Kornél, Bitter István, Sperlágh Beáta (2022) Elevated serum purine levels in schizophrenia: a reverse translational study to identify novel inflammatory biomarkers. INTERNATIONAL JOURNAL OF NEUROPSYCHOPHARMACOLOGY 25: 8 pp. 645-659.

IF: 5,678

DOI:10.14753/SE.2023.2882

12. Appendix A

To extend our studies regarding the developmental changes of the dendritic arborisation, the morphology in dentate granule cells, another type of hippocampal excitatory neuron was also assessed (Fig. 25). Interestingly, there were no differences between genotypes in the granular cells from dentate gyrus from acute hippocampal slices (Fig. 25A-E).

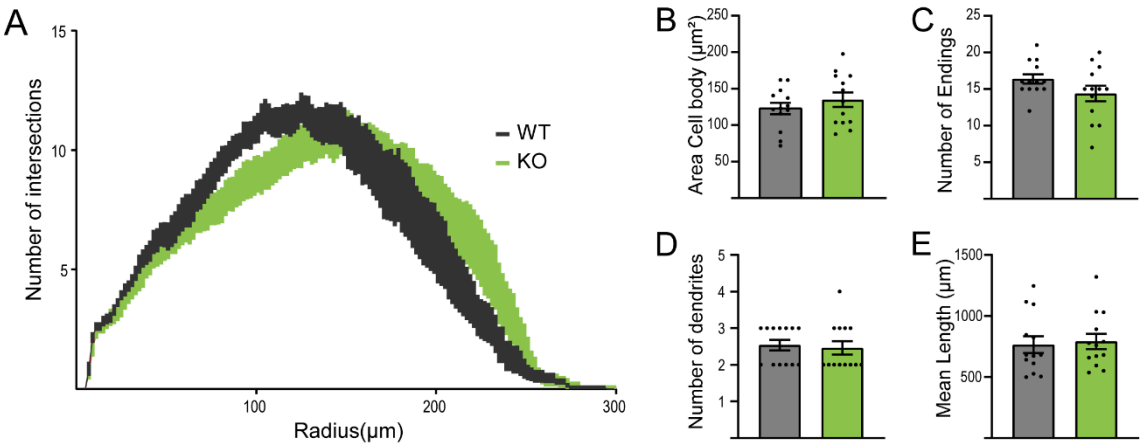

Figure 25. P2X7R does not regulate dendritic branching in dentate granule cells. (A) Sholl analysis presents the number of intersections versus the distance to the soma from granular cells for both genotypes. Quantification of (B) area cell body, (C) number of primary dendrites, (D) number of endings and (E) mean length of the dendrites. There is no statistical difference between WT and KO in two-way Anova nor Unpaired t-test. Figure 3L-O from Huang, L; Mut-Arbona, P; Varga, B; Brunner, J; Arszovszki, A; Iring, A; Kisfali, M; Vizi, S and Sperlágh, B (*2023*). Purinergic Receptor P2X7 Modulates Dentate Gyrus Excitatory Neurotransmission and Alleviates Schizophrenia-like Symptoms in Mouse. *iScience*.

We can conclude that P2X7R depletion led to abnormal dendritic arborisation in pyramidal hippocampal neurons affecting the synapsis in the CA1 region of the hippocampus. Thus, P2X7R is necessary for normal dendritic outgrowth during neuronal development, proliferation, and maturation in a region with cell-type specificity.

DOI:10.14753/SE.2023.2882

13. Acknowledgements

I would like to express my heartfelt gratitude to my supervisor, Beáta Sperlágh, for her invaluable guidance, support, and mentorship throughout my doctoral journey. Bea has been a constant source of inspiration to me, both as a scientist and as a lead woman. Her expertise, insight, and unwavering encouragement have been instrumental in shaping my research and helping me grow as a researcher.

I am also deeply grateful to my colleagues, who have been an integral part of my academic journey. Their intellectual curiosity, enthusiasm, and friendship have made my time in the program all the more rewarding. I would like to thank them all for their support, encouragement, and valuable feedback on my work. Specially, I would like to emphasize the role of Lumei Huang, Andras Iring, Pal Tod, Varga Bernadette and Mari and the immense support on the publication and revision of my main research.

I am also genuinely thankful to my colleagues at Purines DX, for their support, camaraderie, and shared experiences, which have made my time in the program all the more meaningful. I am grateful for the laughs, the trips, the conversations, and the friendships that we have developed over the years.

I would like to extend my appreciation to the city of Budapest, which has been my home for the past five years. The city's vibrant culture, history, and people have provided a stimulating environment that has helped me grow both personally and academically. I am grateful for the opportunities I have had to explore the city, its landmarks, and its hidden gems, and to experience its unique charm and character. I would also like to thank all the friends (and dog-friends) I have made during my time in Budapest, both those who have stayed and those who have moved on. Their friendship, support, and shared experiences have been a source of joy and enrichment, and have made my time in Budapest all the more memorable. I am grateful for the memories we have created together. *Budapest significa familia.*

Last but not least, I would like to thank my family for their love, encouragement, and unwavering support throughout my studies. Their belief in me, even during the most challenging times, has been a constant source of strength and motivation. I am forever grateful for their sacrifices and for being my rock. *Gracias por ser siempre mi fuerza, mi red de apoyo, mi casa, mi techo, mi suerte. Gracias por ser las brasas de una llama que*

DOI:10.14753/SE.2023.2882

siempre se mantendrá viva dentro de mí: la de la fuerza y las ganas. Gracias familia por enseñarme que podía hacer todo aquello que me propusiera y cumplir mis metas.

A ti, que te hubieses ido al mercado a fardar de tu nieta doctoranda.

Gracias a los amigos pasajeros de etapas de mi vida que me han ayudado a llegar hasta aquí, que me vieron ponerme la primera bata y me enseñaron a trabajar en un laboratorio, aquellos que se han quedado conmigo hasta que hemos salido a navegar: los de las maravillosas prácticas en Beniarbeig, los biólogos y neurocientíficos,

Gracias a mis amigos de casa los de siempre, para siempre.

In conclusion, my PhD thesis would not have been possible without the support, guidance, and inspiration of so many people. To all those who have played a role in my academic journey, I offer my sincere thanks and appreciation.